Nitric oxide reactivity of Cu(II) and Co(II) complexes with N-donor ligands

A dissertation submitted to the
Indian Institute of Technology Guwahati as
partial fulfillment for the degree of
Doctor of Philosophy in Chemistry

Submitted by

Hemanta Deka

(Roll No. 11612208)

Supervisor

Prof. Biplab Mondal

Department of Chemistry

Indian Institute of Technology Guwahati

October, 2016

Dedicated to My Family
&
Friends

STATEMENT

I hereby declare that the matter embodied in this thesis is the result of investigations carried out by me in the Department of Chemistry, Indian Institute of Technology Guwahati, India, under the supervision of Prof. Biplab Mondal.

In keeping with the general practice of reporting scientific observations, due acknowledgements have been made wherever the work described is based on the findings of other investigators.

October, 2016

Hemanta Deka

Indian Institute of Technology Guwahati

भारतीय प्रौद्योगिकी संस्थान गुवाहाटी
INDIAN INSTITUTE OF TECHNOLOGY GUWAHATI
North Guwahati, Assam – 781039, India

Prof. Biplab Mondal
Department of Chemistry

Phone : + 91-361-258-2317
Fax: + 91-361-258-2349
E-mail: biplab@iitg.ernet.in

Certificate

This is to certify that **Mr. Hemanta Deka** has been working under my supervision since July, 2011 as a regular Ph. D. student in the Department of Chemistry, Indian Institute of Technology Guwahati. I am forwarding his thesis entitled "**Nitric oxide reactivity of Cu(II) and Co(II) complexes with N-donor ligands**" being submitted for the Ph. D. degree.

I certify that he has fulfilled all the requirements according to the rules of this Institute regarding the investigations embodied in his thesis and this work has not been submitted elsewhere for a degree.

October, 2016 **Biplab Mondal**

Acknowledgements

At the outset, with a deepest sense of gratitude, I would like to express my sincere thanks to my supervisor, Prof. Biplab Mondal, for his invaluable guidance, encouragement, inspiration and moral support which helped me to enhance my knowledge and have inspired me to take right decisions at crucial moments. I am also thankful to him for giving me freedom to pursue my own interests in his lab and I find myself privileged to have worked under his kind guidance.

I would like to acknowledge my doctoral committee members, Prof. J. B. Baruah, Prof. A. Ramesh, Dr. Debasis Manna for their valuable suggestions and advices. My special thanks to Prof. P. K. Iyer for providing me facility of glove box and Dr. A. S Achalkumar for low temperature reaction setup and Dr. Kumar Vanka, NCL Pune for theoretical studies. Also I would like to thank all the faculty members of the department of chemistry for their consistent encouragement.

I would like to thank CSIR-New Delhi for financial support and IIT Guwahati for all the facilities that were made available to me. I am thankful to Dr. Babulal Das, Mr. Aniruddha Gogoi, Mr. Imdadul Islam and Mrs. Abhilasha Baruah of Department of Chemistry and Kesho Singh of Central Instruments Facility (for EPR and LC-MS) and all the non-teaching staff of Department of Chemistry for their help during my Ph.D. tenure.

I must thank my current labmates Somnath, Kuldeep, Soumen, Baishakhi and Dibyajyoti Da and former labmates Moushumi ba, Pankaj Da, Apurba da, Aswini da, Vikash da and Kanhu da for the constant cooperation, support and creating the humourous and pleasant environment in the laboratory. I also would like to thank summer project and MSc project student Samarjit, Nimisha, Aushree, Rini, Arnav, Narayani, Soham, Najmul, Sayantani, Arpan and Plabita whom I had an opportunity to work with. No words can express my thankfulness for giving me their time and companionship, which made the time spent in the laboratory and outside pleasant and memorable.

I would like to give my special thank to my dear friends Dharam, Prasenjit, Manoj, Priya, Sabera, Gargi, Nirmali, Bidyut, Bedanta, Pulakesh and Biju for their help and support during this period.

Finally, I would like to thank my parents and sisters, Riju and Bidya. Without their love and support, this work would not have been completed. I am also thankful to my uncle Sri Gajen Deka and his family for their love and support. I would like to thank all others who are associated with my work directly or indirectly at IIT Guwahati for their help.

Hemanta Deka

Contents

Synopsis

The thesis entitled "**Nitric oxide reactivity of Cu(II) and Co(II) complexes with N-donor ligands**" is divided into five chapters.

Chapter 1: Introduction

Nitric oxide (NO) is a neutral, free radical gas molecule. It has long been recognized as an environmental contaminant and can cause potential health hazard. Later on, NO has been found to play various important roles in biological systems which includes vasodilatation, platelet inhibition, bronchodialation, heart and skeletal muscle contraction, apoptosis facilitation, neurotransmission etc.[1-3] Most of these roles played by NO in biology are attributed to the formation of nitrosyl complexes of the metallo-proteins, mainly iron or copper. The fundamental roles of NO in biological systems and its activation by transition metal ions have attracted a wide range of research.

NO reactivity of ferri- and ferro-heme systems have been studied extensively both with the metallo-enzymes as well as with synthetic models.[4-5] The reduction of Cu(II) centres in laccase and cytochromes by NO is known for a long time. NO induce reduction of Cu(II) to Cu(I) in small molecule models with various ligand frameworks are known. A number of examples reported in literature which demonstrated the reduction of Cu(II) center by NO proceeds through the [Cu(II)-NO] intermediate and afforded N-nitrosation in the ligand frameworks.[6-8] In an other example, Ford and co-workers reported the reduction of Cu(II) center in $[Cu(DAC)]^{2+}$ {DAC = 1,8-*bis*(9-anthracylmethyl)cyclam} by NO with simultaneous N-nitrosation of the ligand.[9] The reaction of NO with $[Cu(dmp)_2(H_2O)]^{2+}$ (dmp = 2,9-dimethyl-1,10-phenanthroline) in methanol was found to result in the formation of $[Cu(I)(dmp)_2]^{+}$ complex along with methyl nitrite and H_2O.[10] It was proposed that this reaction proceeds through the formation of [Cu(II)-NO] intermediate. Lippard's

group reported the examples of several Cu(II) complexes where the NO induced reduction was utilized to develop fluorescence sensors for NO.[11]

On the other hand, NO reactivity of other first row transition metal ions have not been studied to that extent. Caulton and coworkers synthesized $[(TMEDA)Co(NO)_2][BPh_4]$ from the reaction of $CoCl_2$, two equivalents of tetramethylethylenediamine (TMEDA) and NO in dry methanol followed by addition of $NaBPh_4$.[12] Lippard and co-workers reported the formation of mono and dinitrosyl cobalt complexes with tetraazamacrocyclic tropocoronand (TC) ligands.[13-16] They also observed the reductive nitrosylation of cobalt centre to results a carboxylate bridged dinitrosyl complex with *N*-nitrosation of the ligand.[17] Warren *et al.* reported several examples of diazonium dialate formation from the reaction of *C*-nitroso adduct of copper and nickel complexes with NO. In these reactions, oxidation of metal centre takes place with concomitant reduction of NO to NO^-.[18-20]

In addition, redox reaction of coordinated NO is common in biological system as well as in model complexes. In most of the cases NO disproportionate to N_2O and NO_2^- in presence of transition metal ion/s.[21] Oxidation of coordinated NO with reactive oxygen species like peroxide, superoxide, or even molecular oxygen is known to the result in nitrite or nitrate formation.[22]

This thesis has been focused on the redox reaction of NO assisted with transition metal complexes. Initial aim of the thesis was to synthesize stable metal–nitrosyl complexes and to study the redox reactivity of the coordinated nitrosyl. Since most of the roles played by NO in biological systems are attributed to the formation of nitrosyl complexes of the metallo-proteins, this work would have been helpful to understand the basic chemistry involved in biological reactions. To achieve those, the reactivity of Cu(II) complexes of N-

donor ligands have been studied and described in second and third chapters of the thesis. In both the cases, initial attack of NO resulted in the reduction of Cu(II) centre to Cu(I) and the Cu(I) intermediate complex thus formed further reacts with excess NO to afford N_2O.

Since cobalt-nitrosyls having $\{CoNO\}^8$ configuration are known to be stable, the fourth chapter has been originated from our interest to develop stable $\{CoNO\}^8$ complex. It has been reported in literature that Co(II) centres react with different ways with NO. For instance, in some cases, they undergo reductive nitrosylation; on the other hand, simple adduct formation is also known. In this connection, fourth chapter of this thesis describes a comparative account of the roles of ligand frameworks to control the NO reactivity of cobalt complexes. The fifth and final chapter describes the oxidation of NO in presence of a Co(II)- superoxo complex.

Chapter 2: Nitric oxide reactivity of Cu(II) complex of N- donor ligand: Formation of a stable nitrous oxide complex

Ligand, **L1H$_3$** {**L1H$_3$** = 2,2',2''-(((nitrilo-*tris*(ethane-2,1-diyl))*tris*(azanediyl))*tris*(methylene)) triphenol} was prepared by treating *tris*-(2-aminoethyl)amine with 3 equivalent of salicylaldehyde in ethanol followed by the reduction with sodium borohydride. Complex **2.1** was prepared by adding equivalent amount of the ligand into methanol solution of copper(II) perchlorate hexahydrate. Spectroscopic analyses as well as X-ray single crystal structure determination confirmed the formation of mono-nuclear complex **2.1**, $[Cu(L1H_2)](ClO_4)$. The perspective ORTEP view of complex **2.1** is shown in figure 1.

In acetonitrile solution complex **2.1** displayed absorption at 670 nm (ε/ M^{-1} cm^{-1}, 168) and 430 nm (ε/ $M^{-1}cm^{-1}$, 722) with other intra-ligand transitions in the lower wavelengths (Figure 2). The 670 nm absorption is attributed to the *d-d* transition and the band cantered

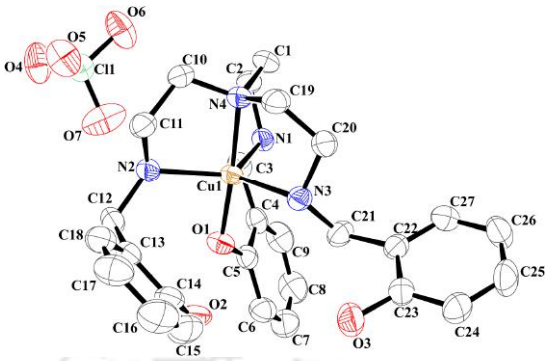

Figure 1 ORTEP diagram of complex **2.1** (30% thermal ellipsoid plot, H-atoms are omitted for clarity).

at 430 nm is assigned as the phenolato→Cu(II) charge transfer. In X-band EPR spectroscopy, the characteristic signal for Cu(II) centre was observed. The observed parameters are $g_{\parallel}$, 2.309, $g_{\perp}$, 2.081 and $A_{\parallel}$, 156.5 × 10^{-4} cm^{-1}.

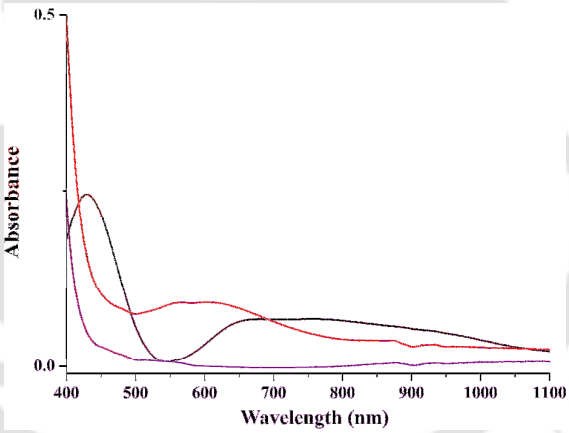

Figure 2 UV-visible spectra of complex **2.1** (black), after adding stoichiometric amount (violet) and excess (red) of NO in acetonitrile at room temperature.

Addition of excess NO to the degassed acetonitrile solution of complex **2.1** at room temperature resulted in the transient colorless species followed by a bluish green solution (Scheme 1). Dry and degassed diethyl ether (~ 20 ml) was added to this and the solution was allowed to stand at room temperature for 3 hrs to precipitate out complex **2.2**. The transient colorless species was characterized as the corresponding Cu(I) complex which

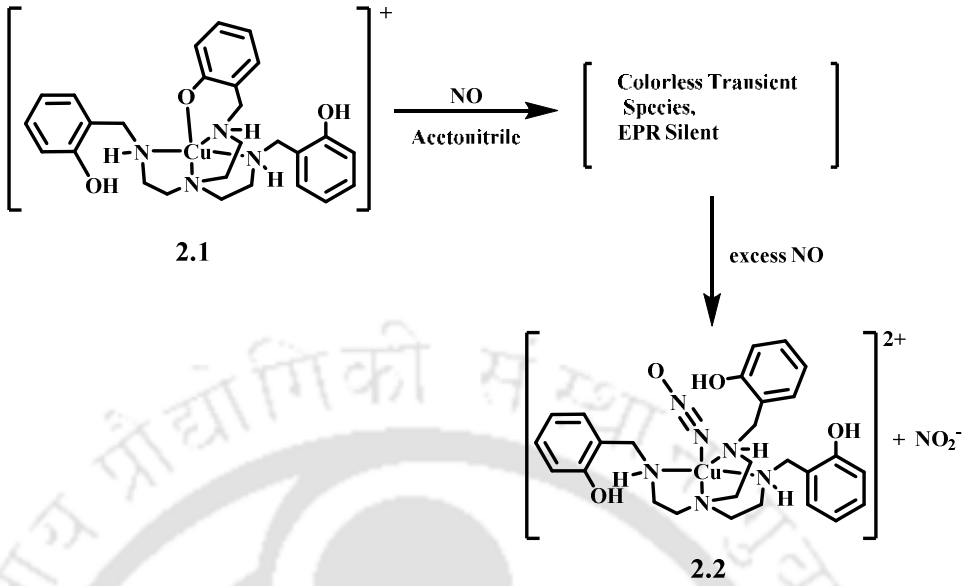

Scheme 1

formed in the reaction of complex **2.1** with NO. It was confirmed by adding equivalent amount of NO into a degassed acetonitrile solution of complex **2.1**. In UV-visible spectroscopy, the *d-d* band of complex **2.1** disappeared after adding stoichiometric amount of NO (Figure 2). In X-band EPR spectroscopy the frozen colorless solution found to be silent (Figure 3). This Cu(I) complex reacted further with excess NO to result in complex **2.2**. In acetonitrile solution it absorbed at 358 nm (ε/ $M^{-1}cm^{-}1$, 17550) and 575 nm (ε /$M^{-1}cm^{-}1$, 260). X-band EPR studies of the acetonitrile solution of complex **2.1** suggest the presence of mono-nuclear Cu(II) centre (Figure 3). In FT-IR spectroscopy of complex **2.2**, stretching frequencies at 2153 cm^{-1} and 1175 cm^{-1} were observed in addition to the others (Figure 4). These frequencies were isotope sensitive and found to appear at 2093 and 1163 cm^{-1}, respectively when the reaction was performed with ^{15}NO (Figure 4). The frequency at 2153 cm^{-1} is assigned to the N-N stretching and the 1175 cm^{-1} to N-O stretching of metal bound N_2O. In $[Ru(NH_3)_5(N_2O)]Br_2$, these frequencies were appeared at 2231 and 1157 cm^{-1}, respectively.[23] In case of only structurally characterized N_2O complex of vanadium,

the NNO stretching frequency appeared at 2289 cm^{-1} which was reported to shift to 2217 cm^{-1} upon ^{15}N labelling.[24] In the present case, the N-N stretching appeared at a lower frequency than those in reported compounds.[23,24]

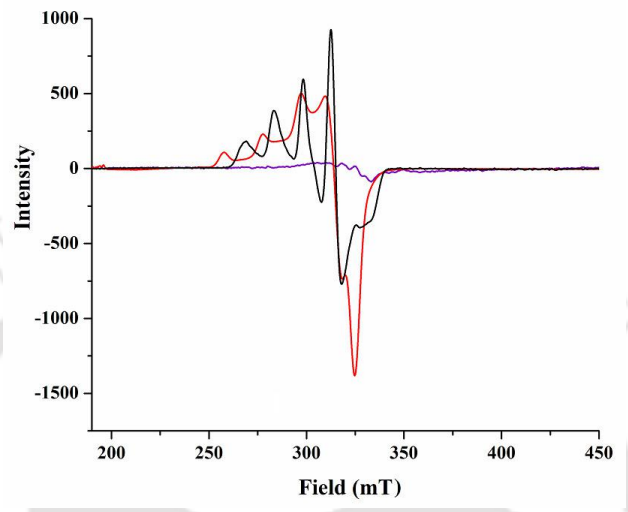

Figure 3 X-band EPR spectra of complex **2.1** (black), after adding stoichiometric amounts (violet) and excess of NO (red) in acetonitrile at 77 K.

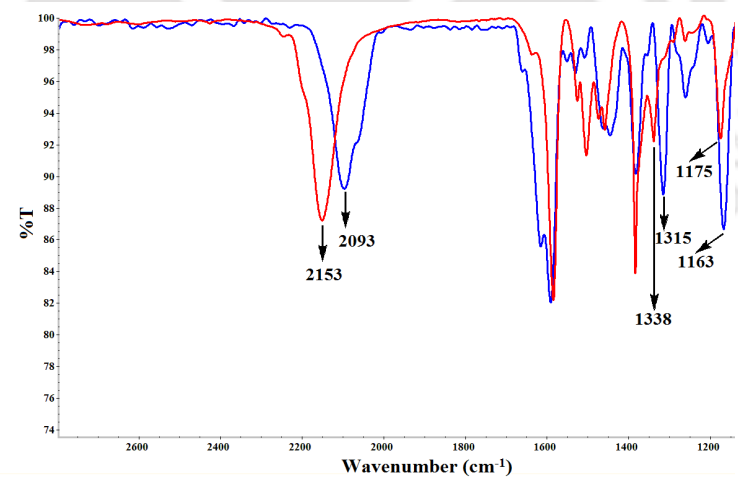

Figure 4 FT-IR spectra of complex **2.2** obtained in the reaction of ^{14}NO (red) and ^{15}NO (blue) with complex **2.1**, respectively, in KBr pellet.

Since X-ray quality crystals were not obtained, DFT calculations were performed to optimize the geometry of complex **2.2** and also to understand the Cu-N_2O bonding. DFT

calculations using Terbomol 7.0 were performed using TZVP basis set. Optimized geometry of complex **2.2** is shown in figure 5. The N_2O moiety is coordinated to the copper center from axial position of overall trigonal bipyramidal geometry. N_2O is bonded to copper through terminal N atom in a bent fashion. In case of $[Ru(NH_3)_5(N_2O)]^{2+}$, DFT calculation showed a linear binding mode of N_2O through terminal N atom.[23] In structurally characterized N_2O complex of vanadium also the N_2O was found to bind linearly.[24] The difference in bonding is also evident in the observed N_2O stretching frequency; which is higher in case of linear $[Ru(NH_3)_5(N_2O)]^{+}$ or vanadium complex compared to the bent [Cu(II)-(N_2O)] complex.

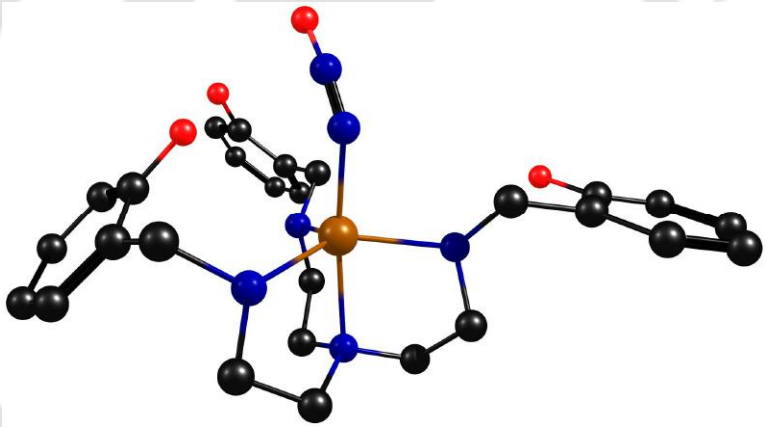

Figure 5 The DFT optimized structure of complex **2.2**. The color scheme is as follows: copper: reddish brown, carbon: black, oxygen: red, nitrogen: blue. The hydrogens have been removed for the purpose of clarity.

Further the formation of complex **2.2** was supported by the ESI mass spectrometry. The m/z ion peak at 285.50 (calculated: 285.61) indicates the existence of $[(L1H_3)Cu(N_2O)]^{2+}$ complex (Figure 6).

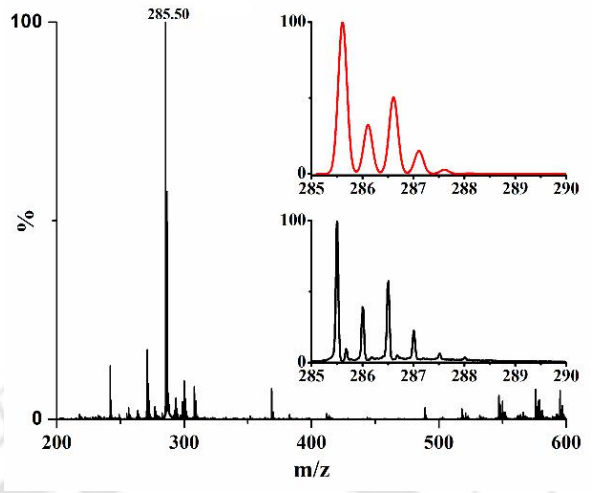

Figure 6 ESI-mass spectra of complex **2.2** in methanol. Inset shows the simulated (red) and experimental (black) isotopic distribution pattern.

Application of vacuum to the acetonitrile or methanol solution of complex **2.2**, stretching frequency at 2153 cm^{-1} was found to diminish. This suggests a weak bonding between the Cu(II) centre and N_2O ligand.

In metal complexes, oxygen atom transfer to triphenylphosphine (PPh_3) from N_2O was reported earlier. Addition of PPh_3 to the solution of complex **2.2** was monitored by solution FT-IR spectroscopy. The band at 2153 cm^{-1} was found to diminish upon addition of PPh_3. ^{31}P-NMR study of the reaction mixture indicates the presence of $OPPh_3$ which supports the oxo transfer from complex **2.2** to PPh_3. It is expected that in oxo transfer reaction, N_2 would be found. Attempts were not made to quantify this N_2.

The formation of N_2O from NO can be envisaged by considering the formation of an intermediate Cu(I)-nitrosyl complex followed by its reaction with excess of NO. This leads to the simultaneous formation of NO_2^- ion. The presence of stretching frequency at ~ 1338 cm^{-1} in the FT-IR spectrum suggests the formation of NO_2^-.

Chapter 3: Nitric oxide reactivty of Cu(II) complex of imidazole based ligand: Aromatic *C*-nitrosation and formation of *N*-nitrosohydroxylaminato complex

A Cu(II) complex, **3.1** of ligand **L2H** {**L2H**= 2-(*bis*(2-ethyl-5-methyl-1H-imidazol-4-yl) methyl)phenol} was synthesized from the reaction of equivalent amount of copper(II) acetate monohydrate and **L2H**. Single crystal structure of complex **3.1** revealed the presence of a diphenolato-bridged di-copper(II) system (Figure 7). It was further characterized by spectroscopic analyses.

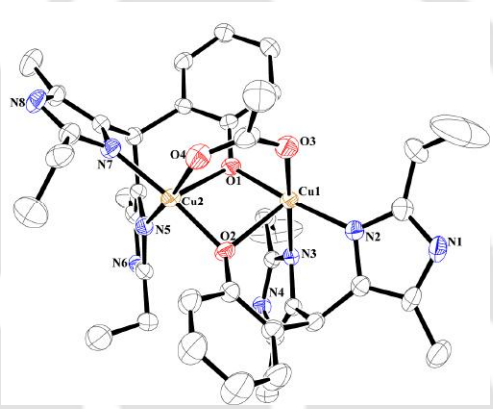

Figure 7 ORTEP diagram of complex **3.1** (30% thermal ellipsoid plot; H-atoms and counter anion are omitted for clearity).

Addition of excess NO to the degassed acetonitrile solution of complex **3.1** at room temperature resulted in the change of color to bluish green *via* the formation of a yellow intermediate. On keeping at room temperature, the bluish green solution afforded complexes **3.2** and **3.3** (Scheme 2). Complexes **3.2** and **3.3** were characterized by X-ray single crystal structure determination. The corresponding ORTEP diagrams are shown in figure 8.

In UV-visible spectroscopy, complex **3.1** in acetonitrile showed *d-d* band at 625 nm along with charge transfer transition at 405 nm. These bands disappeared immediately after

addition of NO (Figure 9a). In X-band EPR spectra, the characteristic signal of Cu(II) diminished (Figure 9b). These are attributed to the reduction of Cu(II) center to Cu(I) by NO.

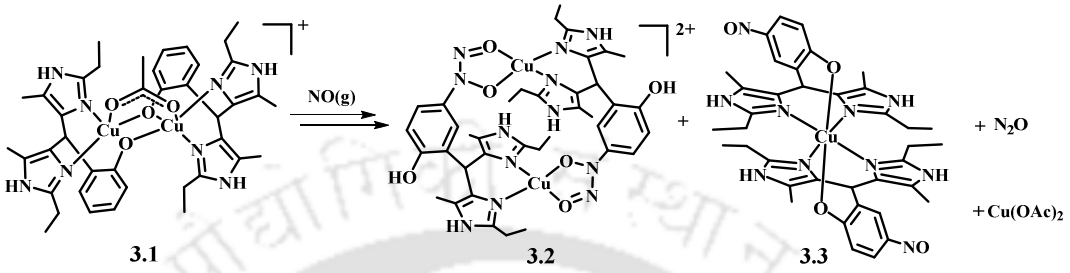

Scheme 2

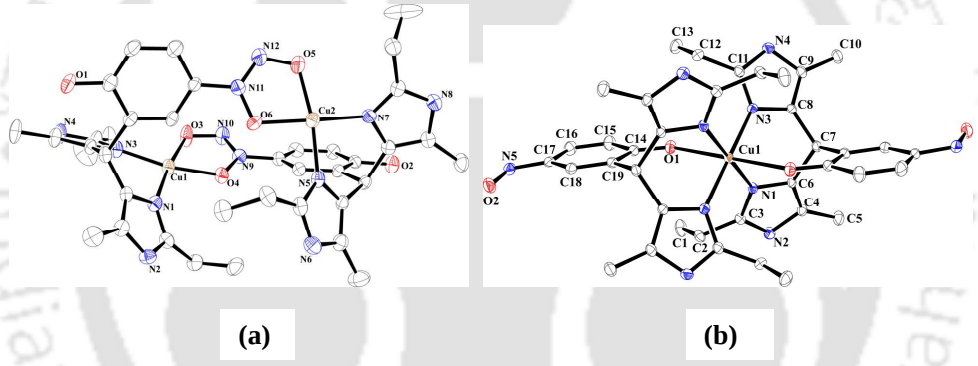

Figure 8 ORTEP diagram of complexes (a) **3.2** and (b) **3.3** (30% thermal ellipsoid plot, H-atoms are omitted for clarity).

Reduction of Cu(II) to Cu(I) resulted in formation of NO^+. This NO^+ is highly reactive and leads to *C*-nitrosation of the ligand (Scheme 2). A trace amount of methyl nitrite was formed in the reaction of methanol and NO^+. The modified *C*-nitroso ligand was isolated and characterized by spectral analyses. The intermediate Cu(I) complex of *C*-nitroso ligand was found to be unstable and undergo rapid oxidation to the corresponding Cu(II) complex. In FT-IR spectroscopy, a new peak at 1712 cm^{-1} assignable to the copper(I)-nitrosyl species was observed (Figure 9c). This reaction mixture upon standing overnight under NO atmosphere resulted in the oxidation of Cu(I) to Cu(II) by NO with simultaneous

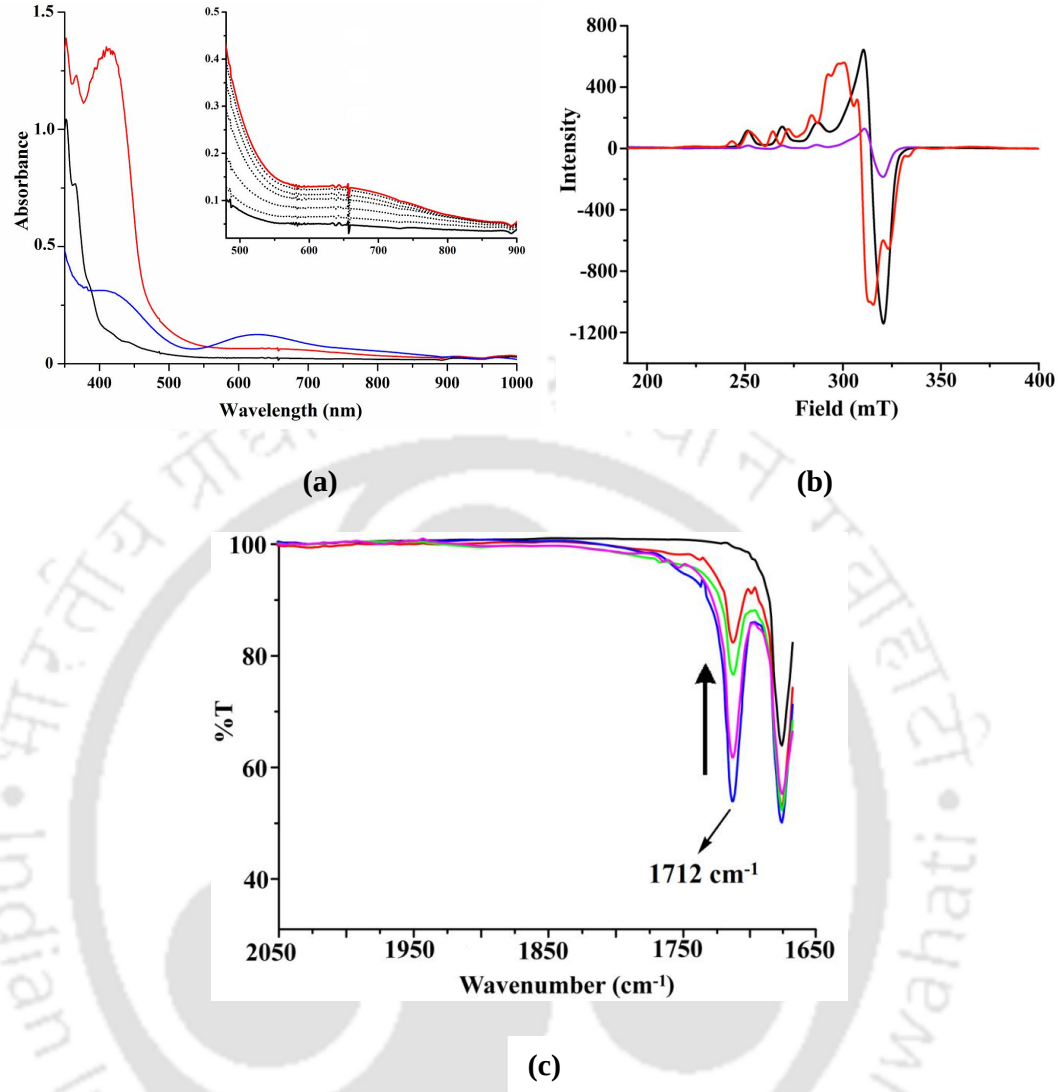

Figure 9 (a) UV-visible spectra of complex **3.1** (blue), after 1 minute (black) and 24 hours (red) of addition of NO in methanol and acetonitrile mixture (1:5, v/v). (b) X-band EPR spectra of complex **3.1** (black), after 1 minute (violet) and 24 hours (red) of addition of NO in methanol and acetonitrile mixture (1:5, v/v) at 77 K. (c) FT-IR spectra of complex **3.1** (black), and after addition of excess NO (blue to red) in methanol and acetonitrile mixture (1:5, v/v).

formation of C-ONNO$^-$. A competitive side reaction also afforded HNO which decomposed to N_2O and H_2O. N_2O was detected using GC-Mass analysis. This supports the low yield of complex **3.2** (40%) and formation of complex **3.3**.

Chapter 4: Effect of ligand denticity on the nitric oxide reactivity of Co(II) complexes

The NO reactivity of three Co(II) complexes, **4.1**, **4.2** and **4.3** with ligands **L3**, **L4** and **L5**, respectively, have been studied. The ligands were prepared by the general reaction of mesitylaldehyde with corresponding amine followed by the reduction of the imine with $NaBH_4$. Metallation was done by stirring the cobalt(II) chloride hexahydrate with required amount of the corresponding ligands in methanol. The complexes were characterized by spectral analyses and single crystal structure determination. The ORTEP diagrams of the complexes are given in figure 10.

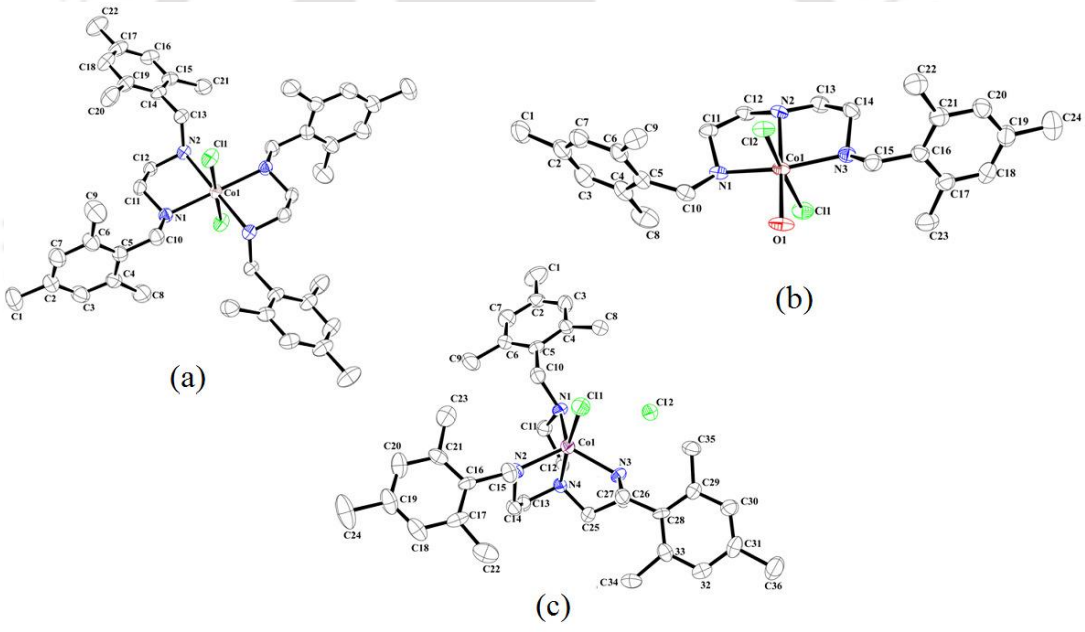

Figure 10 ORTEP diagrams of complexes (a) **4.1**, (b) **4.2** and (c) **4.3** (30% thermal ellipsoid plot, H-atoms are omitted for clarity).

Addition of NO into the dry and degassed methanol solution of complex **4.1** and allowing the mixture to stand for overnight resulted in the formation of complex **4.4a** as brown precipitate (Scheme 3). In FT-IR spectroscopy, complex **4.4a** showed NO stretching frequencies at 1862, 1782 cm^{-1} (Figure 11b) which are assignable to the $\{Co(NO)_2\}^{10}$ unit.

Spectral analyses confirmed the formation of the complex. However, the X-ray quality crystals were not obtained. To get X-ray quality crystals, the counter anion was replaced by perchlorate anion (**4.4b**). Single crystal structure of complex **4.4b** (Figure 12) revealed the presence of Co(I)-dinitronsyl, $\{Co(NO)_2\}^{10}$ moiety where Co(I) in tetrahedrally coordinated by two N-atoms from the ligand and two NO groups.

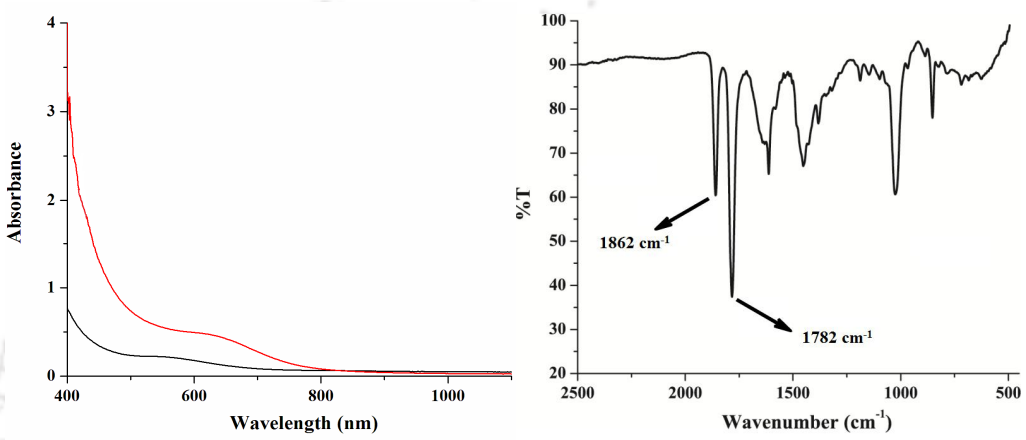

(a) **(b)**

Figure 11 (a) UV-visible spectra of complex **4.1** (black) and upon addition of excess NO (red) in methanol. (b) FT-IR spectrum of complex **4.4a** in KBr pellet.

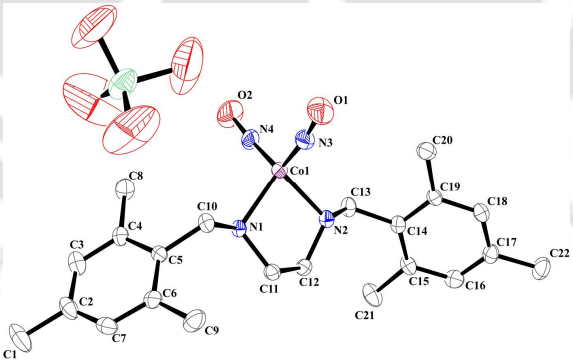

Figure 12 ORTEP diagram of complex **4.4b** (30% thermal ellipsoid plot, H-atoms are omitted for clarity).

In complex **4.1**, there were two **L3** units coordinated to the central metal. In complex **4.4b**, only one **L3** is present. Analyses of complex **4.4a** also support this formulation. When the solution part of the reaction mixture was analyzed, the presence of un-reacted **L3** and

dinitrosation product (**L3′**) were observed in roughly equal proportions. The dinitrosated product was isolated and purified using column chromatography and crystallographic characterization was done. The ORTEP diagram is shown in figure 13.

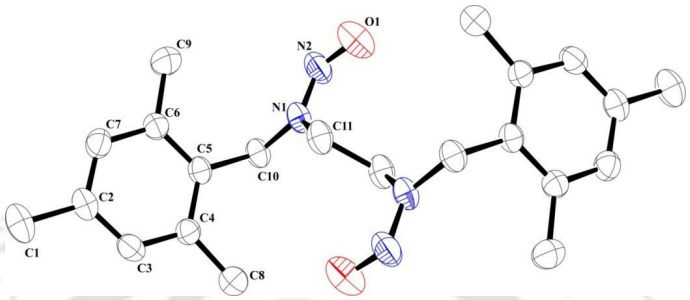

Figure 13 ORTEP diagram of modified ligand **L3′** (30% thermal ellipsoid plot, H-atoms are omitted for clarity).

On the other hand, addition of excess NO in the dry and degassed methanol solution of complex **4.2** led to the formation of complex **4.5** (Scheme 3). In UV-visible study, complexes **4.2** and **4.5** exhibited absorption at 525 nm (ε/ $M^{-1}cm^{-1}$, 300) and 475 nm (ε/ $M^{-1}cm^{-1}$, 521), respectively (Figure 14a). FT-IR spectrum of complex **4.5** in KBr pellet exhibited a strong stretching band at 1659 cm^{-1} assignable to the coordinated NO (Figure 14b). This low energy stretching band for metal-nitrosyl is consistent with Co(III)(NO^-) or $\{Co(NO)\}^8$ formulation. In EPR spectroscopy, complex **4.2** showed characteristic signals, whereas **4.5** was EPR silent. This is also suggesting the trivalency of the cobalt center and thus formally $Co^{III}(NO^-)$ or $\{Co(NO)\}^8$ descriptions. ESI-mass spectrum of complex **4.5** exhibited a molecular ion peak at m/z 491.17. In addition, complex **4.5** was structurally characterized by single-crystal X-ray crystallography. Figure 15 shows the ORTEP diagram of complex **4.5**. Complex **4.3**, in the similar reaction condition was not found to react with NO even after several days.

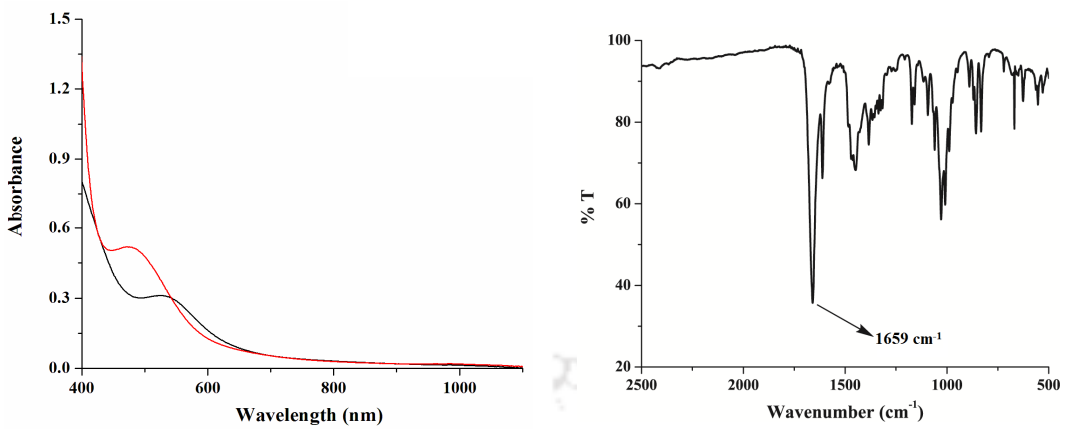

Figure 14 (a) UV-visible spectrum of complex **4.2** (black) and upon addition of excess NO (red) in methanol. (b) FT-IR spectrum of complex **4.5** in KBr pellet.

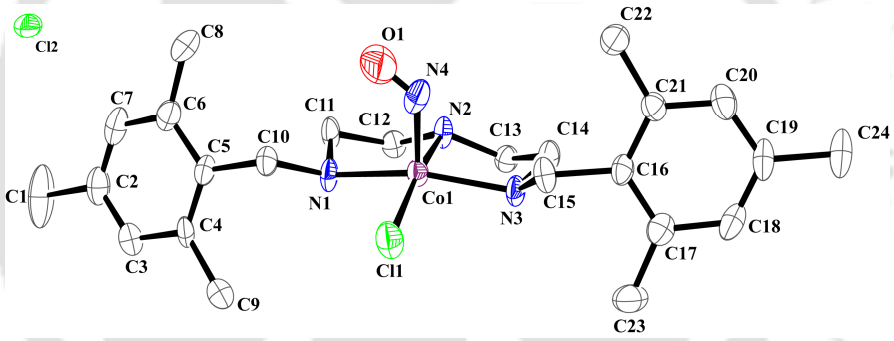

Figure 15 ORTEP diagram of complex **4.5** (30% thermal ellipsoid plot, H-atoms are omitted for clarity).

Thus, while moving from complexes **4.1** to **4.3**, the reactivity of the complexes towards NO changed. In case of complex **4.1**, reductive nitrosylation of the metal ion took place resulting in the corresponding Co(I)-dinitrosyl; while in **4.2**, addition of NO resulted in the formation of $[Co^{III}(NO^{-})]$ and complex **4.3** did not react with NO (Scheme 3). Hence, the ligand framework including denticity has a considerable effect on dictating the NO reactivity of a complex. In case of Co(II) complexes of tropocoronand ligands, it was

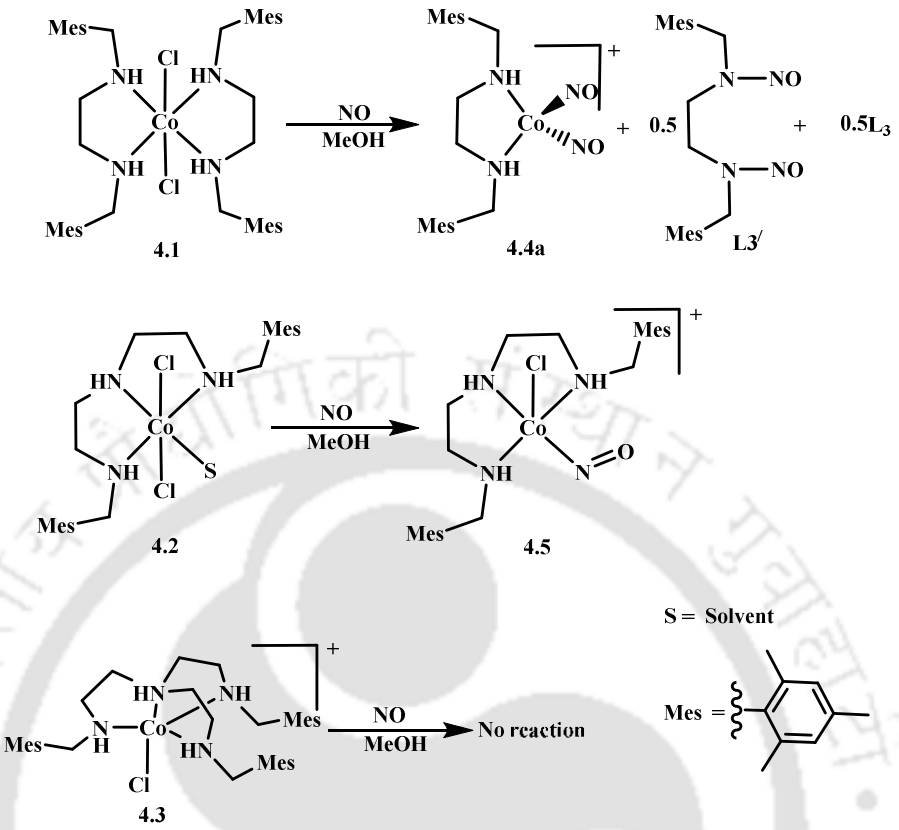

Scheme 3

reported that the ring size of the ligand controls the reactivity by controlling the tetrahedral character of the cobalt dinitrosyls over square planar one.[13] In case of complex **4.1**, the formation of tetrahedral $\{Co(NO)_2\}^{10}$ is favourable from the structural as well as redox potential point of views. In complexes **4.2** and **4.3**, the ligand frameworks do not prefer tetrahedral geometry as such.

Chapter 5: Reaction of a Co(II)-superoxo complex with nitric oxide: Formation of Co(III)-nitrite complex

In chapter 4, it has been observed that complex **4.3** did not react with NO. Addition of KO_2 to acetonitrile solution of complex **4.3** at -40 °C resulted in a dark green solution of complex **5.1** (Scheme 4). Complex **5.1** is stable for a couple of days at bellow 0 °C.

Addition of pre-cooled ether followed by keeping the mixture in freezer for 2 days afforded the precipitate of complex **5.1**.

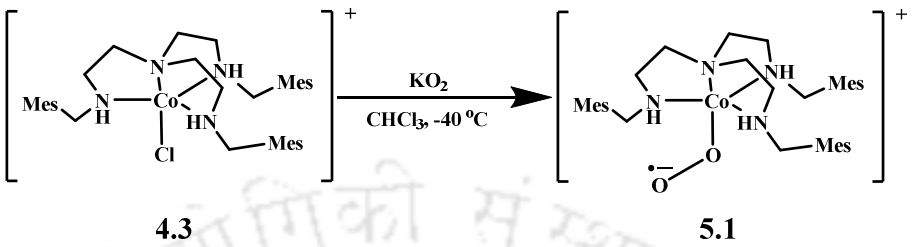

Scheme 4

ESI-mass spectrum of complex **5.1** displayed a peak at m/z = 633.51 which corresponds to the Co(II) superoxo complex. The isotopic distribution pattern also corresponds to the same. In FT-IR spectrum, a stretching frequency at 1067 cm^{-1} assignable to the metal bound superoxo species was observed. Upon addition of NO to the acetonitrile solution of complex **5.1** at -40 °C, the green solution changed to pink. It was found to decompose to afford complex **5.2** (Scheme 5).

UV-visible monitoring in acetonitrile solution, complex **4.3** absorbs at 480 and 590 nm (Figure 16). Upon addition of equivalent amount of KO_2, these bands disappeared with the formation of ~420 nm band corresponding to metal bound superoxide. In presence of NO, the absorption at 420 nm disappeared with the formation of new absorption centred at 560 nm. It was found to be unstable and gradually shifted to 545 nm. In FT-IR spectrum, the peak around 1067 cm^{-1} also disappeared after addition of NO. Isolation of the decomposition product revealed the formation of complex **5.2**. Analyses confirmed the formulation of **5.2** as the corresponding nitrite complex. It was characterized by X-ray structure determination, also. The perspective ORTEP view of the complex is given in figure 17. The formation of **5.2** suggests that the reaction proceeds *via* the formation of

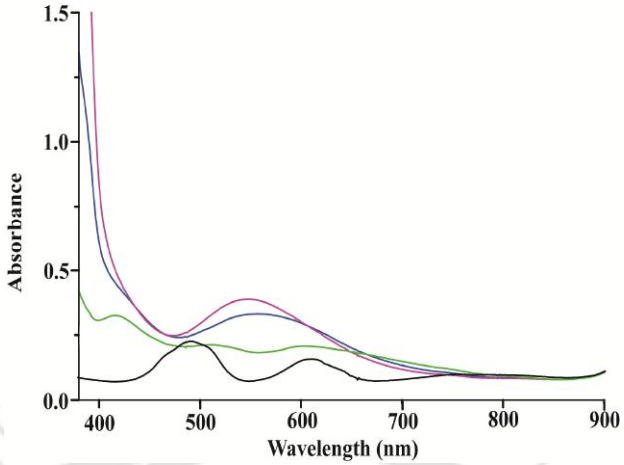

Figure 16 UV-visible spectra of complex **4.3** (black), upon addition of 1 equiv of KO_2 (green), after 1 minute (blue) and 30 minute (pink) of purging NO chloroform at -40 °C.

corresponding peroxynitrite intermediate. It was further supported by the characteristic oxidative dimerization reaction of 2,4-di-*tert*butylphenol to result in 2,2′-dihydroxy-3,3′,5,5′-tetra-*tert*-butylbiphenol (~35%).

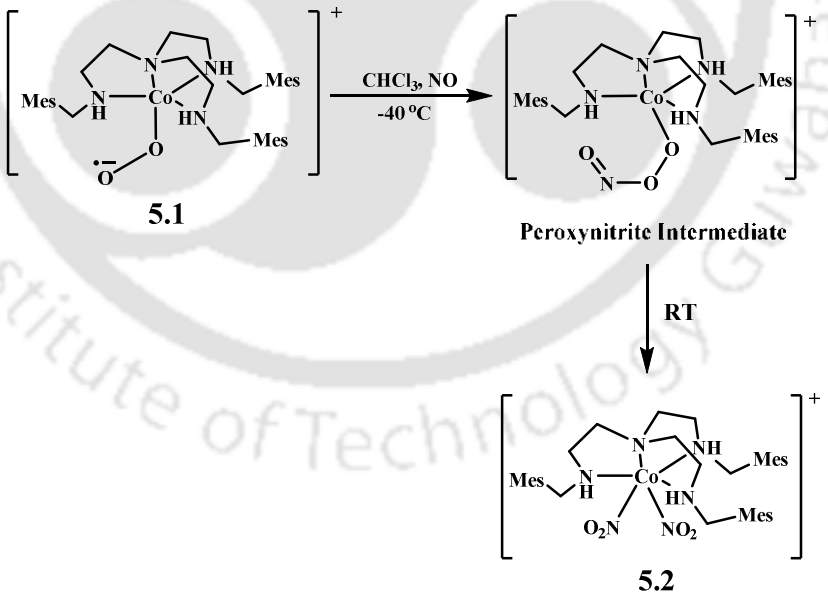

Scheme 5

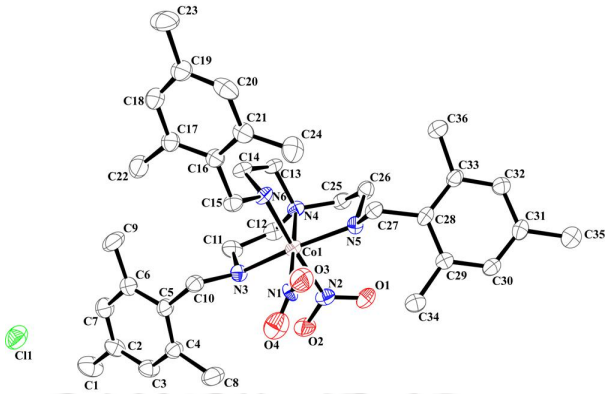

Figure 17 ORTEP diagram of complex **5.2**. (30% thermal ellipsoid plot, H-atoms are omitted for clarity).

References

(1) (a) Culotta, E.; Koshland, D. E. Jr. *Science* **1992**, *258*, 1862. (b) Moncada, S.; Palmer, R. M. J.; Higgs, E. A. *Pharmacol. Rev.* **1991**, *43*, 109.

(2) (a) Furchgott, R. F. *Angew. Chem. Int. Ed.* **1999**, *38*, 1870. (b) Ignarro, L. J.; Buga, G. M.; Wood, K. S.; Byrns, R. E.; Chaudhuri, G. *Proc. Natl. Acad. Sci. USA* **1987**, *84*, 9265. (c) Palmer, R. M. J.; Ferrige, A. G.; Moncada, S. *Nature* **1987**, *327*, 524.

(3) (a) Ignarro, L. J. *Nitric Oxide, Biology and Pathobiology* Ed. Academic Press, San Diego, CA, **2000**. (b) Richter-Addo, G. B.; Legzdins, P. *Metal Nitrosyls*, Oxford University Press, New York, **1992**. (c) Butler, A. R.; Williams, D. *Chem. Soc. Rev.* **1993**, 233. (d) Feelisch, M. Stamler, J. S. *Methods in Nitric Oxide Research* John Wiley and Sons, Chichester, England, **1996**. (e) Jia, L.; Bonaventura, C.; Bonaventura J.; Stamler, J. S. *Nature* **1996**, *380*, 221. (f) Hulse, C. L.; Averill, B. A.; Tiedje, J. M. *J. Am. Chem. Soc.* **1989**, *111*, 232.

(4) Kim, S.; Deinum, G.; Gardner, M. T.; Marletta, M. A.; Babcock, G. T. *J. Am. Chem. Soc.* **1996**, *118*, 8769.

(5) Burstyn, J. N.; Yu, A. E.; Dierks, E. A.; Hawkins, B. K.; Dawson, B. K. *Biochemistry* **1995**, *34*, 5896.

(6) Sarma, M.; Kalita, A.; Kumar, P.; Singh, A.; Mondal, B. *J. Am. Chem. Soc*. **2010**, *132*, 7846.

(7) Sarma, M.; Kumar, V.; Kalita, A.; Deka, R. C.; Mondal, B. *Dalton Trans*. **2012**, *41*, 9543.

(8) Kumar, P.; Kalita, A.; Mondal, B. *Dalton Trans*. **2011**, *40*, 8656.

(9) Fernandez, B. O.; Lim, M. D.; Ford, P. C. *Chem. Rev.* **2005**, *105*, 2439.

(10) Tran, D.; Ford, P. C. *Inorg. Chem*. **1996**, *35*, 2411.

(11) (a) Lim, M. H.; Lippard, S. J. *Acc. Chem. Res.* **2007**, *40*, 41. (b) Lim, M. H.; Lippard, S. J. *J. Am. Chem. Soc*. **2005**, *127*, 12170.

(12) (a) Gwost, D. G.; Caulton, K. G. *Inorg. Chem.* **1973**, *12*, 2095. (b) Gwost, D. G.; Caulton, K. G. *Inorg. Synth*. **1976**, *16*, 16.

(13) Kozhukh, J; Lippard, S. J. *J. Am. Chem. Soc*. **2012**, *134*, 11120.

(14) Scott, M. J.; Lippard, S. J. *J. Am. Chem. Soc*. **1997**, *119*, 341.

(15) Villacorta, G. M.; Lippard, S. J. *Pure Appl. Chem*. **1986**, *58*, 1474.

(16) Jaynes, B. S.; Doerrer, L. H.; Liu, S.; Lippard, S. J. *Inorg. Chem*. **1995**, *34*, 5735.

(17) Hilderbrand, S. A.; Lippard, S. J. *Inorg. Chem*. **2004**, *43*, 5294.

(18) Wiese, S.; Kapoor, P.; Williams, K. D.; Warren, T. H. *J. Am. Chem. Soc*. **2009**, *131*, 18105.

(19) Williams, K. D.; Cardenas, A. J. P.; Oliva, J. D.; Warren, T. H. *Eur. J. Inorg. Chem.* **2013**, 3812.

(20) Weiner, W. P.; Bergman, R. G. *J. Am. Chem. Soc*. **1983**, *105*, 3922.

(21) Wang, J.; Schopfer, M. P.; Sarjeant, A. A. N; Karlin, K. D. *J. Am. Chem. Soc*. **2009**, *131*, 450.

(22) Kumar, P.; Lee, Y. M.; Park, Y. J.; Siegler, M. A.; Karlin, K. D.; Nam, W. *J. Am. Chem. Soc*. **2015**, *137*, 4284.

(23) Paulat, F.; Kuschel, T.; Nather, C.; Praneeth, V. K. K.; Sander, O.; Lehnert, N. *Inorg. Chem*. **2004**, *43*, 6979.

(24) Piro, N. A.; Lichterman, M. F.; Harman, W. H.; Chang, C. J. *J. Am. Chem. Soc.* **2011**, *133*, 2180.

Chapter 1

Introduction

1.1 General aspect of nitric oxide

Nitric oxide (NO) is a neutral free radical gas molecule. It has attracted a considerable research interest since its discovery as a signalling molecule in cardiovascular system.[1,2] Later on, it has been found to play the key roles in vasodilatation, muscle contraction, apoptosis facilitation and neurotransmission.[3] Subsequently, a number of disease states have been identified involving NO imbalances and this has triggered an extensive research activity into the chemistry, biology, and pharmacology of NO.[1,4] Most of the roles played by NO in biology are attributed to the formation of nitrosyl complexes of the metallo-proteins, mostly iron or copper.[5] Hence, the binding and activation of NO with/by transition metal ions/complexes is a potential field of research. In this direction, iron, both in the protein and model systems, has been studied extensively. NO reactivity of copper and other first row transition metal ions and their complexes has been reported to some extent, though not as extensive as iron.[6]

In a metal complex, the character of the NO ligand can range from that of a nitrosyl cation (NO^+), which binds to the metal with an M-NO angle of ~180°, to that of a nitroxyl anion (NO^-), for which a bond angle of ~120° might be anticipated. The ability to form a stable NO complex and the structure of that species depend strongly on the oxidation state of the metal. NO has been found to interact reversibly with many metal complexes to form stable nitrosyls.[7] The binding in these complexes is similar to the coordination of dioxygen to such metal centres, although the nitrosyl products are far more stable and easy to characterize than are their superoxo analogues. For example, nitroprusside anion,

$[Fe(CN)_5(NO)]^{2-}$ is perhaps the earliest discovered nitrosyl complex, and it remains the subject of intense research efforts.[8-11]

Solomon and co-workers have studied the $\{Fe\text{-}NO\}^7$ coordination complexes such as [Fe(NO)(EDTA)] and $[Fe(L)(NO)(N_3)_2]$ (L= triazacyclononane and derivatives) in a great detail using diverse spectroscopic and analytical techniques. These studies revealed that the $\{Fe\text{-}NO\}^7$ complexes to be best described as a high-spin ferric ion (S = 5/2) antiferromagnetically coupled to NO^- (S = 1).[12-18] Borovik and co-workers reported a series of trigonal bipyramidal $\{Fe\text{-}NO\}^7$ complexes with tripodal ligands derived from *tris*-(carbamoylmethyl) amine. Spectral analyses suggest an electronic configuration of [Fe(III)-NO^-].[19,20] Examples of the diiron dinitrosyl complexes, $[Fe_2(\mu\text{-Et-HPTB})(\mu\text{-}O_2CPh)(NO)_2][BF_4]_2.3MeCN$ {Et-HPTB=N,N,N′,N′-*tetrakis*(N-ethyl-2-benzimidazolyl methyl)-2-hydroxy-1,3,diaminopropane} as a model for the binding of O_2 to non-heme iron proteins have been reported by the Lippard's group.[21] The iron nitrosyl complexes $[Fe(NO)X(CH_2CH_2SC_6H_4\text{-}o\text{-}S)_2]$ (X = NR, S) have also been cited as models for the active sites in nitrogenase enzymes.[22-24]

1.2 Nitric oxide reactivity of cobalt and copper complexes

In an early report, Caulton and co-workers, synthesized $[(TMEDA)Co(NO)_2][BPh_4]$ from the reaction of $CoCl_2$, two equivalents of tetramethylethylenediamine (TMEDA) and NO in dry methanol followed by addition of $NaBPh_4$.[25] Later on, this dinitrosyl was used for synthesis of other cobalt nitrosyl complexes.[26] Lippard's and Hayton's group extensively studied the formation of different type of metal nitrosyl with Fe, Co, Mn, and Ni metal.[27] Lippard and co-workers reported the formation of a β-diketiminate supported cobalt

dinitrosyl, (Ar_2nacnac) $Co(NO)_2$ complex which. Chemical reduction of this dinitrosyl afforded corresponding $\{Co(NO)_2\}^{11}$ system (Scheme 1.1).[28]

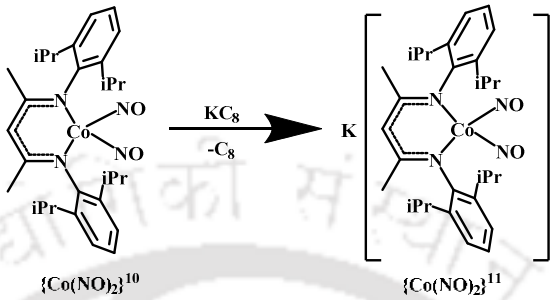

Scheme 1.1

Recently, they demonstrated the influence of tetraazamacrocyclic tropocoronand (TC) ligands on the NO reactivity of their Co(II) complexes. They reported that [Co(TC-3,3)], [Co(TC-4,4)] and [Co(TC-5,5)] reacts with excess NO to give mononitrosyl complexes which have been isolated and structurally characterized. On the other hand, [Co(TC-6,6)] upon reaction with NO, resulted in $\{Co(NO)_2\}^{10}$ species. This further decomposed to [$Co(NO_2)$(TC-6,6)] complex (Figure 1.1).[29]

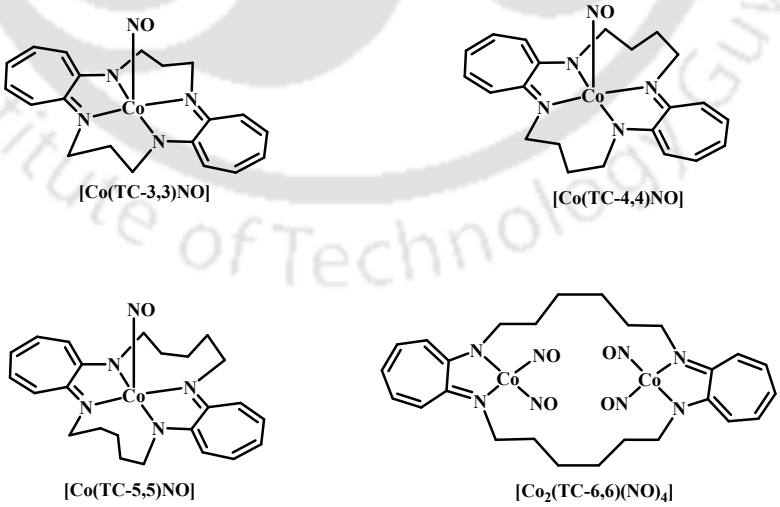

Figure 1.1 Some of structurally characterized cobalt nitrosyls.

Darensbourg and co-workers reported a series of cobalt nitrosyl complexes supported by a number of N_2S_2 ligands, including bme-daco (N,N′-*bis*(2-mercaptoethyl)-1,5 diazacyclooctane), bme*-daco (N,N′-*bis*(2-methyl-2-mercaptoethyl)-1,5-diazacyclo octane) and bme-dach (N,N′-*bis*(2-mercaptoethyl)-1,5-diazacycloheptane) (Scheme 1.2). These complexes exhibit a square pyramidal coordination environment and a $\{Co(NO)\}^8$ electronic configuration.[30]

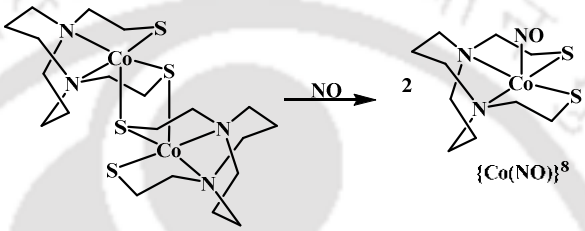

Scheme 1.2

The reactivity of NO with cobalt porphyrins is also well-studied.[31] One notable recent development was the detection of a series of six coordinate cobalt(nitrosyl) porphyrin complexes in the solid state by Kurtikyan and co-workers (Scheme 1.3). Low-temperature interaction of nitrogen base ligands with layered Co(TTP)(NO) {(TTP=meso-tetratolylporphyrinato dianion} as well as its toluene solution leads to the formation of the first six-coordinate species of the general formula (B)Co(TTP)(NO) (where B = piperidine and pyridine). The ν(NO) stretching bands of these species appear at lower frequencies compared with the five-coordinate nitrosyl derivative and depend on the nature of the trans axial ligand.[32]

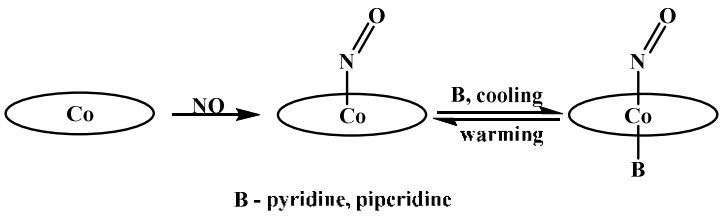

Scheme 1.3

Lippard and co-workers reported the formation of N-nitroso amine in dansyl substituted piperizine ligand of carboxylate bridged cobalt complexes. They observed reductive nitrosylation of cobalt centre to produce a carboxylate bridged cobalt dinitrosyl complex (Scheme 1.4).[33]

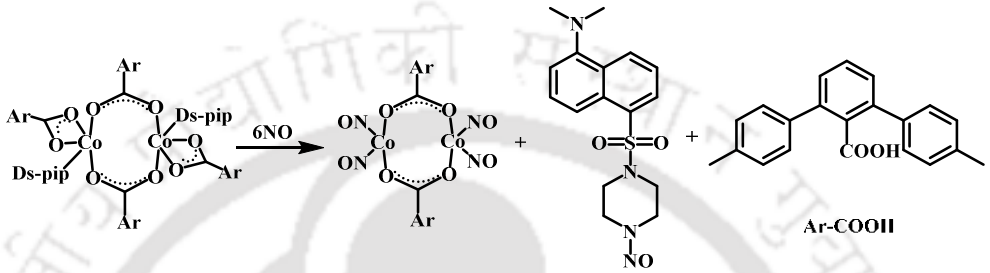

Scheme 1.4

Unlike cobalt nitrosyls, copper(II)-nitrosyls are rarely characterized. Several theoretical and matrix-isolation studies on copper(II)–nitrosyl complexes have been reported.[34-38] There have been a number of examples from our group which demonstrated that reduction of Cu(II) centre by NO proceeded through the unstable [Cu(II)-NO] intermediate and afforded N-nitrosation in the ligand frameworks. For example, copper(II) complex of *tris*-(2-isopropyl aminoethyl)amine on reaction with NO afforded reduction of Cu(II) centre with simultaneous tri-nitrosation of the ligand (Scheme 1.5).[39]

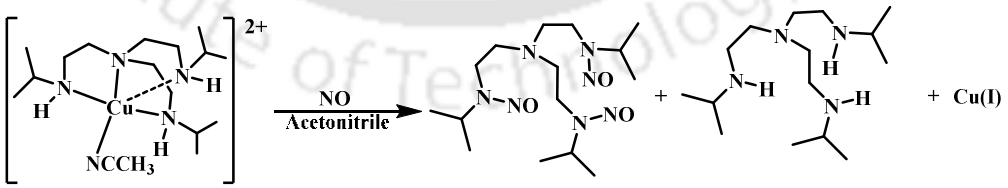

Scheme 1.5

Copper(II) complexes of ethylenediamine and its substituted derivatives react with NO to result in the reduction of Cu(II) and mono- and di -nitrosation of the ligand (Scheme 1.6).[40]

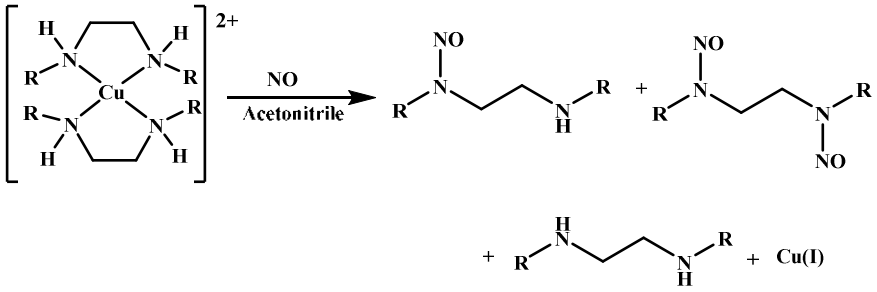

R = Methyl, ethyl and *iso*-butyl

Scheme 1.6

It has been found that N-bound nitrosyls are more stable than O-bound nitrosyls. Hayton and co-workers reported the isolation and structural characterization of a copper nitrosyl $[Cu(CH_3NO_2)_5(NO)][PF_6]_2$, with a $\{Cu(NO)\}^{10}$ configuration (Figure 1.2). Here, Cu-N-O angle is found to be 121.0(3)^o. This complex shows ν_{NO} at 1933 cm^{-1} in FT-IR spectrum in nujol. This complex was reported to react with mesitylene to form [mesitylene, NO][PF_6] and [Cu(η^2-1,3,5-$Me_3C_6H_3)_2$][PF_6] by transfer of NO^+ to the mesitylene ring.[41]

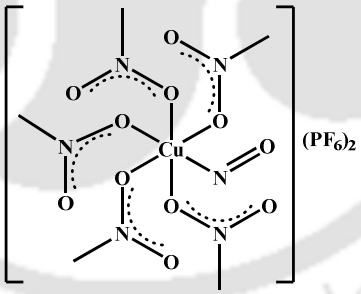

Figure 1.2 Example of structurally characterized copper(II) nitrosyl.

From our group, it is reported that addition of NO to Cu(II) complex of *bis*(2-ethyl-4-methyl-imidazole-5-yl)methane results in generation of corresponding [Cu(II)-NO], which can be isolated as a solid (Scheme 1.7). The product was characterized by elemental analysis, ESI-mass spectrometry, UV-visible, EPR, and IR spectroscopy. The complex is EPR silent and exhibits a low NO stretch (1662 cm^1). A DFT study predicts a $Cu^{II}(NO^{\bullet})$

electronic configuration for this complex, in which the NO moiety is bound to the equatorial plane of square pyramidal complex. This [Cu(II)-NO] species was found to react with H_2O_2 to resulted Cu(I)-NO_3 *via* formation of a unstable peroxynitrite intermediate.[42]

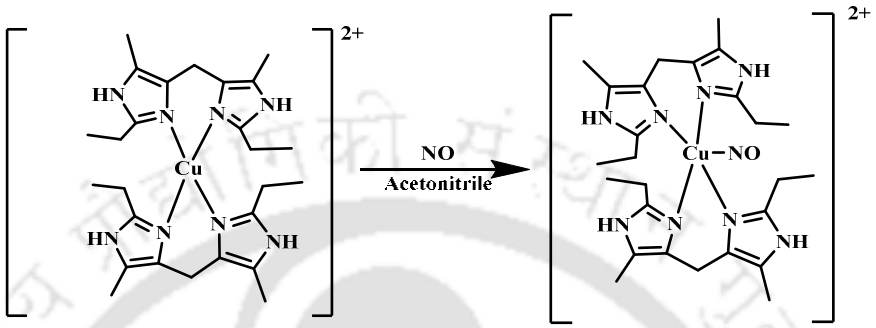

Scheme 1.7

In another report a stable Cu(II)-NO complex of histidine derived ligand {methyl (2-hydroxyphenyl)histidinate} was synthesized and characterized by various spectroscopic techniques. Addition of H_2O_2 to this complex at -20 ºC results in the reduction of Cu(II) centre and nitration of ligand *via* putative formation of peroxynitrite intermediate (Scheme 1.8).[43]

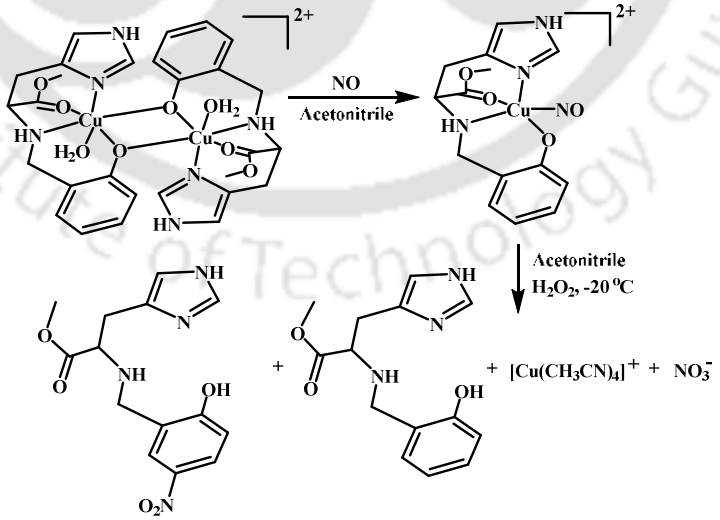

Scheme 1.8

1.3 Scope of the thesis

This thesis originates from our interest to study the redox reaction of NO assisted with transition metal complexes. Initial aim of the thesis was to synthesize stable metal–nitrosyl complexes and to study the redox reactivity of the coordinated nitrosyl. Since most of the roles played by NO in biological systems are attributed to the formation of nitrosyl complexes of the metallo-proteins, this work would have been helpful to understand the basic chemistry involved in biological reactions. To achieve those, the reactivity of Cu(II) complexes of N-donor ligands have been studied and described in second and third chapters of the thesis. In both the cases, initial attack of NO resulted in the reduction of Cu(II) centre to Cu(I) and the Cu(I) intermediate complex thus formed further reacts with excess NO to afford N_2O. In chapter 2, the N_2O moiety is found to bind with metal centre to give a stable nitrous oxide complex. DFT calculation suggests that N_2O binds to copper centre through nitrogen atom. It loses N_2O easily in solution indicating a weak binding of N_2O to the metal ion.

In chapter 3, NO reactivity of a copper complex of imidazole based ligand is studied. The reaction describes *c*-nitrosation of a ligand by NO with concomitant reduction of Cu(II) to Cu(I). The corresponding Cu(I) complex with *C*-nitrosylated ligand further reacts with NO to give Cu(I)-NO intermediate. This Cu(I)-NO intermediate reacts with another equivalent of NO to form N-nitrosohydroxylaminato complex or decomposes to Cu(II) complex of *c*-nitrosylated ligand and N_2O.

Since cobalt-nitrosyls having $\{CoNO\}^8$ configuration are known to be stable, the fourth chapter has been originated from our interest to develop stable $\{CoNO\}^8$ complex. It has been reported in literature that Co(II) centres react with different ways with NO. For

instance, in some cases, they undergo reductive nitrosylation; on the other hand, simple adduct formation is also known. In this connection, fourth chapter of this thesis describes a comparative account of the roles of ligand frameworks to control the NO reactivity of cobalt complexes. The fifth and final chapter describes the oxidation of NO in presence of a Co(II)- superoxo complex.

1.4 References

(1) (a) Culotta, E.; Koshland, D. E. Jr. *Science* **1992**, *258*, 1862. (b) Moncada, S.; Palmer, R. M. J.; Higgs, E. A. *Pharmacol. Rev.* **1991**, *43*, 109.

(2) (a) Furchgott, R. F. *Angew. Chern. Int. Ed.* **1999**, *38*, 1870. (b) Ignarro, L. J.; Buga, G. M.; Wood, K. S.; Byrns, R. E.; Chaudhuri, G. *Proc. Natl. Acad. Sci. U.S.A.* **1987**, *84*, 9265. (c) Palmer, R. M. J.; Ferrige, A. G.; Moncada, S. *Nature* **1987**, *327*, 524.

(3) (a) Ignarro, L. J. *Nitric Oxide, Biology and Pathobiology* Ed. Academic Press, San Diego, CA, **2000**. (b) Richter-Addo, G. B.; Legzdins, P. *Metal Nitrosyls* Oxford University Press, New York, **1992**. (c) Bredt, D. S.; Snyder, S. H. *Annu Rev. Biochem.* **1994**, *63*, 175. (d) Butler, A. R.; Williams, D. *Chem. Soc. Rev.* **1993**, 233. (e) Feelisch, M.; Stamler, J. S. *Methods in Nitric Oxide Research*, John Wiley and Sons, Chichester, England, **1996**. (f) Jia, L.; Bonaventura, C.; Bonaventura J.; Stamler, J. S. *Nature* **1996**, *380*, 221. (g) Hulse, C. L.; Averill, B. A.; Tiedje, J. M. *J. Am. Chem. Soc.* **1989**, *111*, 232.

(4) Fang, F. C. *Nitric Oxide and Infection* Ed. Kluwer Academic/ Plenum Publishers, New York, **1999**.

(5) (a) Kim, S.; Deinum, G.; Gardner, M. T.; Marletta, M. A.; Babcock, G. T. *J. Am. Chem. Soc.* **1996**, *118*, 8769 and references therein. (b) Burstyn, J. N.; Yu, A. E.; Dierks, E. A.; Hawkins, B. K.; Dawson, J. H. *Biochemistry* **1995**, *34*, 5896.

(6) Li, L.; Li, L. *Coord. Chem. Rev*. **2016**, *306*, 678.

(7) (a) Franz, K. J.; Lippard, S. J. *J. Am. Chem. Soc.* **1999**, *121*, 10504. (b) Inoue, H.; Narino, S.; Yoshioka, N.; Fluck, E. *Z. Naturforsch., B: Chem. Sci.* **2000**, *55*, 685.

(8) Haskin, C. J.; Ravi, N.; Lynch, J. B.; Munck, E.; Que, L. Jr. *Biochemistry* **1995**, *34*, 11090.

(9) Estrin, D. A.; Baraldo, L. M.; Slep, L. D.; Barja, B. C.; Olabe, J. A.; Paglieri, L.; Corongiu, G. *Inorg. Chem.* **1996**, *35*, 3897.

(10) Nikol'skii, A. B.; Kotov, V. Y.; Vitalii, Y. *Mendeleev Commun.* **1995**, *4*, 139.

(11) Gomez, J. A.; Guenzburger, D. *Chem. Phys.* **2000**, *253*, 73.

(12) Brown, C. A.; Pavlosky, M. A.; Westre, T. E.; Zhang, Y.; Hedman, B.; Hodgson, K. O.; Solomon, E. I. *J. Am. Chem. Soc.* **1995**, *117*, 715.

(13) Westre, T. E.; Dicicco, A.; Filipponi, A.; Natoli, C. R.; Hedman, B.; Solomon, E. I.; Hodgson, K. O. *J. Am. Chem. Soc.* **1994**, *116*, 6757.

(14) Westre, T. E.; Di Cicco, A.; Filipponi, A.; Natoli, C. R.; Hedman, B.; Solomon, E. I.; Hodgson, K. O. *Physica B* **1995**, *208/209*, 137.

(15) Zhang, Y.; Pavlosky, M. A.; Brown, C. A.; Westre, T. E.; Hedman, B.; Hodgson, K. O.; Solomon, E. I. *J. Am. Chem. Soc.* **1992**, *114*, 9189.

(16) Farrar, J. A.; Grinter, R.; Pountney, D. L.; Thomson, A. J. *J. Chem. Soc., Dalton Trans.* **1993**, 2703.

(17) Hauser, C.; Glaser, T.; Bill, E.; Weyhermuller, T.; Wieghardt, K. *J. Am. Chem. Soc.* **2000**, *122*, 4352.

(18) Marlin, D.; Mascharak, P. *Chemtracts* **2000**, *13*, 539.

(19) Hammes, B. S.; Ramos-Maldonado, D.; Yap, G. P. A.; Liable-Sands, L.; Rheingold, A. L.; Young, V. G.; Borovik, A. S. *Inorg. Chem.* **1997**, *36*, 3210.

(20) Ray, M.; Golombek, A. P.; Hendrich, M. P.; Yap, G. P. A.; Liable-Sands, L. M.; Rheingold, A. L.; Borovik, A. S. *Inorg. Chem.* **1999**, *38*, 3110.

(21) Feig, A. L.; Bautista, M. T.; Lippard, S. J. *Inorg. Chem.* **1996**, *35*, 6892.

(22) Sellmann, D.; Becker, T.; Hofmann, T.; Knoch, F.; Moll, M. *Inorg. Chim. Acta* **1994**, *219*, 75.

(23) Sellmann, D.; Hohn, K.; Moll, M. *Z. Naturforsch., B: Chem. Sci.* **1991**, *46*, 665.

(24) Sellmann, D.; Hohn, K.; Moll, M. *Z. Naturforsch., B: Chem. Sci.* **1991**, *46*, 673.

(25) (a) Gwost, D. G.; Caulton, K. G. *Inorg. Chem.* **1973**, *12*, 2095. (b) Gwost, D. G.; Caulton, K. G. *Inorg. Synth*. **1976**, *16*, 16.

(26) Tomson, N. C.; Crimmin, M. R.; Petrenko, T.; Rosebrugh, L. E.; Sproules, S.; Boyd, W. C.; Bergman, R. G.; DeBeer, S.; Toste, F. D.; Wieghardt, K. *J. Am. Chem. Soc.* **2011**, *133*, 18785.

(27) (a) Franz, K. J.; Lippard, S. J. *Inorg. Chem.* **2000**, *39*, 3722. (b) Franz, K. J.; Doerrer, L. H.; Spingler, B.; Lippard, S. J. *Inorg. Chem.* **2001**, *40*, 3774. (c) Franz, K. J.; Singh, N.; Lippard, S. J. *Angew. Chem. Int. Ed.* **2000**, *39*, 2120. (d) Wright, A. M.; Wu, G.; Hayton, T. W. *J. Am. Chem. Soc.* **2012**, *134*, 9930. (e) Wright, A. M.; Zaman, H. T.; Wu, G.; Hayton, T. W. *Inorg. Chem.* **2014**, *53*, 3108.

(28) Tonzetich, Z. J.; Heroguel, F.; Do, L. H.; Lippard, S. J. *Inorg. Chem.* **2011**, *50*, 1570.

(29) (a) Kozhukh, J; Lippard, S. J. *J. Am. Chem. Soc.* **2012**, *134*, 11120. (b) Scott, M. J.; Lippard, S. J. *J. Am. Chem. Soc*. **1997**, *119*, 341. (c) Villacorta, G. M.; Lippard,

S. J. *Pure Appl. Chem*. **1986**, *58*, 1474. (d) Jaynes, B. S.; Doerrer, L. H.; Liu, S.; Lippard, S. J. *Inorg. Chem*. **1995**, *34*, 5735.

(30) Chiang, C.-Y.; Lee, J.; Dalrymple, C.; Sarahan, M. C.; Reibenspies, J. H.; Darensbourg, M. Y. *Inorg. Chem.* **2005**, *44*, 9007.

(31) (a) Richter-Addo, G. B.; Hodge, S. J.; Yi, G.-B.; Khan, M. A.; Ma, T.; Van Caemelbecke, E.; Guo, N.; Kadish, K. M. *Inorg. Chem*. **1996**, *35*, 6530. (b) Cheng, S.-H.; Su, Y. O. *Inorg. Chem*. **1994**, *33*, 5847. (c) Tsuji, K.; Imaizumi, M.; Oyoshi, A.; Mochida, I.; Fujitsu, H.; Takeshita, K. *Inorg. Chem.* **1982**, *21*, 721. (d) Mochida, I.; Suetsugu, K.; Fujitsu, H.; Takeshita, K. *J. Chem. Soc. Chem. Commun*. **1982**, 166.

(32) Kurtikyan, T. S.; Markaryan, E. R.; Mardyukov, A. N.; Goodwin, J. A. *Inorg. Chem.* **2007**, *46*, 1526.

(33) Hilderbrand, S. A.; Lippard, S. J. *Inorg. Chem*. **2004**, *43*, 5294.

(34) Zhou, M. F.; Andrews, L. *J. Phys. Chem. A* **2000**, *104*, 2618.

(35) Dobos, S.; Cesaro, S. N. *High Temp. Mater. Sci.* **1997**, *37*, 81.

(36) Spoto, G.; Bordiga, S.; Scarano, D.; Zecchina, A. *Catal. Lett.* **1992**, *13*, 39.

(37) Spoto, G.; Zecchina, A.; Bordiga, S.; Ricchiardi, G.; Martra, G.; Leofanti, G.; Petrini, G. *Appl. Catal., B* **1994**, *3*, 151.

(38) Kohlschutter, V.; Kutscheroff, M. *Chem. Ber.* **1904**, *37*, 3044.

(39) Sarma, M.; Kalita, A.; Kumar, P.; Singh, A.; Mondal, B. *J. Am. Chem. Soc*. **2010**, *132*, 7846.

(40) Sarma, M.; Mondal, B. *Dalton Trans*. **2012**, *41*, 2927.

(41) Wright, A. M.; Wu, G.; Hayton, T. W. *J. Am. Chem. Soc*. **2010**, *132*, 14336.

(42) Kalita, A.; Kumar, P.; Deka, R. C.; Mondal, B. *Chem. Commun*. **2012**, *48*, 1251.

(43) Kalita, A.; Deka, R. C.; Mondal, B. *Inorg. Chem.* **2013**, *52*, 10897.

Chapter 2

Nitric oxide reactivity of Cu(II) complex of N- donor ligand: Formation of a stable nitrous oxide complex

Abstract

A Cu(II) complex, **2.1** of ligand **L1H$_3$** {**L1H$_3$** = 2,2',2''-(((nitrilo-*tris*(ethane-2,1-diyl))*tris*(azanediyl))*tris*(methylene)) triphenol}, was synthesized and characterized structurally. Addition of excess nitric oxide to the degassed acetonitrile solution of complex **2.1** at room temperature resulted in a transient colorless species followed by a deep bluish green solution. This solution afforded a dark precipitate of complex **2.2** when allowed to stand at room temperature for 3 hours. Complex **2.2** was characterized as stable [Cu(II)-N_2O] complex of the ligand **L1H$_3$**. Spectroscopic and analytical techniques confirmed the formulation of **2.2** unambiguously. DFT studies suggest that N_2O is bonded to the Cu(II) centre through terminal N atom in with Cu-N-N angle of 135.2º.

2.1 Introduction

Nitrous oxide (N_2O) is a potential greenhouse gas and is involved in the depletion of stratospheric ozone.[1] The N_2O level in the atmosphere is primarily modulated by the biological nitrification and denitrification processes involving metalloenzymes.[2] For example, nitrous oxide reductase (N_2OR), a copper containing enzyme, catalyses the reduction of N_2O to N_2 [equation 2.1][2,3].

$$N_2O + 2H^+ + 2e^- \longrightarrow N_2 + H_2O \qquad (2.1)$$

These metalloenzyme promoted processes have triggered a wide range of research including the binding and reactivity of N_2O with transition metal ions. For instance, a set of Cu-ZSM-5 material has been developed where N_2O decomposes to N_2.[4] However, N_2O is known to be a poor ligand because of its low dipole moment as well as weak σ- donor and π- acceptor properties.[5] Despite intense interest in transition metal mediated N_2O activation, only a very limited number of examples of metal complexes containing the N_2O ligand have been identified since the report of $[Ru(NH_3)_5(N_2O)]^{2+}$ and $[\{Ru(NH_3)_5\}_2(\mu\text{-}N_2O)]^{4+}$ by Taube.[6] Initially, $[Ru(NH_3)_5(N_2O)]^{2+}$ was characterized in solution; but it was isolated later as a solid with different counter anions (*i.e.* Cl^-, Br^-, BF_4^- etc.).[7] James *et al.* reported an *in situ* synthesis and NMR spectroscopic characterization of the $Ru^{II}(N_2O)$ complex, $[RuCl_2(\eta^1\text{-}N_2O)(P{-}N)(PPh_3)]$ {P−N = [*o*-(*N*,*N*-Dimethylamino)phenyl]diphenyl phosphine}.[8] However, none of these was characterized structurally. All other attempts to isolate N_2O complexes of other transition metal ions resulted in the corresponding metal oxide, nitride or nitrosyls.[9] Recently, Chang *et al.* reported the single crystal X-ray structure of the metal-N_2O complex, $[(tpa^{Mes})V(N_2O)]$ {tpa^{Mes} = *tris*-mesityl pyrrolide} in a vanadium-pyrrolide system.[10] Zhou *et al.* reported the

synthesis of [ClCu(N_2O)] trapped in solid argon by co-deposition of laser-evaporated metal chlorides with N_2O in excess argon.[11] However, till date, there is not even a single example of a stable N_2O complex of copper in any oxidation state that is known in literature.

This chapter describes the formation of a Cu(II)-N_2O complex which has been isolated as solid. Even after many efforts we could not get the X-ray quality crystal of the complex **2.2**. However other spectral analyses and physical measurements establish the formation of the complex unambiguously.

2.2 Results and Discussion

The ligand, $\mathbf{L1H_3}$ ($\mathbf{L1H_3}$ = 2,2',2''-(((nitrilo-*tris*-(ethane-2,1-diyl))-*tris*-(azanediyl))-*tris*-(methylene)) triphenol) was prepared by treating *tris*-(2-aminoethyl)amine with 3 equivalents of salicylaldehyde in ethanol solution followed by the reduction of the corresponding imine with sodium borohydride (Experimental Section). Microanalysis, FT-IR, ^{1}H and ^{13}C NMR and mass spectral analyses confirmed the formation of the ligand (Experimental Section). Complex **2.1** was prepared by the reaction of copper(II) perchlorate hexahydrate with an equivalent amount of ligand in methanol (Scheme 2.1; Experimental Section). Spectroscopic analyses as well as a X-ray single crystal structure determination confirmed the formation of the mono-nuclear complex **2.1**, [($L1H_2$)Cu](ClO_4) (Experimental Section). The ORTEP view of complex **2.1** is shown in Figure **2.1**. The list of crystallographic data is given in table 2.1. The structure revealed that the Cu(II) ion is surrounded by four N-atoms and one phenolato-O atom from the $\mathbf{L1H_2^-}$ moiety in a trigonal bipyramidal geometry. The calculated structural parameter, τ (0.88), also suggests the existence of a trigonal bipyramidal geometry.

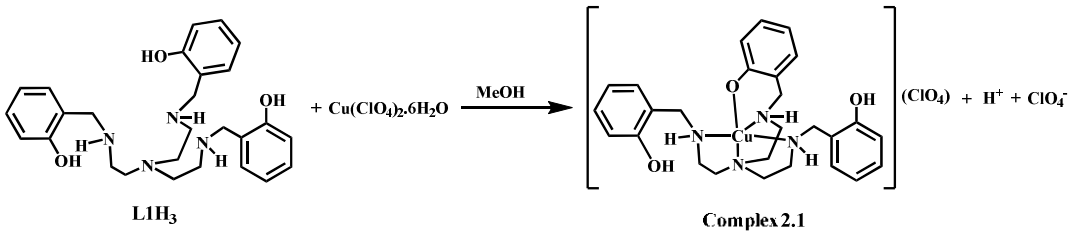

Scheme 2.1

In UV-visible spectroscopy, the acetonitrile solution of complex **2.1** displayed an absorption centered at 670 nm (ε, 168 $M^{-1}cm^{-1}$) and 430 nm (ε, 722 $M^{-1}cm^{-1}$) along with other intra-ligand transitions in the lower wavelengths (Appendix I and figure 2.2). The absorption band at 670 nm is assignable to a *d-d* transition and the 430 nm band is attributed to the phenolate→Cu(II) charge transfer.[12] Complex **2.1** in the acetonitrile at 77 K showed the characteristic signal for a Cu(II) ion in the trigonal bipyramidal geometry in the X-band EPR spectroscopy.[13] The observed parameters are $g_{\parallel}$, 2.30, $g_{\perp}$, 2.08 and $A_{\parallel}$, 156.5 × 10^{-4} cm^{-1} (Appendix I).

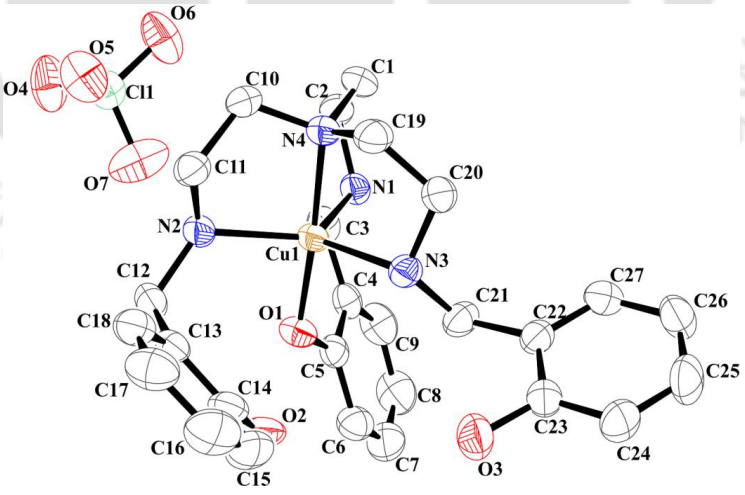

Figure 2.1 ORTEP diagram of complex **2.1** (30% thermal ellipsoid plot, H-atoms are omitted for clarity).

Table 2.1 Crystallographic data table for complex **2.1**.

	2.1
Formulae	C_{27} H_{35} Cl_1 Cu_1 N_4 O_7
Mol. wt.	626.58
Crystal system	Orthorhombic
Space group	Pbca
Temperature /K	293(2)
Wavelength /Å	0.71073
a /Å	10.9282(3)
b /Å	16.9760(4)
c /Å	30.7783(6)
α/°	90
β/°	90
γ/°	90
V/ $Å^3$	5709.9(2)
Z	8
Density/Mgm^{-3}	1.458
Abs. Coeff. /mm^{-1}	0.910
Abs. correction	None
F(000)	2616.0
Total no. of reflections	5163
Reflections, $I > 2\sigma(I)$	4304
Max. 2θ/°	25.25
Ranges (h, k, l)	$-13 \leq h \leq 10$ $-21 \leq k \leq 20$ $-29 \leq l \leq 38$
Complete to 2θ (%)	99.8
Refinement method	Full-matrix least-squares on F^2
Goof (F^2)	1.119
R indices [$I > 2\sigma(I)$]	0.0375
R indices (all data)	0.0479

Nitric oxide reactivity

Addition of excess $NO_{(g)}$ to the degassed acetonitrile solution of complex **2.1** at room temperature resulted in a transient colorless species followed by a deep bluish green solution (Scheme 2.2). Upon keeping the solution at room temperature for 3 h,

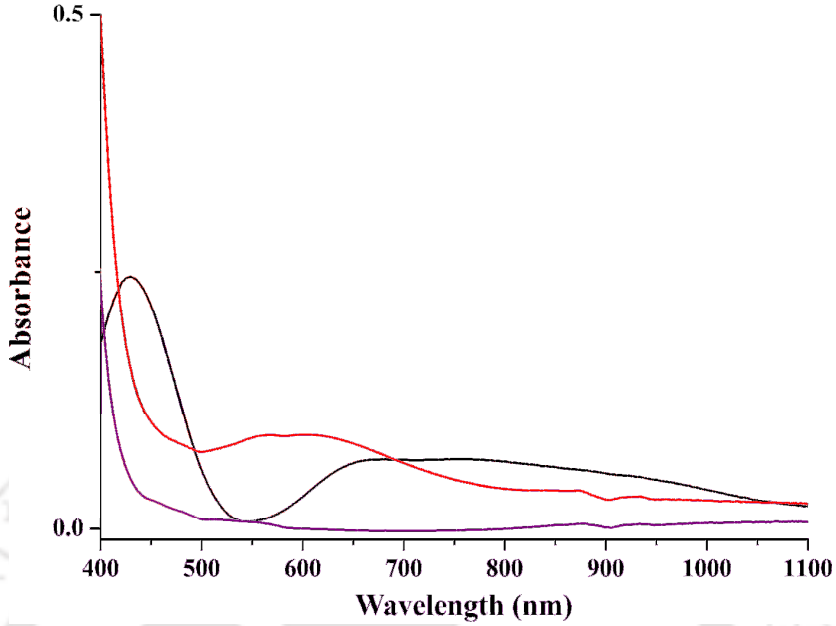

Figure 2.2 UV-visible spectra of complex **2.1** (black), after addition of stoichiometric amount (violet) and excess (red) of NO(g) in acetonitrile solution at room temperature.

dark brown precipitate of complex **2.2** was obtained (Scheme 2.2). It is to be noted that addition of an equivalent amount of $NO_{(g)}$ into a degassed acetonitrile solution of complex **2.1** resulted in the same colorless species. In the UV-visible spectrum, the *d-d* band of complex **2.1** disappeared after the addition of a stoichiometric amount of $NO_{(g)}$ (Figure 2.2).[13] The reaction mixture was found to be EPR silent at 77 K (Figure 2.3).[13] Furthermore, it displayed well resolved signals in the ^{1}H-NMR

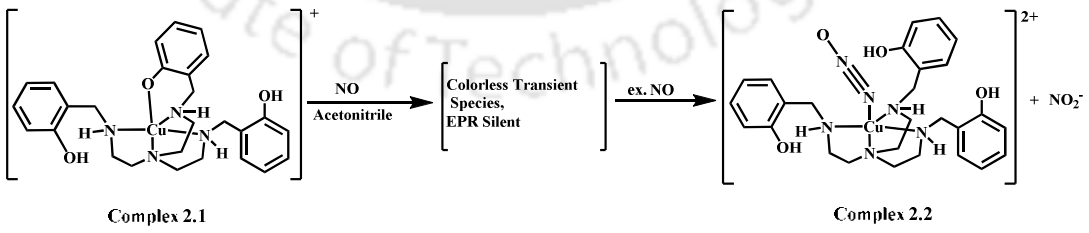

Scheme 2.2

spectrum (Appendix I). In addition, when the reaction was carried out in the presence of a drop of methanol, GC-Mass analyses of the reaction mixture revealed the formation of methylnitrite ($MeNO_2$) (Equation 2.2). Thus the spectral studies suggest the reduction of the Cu(II) center by NO.[13]

$$[(L1H_2)Cu^{II}](ClO_4) + NO + CH_3OH \longrightarrow [(L1H_3)Cu^{I}](ClO_4) + CH_3NO_2 \text{ ----- } (2.2)$$

When this solution was stored in a freezer under an argon atmosphere for 10-12 days, $[Cu(CH_3CN)_4](ClO_4)$ was crystallized out and unreacted ligand was isolated almost quantitatively (Appendix I). This is attributed to the higher thermodynamic stability of $[Cu(CH_3CN)_4](ClO_4)$ compared to $[(L1H_3)Cu^{I}](ClO_4)$ (Equation 2.2).[13a] However, air and moisture sensitivity of the colorless solution precluded its isolation and characterization as a solid. Thus, the colorless species is presumably the corresponding Cu(I) complex which is formed in the reaction of the complex **2.1** with NO (Equation 2.2).

This Cu(I) intermediate reacted further with excess $NO_{(g)}$ to result in complex **2.2**. The acetonitrile solution of complex **2.2** displayed absorption at 358 nm (ε, 17,550 $M^{-1}cm^{-1}$) and 575 nm (ε, 260 $M^{-1}cm^{-1}$) (Appendix I). The phenolate→Cu^{II} charge transfer band of complex **2.1** disappeared in complex **2.2**. This is attributed to the fact that the phenolate group is no longer coordinated to the Cu^{II} center in complex **2.2**. The presence of a mono-nuclear Cu^{II} ion in complex **2.2** was further confirmed by the characteristic signals in the X-band EPR spectrum in acetonitrile (Figure 2.3). In the FT-IR spectroscopy of complex **2.2**, two new stretching frequencies at 2153 cm^{-1} and 1175 cm^{-1} were observed in addition to the others (Figure 2.4). These are

isotope sensitive and appeared at 2093 and 1163 cm^{-1}, respectively, upon ^{15}N labelling (Figure 2.4). The band at 2153 cm^{-1} and 1175 cm^{-1} are assignable to the N-N and N-O stretching frequency of the metal bound N_2O. In $[Ru(NH_3)_5(N_2O)]Br_2$, these bands appeared at 2231 and 1157 cm^{-1}, respectively.[14] In case of the structurally characterized vanadium-N_2O complex, the N_2O stretching frequency was observed at 2289 cm^{-1}, which was shifted to 2217 cm^{-1} upon ^{15}N labelling.[10] In the present case, the observed N-N stretching frequency is lower than that in reported compounds. The application of vacuum to the methanol solution of complex **2.2** at 25 ºC, resulted in the disappearance of the stretching frequency at

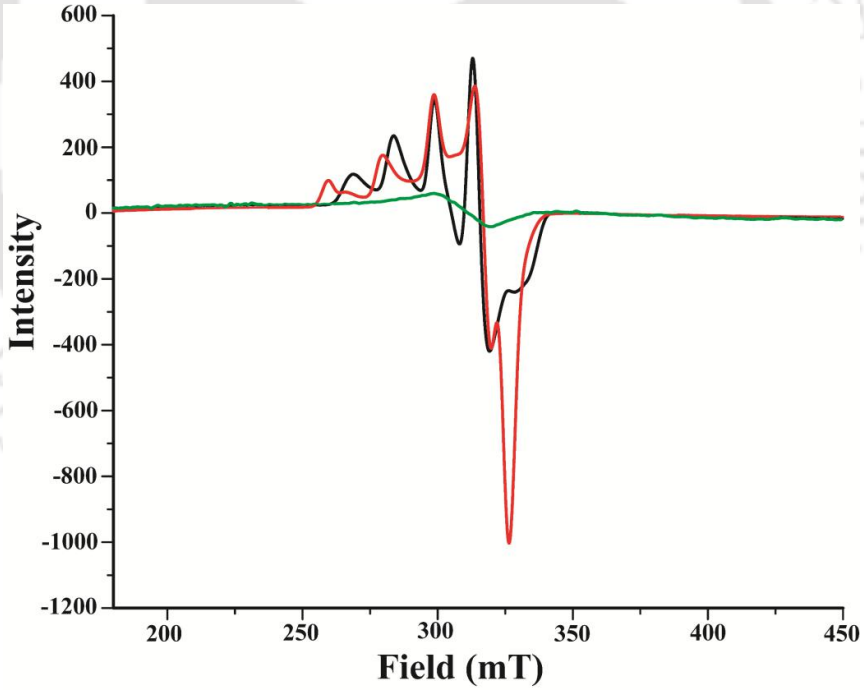

Figure 2.3 X-band EPR spectra of complex **2.1** (black), after addition of equivalent amount (green) and excess (red) of NO(g) in the acetonitrile at 77 K. (The spin quantification data are given in Appendix I).

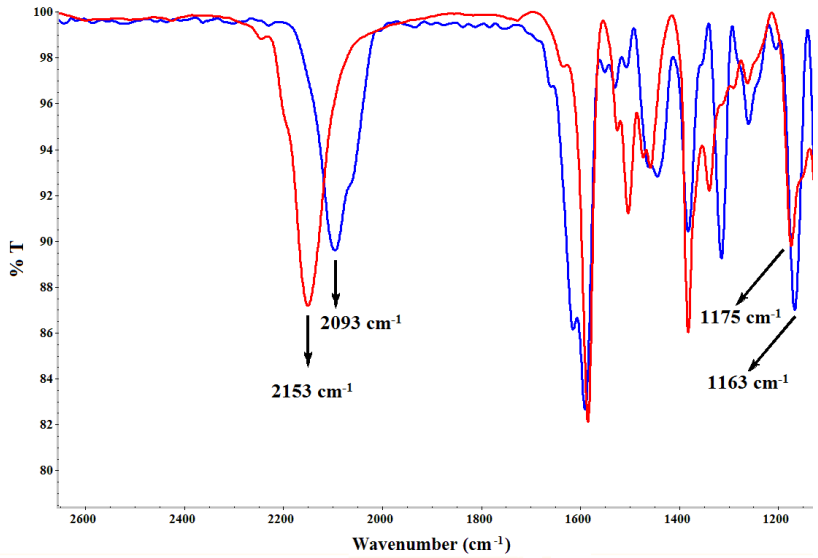

Figure 2.4 FT-IR spectra of complex **2.2** from the reaction of ^{14}NO (red) and ^{15}NO (blue) with complex **2.1**, respectively, in KBr pellet.

2153 cm^{-1} leading to the precipitation of complex **2.1** with a small amount of $[(L1H_2)Cu](NO_2)$ (*ca.* 8-10%) (Appendix I). When complex **2.2** in solid state was subjected to the application of vacuum at the same temperature, the 2153 cm^{-1} band diminished slowly. This suggests a weak bonding between the Cu(II) center and the N_2O ligand. It would be worth mentioning that the application of vacuum to the solution of $[(tpa^{Mes})V(N_2O)]$ leads to the disappearance of N_2O stretching. However, in solid even after 18 h of vacuum application, it remains unchanged.[10] This difference suggests that the metal-N_2O binding is much weaker in case of the present Cu(II)-N_2O complex compared to the $[(tpa^{Mes})V(N_2O)]$.

In addition, heating to a temperature of 120 °C also resulted in the loss of N_2O from complex **2.2**. TGA-DSC studies suggest that the loss corresponds to one unit of N_2O (Appendix I).

Further, the formation of complex **2.2** was supported by ESI mass spectrometry. The calculated formula weight of the dicationic $[(L1H_3)Cu^{II}(N_2O)]^{2+}$ is 571.22. In the mass spectrum, the m/z ion peak appeared at 285.50 (calculated: 285.61) which corresponds to the m/2 ion peak. Thus, it indicates the existence of the $[(L1H_3)Cu^{II}(N_2O)]^{2+}$ complex (Figure 2.5).

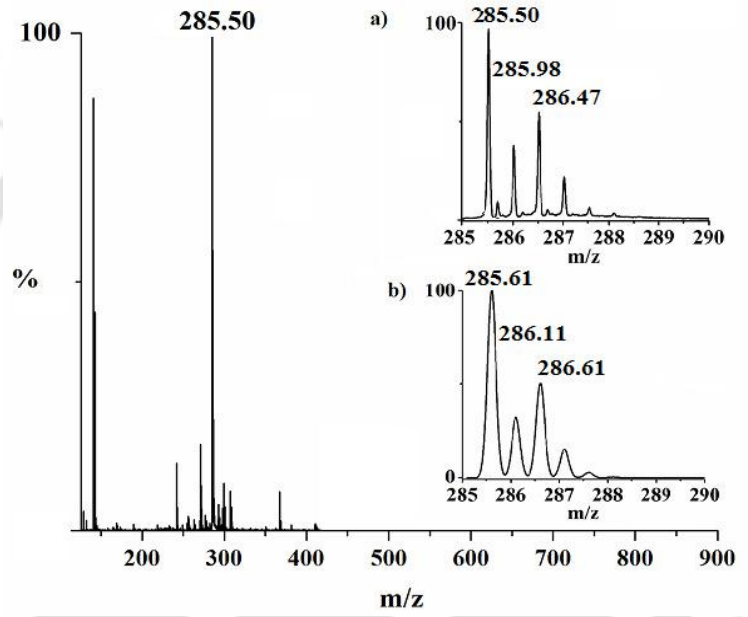

Figure 2.5 ESI mass spectrum of complex **2.2** [Inset: (a) Experimental and (b) Simulated isotropic distribution pattern] in methanol.

Along with the spectroscopic characterization, we sought chemical evidence of the formation of complex **2.2**. In metal-N_2O complexes, oxygen atom transfer to triphenylphsphene (PPh_3) from N_2O has been reported earlier as a characteristic reaction.[15] Upon addition of PPh_3 to the methanol of complex **2.2** under an Ar atmosphere, the band at 2153 cm^{-1} was found to disappear (Appendix I). ^{31}P-NMR study of the reaction mixture indicates the presence of $OPPh_3$. Thus, the oxo transfer

from complex **2.2** to PPh_3 is evident (Appendix I). It is expected that in the oxo transfer reaction, N_2 would be found.[15] Attempts were not made to quantify this N_2. The formation of N_2O from NO can be envisaged by considering the formation of an intermediate Cu(I)-nitrosyl complex followed by its reaction with excess NO. This has been confirmed by FT-IR and ESI-mass spectrometric studies of the reaction mixture. In mass spectrometry, just after addition of 2-3 equivalent of NO in acetonitrile solution of complex **2.1**, a peak at m/z, 557.13 was observed (Appendix I). This is attributed to the corresponding $\{CuNO\}^{10}$ intermediate (calculated; m/z, 557.21) In the FT-IR spectrum of the reaction mixture, the appearance of the 1695 cm^{-1} band indicated the formation of the $[CuNO]^{10}$ intermediate (Appendix I).

This leads to the simultaneous formation of the NO_2^- ion.[16] The presence of a stretching frequency at ~1338 cm^{-1} in the FT-IR spectrum of complex **2.2** suggests the formation of NO_2^-. This peak was found to shift to 1315 cm^{-1} when ^{15}NO was used. The highly reactive nature of the $\{CuNO\}^{10}$ intermediate precluded its isolation and further characterization.

DFT studies

Since X-ray quality single crystals were not available, DFT calculations have been performed to optimize the geometry of complex **2.2** and also to understand the Cu-N_2O bonding. DFT calculations using Turbomol 7.0 were performed with the TZVP basis set (Appendix I).[17] The structure of the cation of complex **2.1** was optimized using the LanL2DZ basis set (Appendix I). Then complex **2.2** was optimized to a stable minimum. The optimized structure of complex **2.2** is shown in Figure 2.6. The N_2O moiety is coordinated to the Cu center from the axial position of the

overall trigonal bipyramidal geometry. N_2O is bonded to Cu through the terminal N-atom in a bent geometry. The calculated Cu-N-N angle is 135.2° and the N-N-O

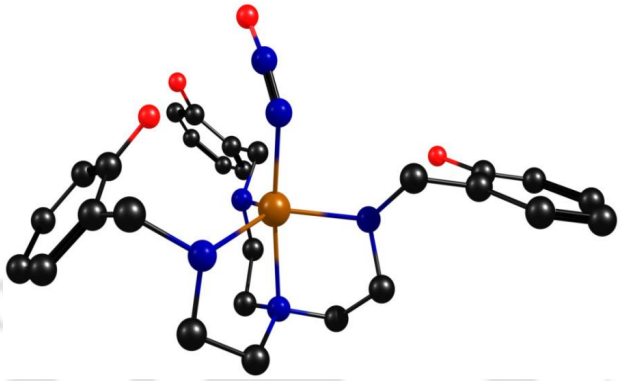

Figure 2.6 The optimized structure of complex **2.2** (color scheme: copper: reddish brown, carbon: black, oxygen: red, nitrogen: blue. Hydrogen atoms are removed for clarity).

angle is 169.9°. In case of $[Ru(NH_3)_5(N_2O)]^{2+}$, DFT calculations shows a linear binding mode of N_2O through the terminal N-atom.[14] In the structurally characterized N_2O complex of vanadium as well the N_2O is found to bind linearly. The difference in bonding is in agreement with the observed N_2O stretching frequency.[10] The linear $[Ru(NH_3)_5(N_2O)]^{+}$ or vanadium complex show higher stretching frequency compared to that in the bent Cu-N_2O.[10,14] The calculated Cu-NNO distance is 2.05 Å. N-N and N-O distances of coordinated N_2O are 1.16 and 1.20 Å, respectively. In the $[Ru(NH_3)_5(NNO)]^{2+}$ complex, the calculated Ru-NNO, N-N and N-O distances are 2.027 Å, 1.164 Å and 1.233 Å, respectively.[14] On the other hand, in the $[(tpa^{MES})V(N_2O)]$ complex, the metal–N_2O distance is 2.138 Å; whereas N-N and N-O distances of N_2O are 1.119 and 1.186 Å, respectively.[10] Thus, the calculated bond distances are closer to those of the $[Ru(NH_3)_5(N_2O)]^{2+}$ complex.[14]

In order to understand the bonding from the IR frequency perspective, the IR frequencies for the free N_2O molecule were calculated first. The calculated N-N stretch was at 2273.81 cm^{-1}. This stretching frequency was found to decrease to 2152.58 cm^{-1} while calculated for complex **2.2** (Appendix I). The FT-IR studies of the experimentally isolated complex **2.2** shows this υ(N-N) at 2153 cm^{-1}.

The UV-Visible spectrum for the complex **2.2** has been calculated at the same level of theory as taken for the calculation of the IR spectrum. It would be worth mentioning that the calculated and experimentally observed UV-visible spectra of complex **2.2** are in very good agreement.

Natural bond orbital (NBO) analysis was done in order to understand the nature of metal–N_2O bonding in complex **2.2**. Emphasis was given on the Cu-N and N-Cu bonding interactions since these are the most significant ones. The lone pair (π) of N=N of N_2O donates to the Cu orbital through sigma donation (Figure 2.7). The

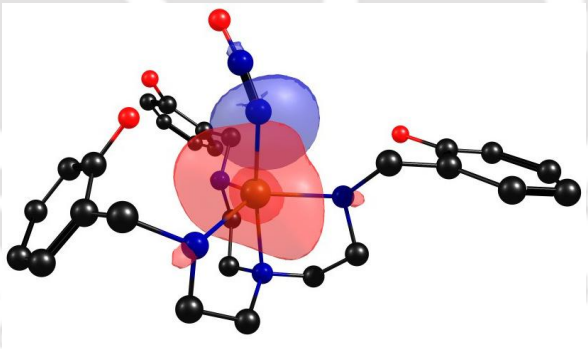

Figure 2.7 The picture shows the strong sigma (σ) interaction between the lone pair of N and d-orbital of Cu in complex **2.2**. The hydrogen (H) atoms have been removed for clarity. The iso-value is 0.05.

calculated interaction energy is 36.0 kcal/mol(Appendix I). The DFT calculations suggest that an increased transfer of electron density from the reduced Cu-centers to the bridged N_2O unit is responsible for the N_2O binding in N_2OR enzyme.[3b, 18] On

the other hand, in the $[Ru(NH_3)_5(N_2O)]^{2+}$ complex as well the π-back bonding was found to be the key to stabilizing the metal-N_2O bond.[14]

2.3 Experimental Section

2.3.1 Materials and methods

All reagents and solvents of reagent grade were purchased from commercial sources and used as received except specified. ^{15}NO was purchased from Icon Isotopes. Deoxygenation of the solvent and solutions was effected by bubbling with nitrogen or argon for 30 minutes. NO gas was used from a cylinder after purification using standard procedure. The dilution of NO was effected with argon gas using Environics Series 4040 computerized gas dilution system. UV-visible spectra were recorded on Agilent HP 8454 dioad arrey UV-visible spectrophotometer. FT-IR spectra of the solid samples were taken on a Perkin Elmer spectrophotometer with samples prepared as KBr pellets. Solution electrical conductivity was measured using a Systronic 305 conductivity bridge. ^{1}H-NMR spectra were recorded in a 400 MHz Varian FT spectrometer. Chemical shifts (ppm) were referenced either with an internal standard (Me_4Si) or to the residual solvent peaks. The X-band Electron Paramagnetic Resonance (EPR) spectra were recorded on a JES-FA200 ESR spectrometer, at room temperature or at 77 K with microwave power, 0.998 mW; microwave frequency, 9.14 GHz and modulation amplitude, 2. Mass spectra of the compounds were obtained in a Waters Q-Tof Premier and Aquity instrument. Elemental analyses were obtained from a Perkin Elmer Series II Analyzer. The magnetic moment of complexes was measured on a Cambridge Magnetic Balance.

Single crystals were grown by slow evaporation technique. The intensity data were collected using a Bruker SMART APEX-II CCD diffractometer, equipped with a fine

focus 1.75 kW sealed tube MoK_α radiation (λ = 0.71073 Å) at 273(3) K, with increasing ω (width of 0.3° per frame) at a scan speed of 3 s/frame. The SMART software was used for data acquisition.[19] Data integration and reduction were undertaken with SAINT and XPREP software.[20] Structures were solved by direct methods using SHELXS-97 and refined with full-matrix least squares on F^2 using SHELXL-97.[21] Structural illustrations have been drawn with ORTEP-3 for Windows.[22]

2.3.2 Computational details

The intermediate that has been proposed in the scheme shown above has been studied computationally through quantum chemical calculations with density functional theory (DFT). The calculations have been carried out with Turbomole 7.0[23] using the TZVP basis set.[24] Geometry optimizations were performed using the Perdew, Burke, and Ernzerhof functional (PBE).[25] Dispersion corrections have been included in all the calculations.[26] The resolution of identity (RI)[27] along with the multipole accelerated RI (marij)[28] approximations have been used for an accurate and efficient treatment of the electronic Coulomb term in the DFT calculations. Solvent corrections have also been included in all the calculations using the cosmo model,[29] with epsilon (ε) = 37.5 employed, to model the acetonitrile solvent. Frequency analysis has been done for the Cu-N_2O complex intermediate. Furthermore, natural bond orbital (NBO) analysis and time dependent density functional theory (TDDFT) calculations have also been performed for this complex. The NBO analysis was done with Gaussian 09 with the PBEPBE functional and the TZVP basis set and the solvent correction was done with PCM (10) with acetonitrile {(ε) = 37.5} as the solvent.[30]

2.3.3 Synthesis of ligand $L1H_3$

Tris-(2-aminoethyl)amine, (1.46 g, 10 mmol) was added in 50 ml ethanol in a round bottom flask. To this salicylaldehyde (3.66 g, 30 mmol) was added drop wise with constant stirring. The reaction mixture was stirred for 1 hour at 60 °C. The volume of the solution was reduced to 15 ml and kept in the freezer for 12 hours which resulted in the precipitate of the corresponding Schiff base. The Schiff base was filtered out and dried. Yield: 4.00 g (90%). It was then reduced by sodium borohydride in ethanol. The solvent was dried under reduced pressure. 50 ml of water was added to the crude mass and then neutralized with dilute acetic acid. The organic part was extracted using chloroform (25 ml × 3 portion) and dried under vacuum to give pure ligand **$L1H_3$**. Yield: 2.5g (60%). Elemental analyses for $C_{27}H_{36}N_4O_3$, calcd (%): C, 69.80; H, 7.81; N, 12.06; found (%): C, 69.70; H, 7.82; N, 12.15. FT-IR (in KBr): 3230, 1590, 1455, 1416, 1352, 1258, 1105, 1034, 754 cm^{-1}. ^{1}H-NMR (400 MHz, $CDCl_3$) δ_{ppm}: 2.56 (t, 6H), 2.69 (t, 6H), 3.95 (s, 6H), 6.76 (m, 6H), 6.93 (d, 3H), 7.12 (t, 3H). ^{13}C-NMR (100 MHz, $CDCl_3$) δ_{ppm}: 46.2, 52.6, 54.4, 116.5, 119.2, 122.5, 128.6, 128.9, and 158.2. Mass (m/z): Calcd: 464.28, found: 465.43 (M+1).

2.3.4 Synthesis of complex 2.1, $[Cu(L1H_2)](ClO_4)$

Copper(II) perchlorate hexahydrate (0.370 g) was dissolved in 20 ml of MeOH in a 50 ml round bottom flask. 0.464 g of ligand **$L1H_3$** in methanol was added to this solution and stirred for 1 hour. The green precipitate resulted was filtered and dried in vacuum. Yield, 0.50g (80%). Elemental analyses for $C_{27}H_{35}ClN_4O_7$, calcd (%): C, 51.76; H, 5.63; N, 8.94; found (%): C, 51.80; H, 5.60; N, 9.02. FT-IR (in KBr): 3260, 3229, 1610, 1597, 1572, 1450, 1247, 1088, 761, 622 cm^{-1}. UV-visible (in acetonitrile): 670 nm (ε/ M^{-1} cm^{-1}, 168), 430 nm (ε/ M^{-1} cm^{-1}, 722); $\mu_{obs.}$: 1.51 BM; Molar conductivity: 142 S cm^2 mol^{-1}; $g_{\|}$ = 2.30;

$g_{\perp}$ = 2.07 and $A_{\parallel}$ = 156.5×10^{-4} cm^{-1}. Mass (m/z): Calcd: 526.20 for $[Cu(L1H_2)]^+$, found: 526.21.

2.3.5 Synthesis of complex 2.2, $[Cu(L1H_3)(N_2O)](ClO_4)(NO_2)$

To 20 ml of distilled and degassed acetonitrile solution of complex **2.1** (500 mg), freshly prepared NO was bubbled for 5 minutes. The green color of the solution turned bluish green. After 1 hour, the solution was degassed to remove excess NO and 50 ml of diethyl ether was added to give dark green precipitate of complex **2.2** (yield, 350 mg, 65%). Elemental analyses for $C_{27}H_{36}ClCuN_7O_{10}$, calcd (%): C, 45.19; H, 5.06; N, 13.66; found (%): C, 45.00; H, 5.06; N, 13.60. FT-IR (in KBr): 3235, 2924, 2153, 1590, 1460, 1384, 1338, 1285, 1175, 1090, 750, 624 cm^{-1}. UV-visible (in methanol): 358 nm ($\varepsilon/M^{-1}cm^{-1}$ 17,550), 575 nm ($\varepsilon/M^{-1}cm^{-1}$, 260). $\mu_{obs.}$: 1.41 BM. Molar conductivity: 210 S cm^2 mol^{-1}. $g_{\parallel}$ = 2.34; $g_{\perp}$ = 2.0 and $A_{\parallel}$ = 219×10^{-4} cm^{-1}. Mass (m/z): Calcd: 285.61 for $[Cu(L1H_3)]^{2+}/2$, found: 285.50.

2.4 Conclusion

In summary, a stable Cu(II)-N_2O complex has been isolated as a solid. Spectroscopic and chemical analyses confirm the formation of the complex unambiguously. This complex loses N_2O easily in solution indicating a weak binding of N_2O to the metal ion. DFT studies indicate that the N_2O moiety is bonded to the Cu^{II} center through the terminal N atom in a bent geometry. In contrast, computational studies with density functional theory (DFT) on the $[Ru(NH_3)_5(N_2O)]^{2+}$, indicate that N_2O is bonded to the metal ion in a linear fashion.

2.5 References

(1) (a) Dickinson, R. E.; Cicerone, R. J. *Nature* **1986**, *319*, 109. (b) Cicerone, R. J. *Science* **1987**, *237*, 35. (c) Cicerone, R. J. *Geophys. Res.* **1989**, *94*, 18265. (d) Badr, O.; Probert, S. D. *Appl. Energy* **1993**, *44*, 197.

(2) (a) Averill, B. A. *Chem. Rev*. **1996**, *96*, 2951. (b) Beauchamp, E. G. *Can. J. Soil Sci*. **1997**, *77*, 113. (c) Zumft, W. G. *Microbiol. Mol. Biol. Rev*. **1997**, *61*, 533. (d) Naqvi, A.; Jayakumar, D. A.; Narvekar, P. V.; Nalk, H.; Sarma, S. S.; D'Souza, W.; Joseph, S.; George, N. D. *Nature* **2000**, *408*, 346.

(3) (a) Pomowski, A.; Zumft, W. G.; Kroneck, P. M. H.; Einsle, O. *Nature* **2011**, *477*, 234. (b) Chen, P.; DeBeer George, S.; Cabrito, I.; Antholine, W. E.; Moura, J. J.; Moura, I.; Hedman, B.; Hodgson, K. O.; Solomon, E. I. *J. Am. Chem. Soc.* **2002**, *124*, 744.

(4) Tsai, M-L.; Hadt, R. G.; Vanelderen, P.; Sels, B. F.; Schoonheydt, R. A.; Solomon, E. I. *J. Am. Chem. Soc*. **2014**, *136*, 3522.

(5) (a) Groves, J. T.; Roman, J. S. *J. Am. Chem. Soc.* **1995**, *117*, 5594. (b) Tolman, W. B. *Angew. Chem. Int. Ed.* **2010**, *49*, 1018.

(6) Armor, J. N.; Taube, H. *J. Am. Chem. Soc.* **1969**, *91*, 6874. (b) Armor, J. N.; Taube, H. *Chem. Commun.* **1971**, 287.

(7) (a) Diamantis, A. A.; Sparrow, G. J. *Chem. Commun.* **1970**, 819. (b) Diamantis, A. A.; Sparrow, G. J. *J. Colloid Interface Sci.* **1974**, *47*, 455. (c) Diamantis, A. A.; Sparrow, G. J.; Snow, M. R.; Norman, T. R. *Aust. J. Chem.* **1975**, *28*, 1231. (d) Bottomley, F.; Brooks, W. V. F. *Inorg. Chem.* **1977**, *16*, 501. (e) Bottomley, F.; Crawford, J. R. *Chem. Commun.* **1971**, 200. (f) Bottomley, F.; Crawford, J. R. *J. Am. Chem. Soc*. **1972**, *94*, 9092.

(8) Pamplin, C. B.; Ma, E. S. F.; Safari, N.; Rettig, S. J.; James, B. R. *J. Am. Chem. Soc.* **2001**, *123*, 8596.

(9) (a) Yamamoto, A.; Kitazume, S.; Pu, L. S.; Ikeda, S. *J. Am. Chem. Soc.* **1971**, *93*, 371. (b) Bottomley, F.; Lin, I. J. B.; Mukaida, M. *J. Am. Chem. Soc.* **1980**, *102*, 5238. (c) Bottomley, F. Paez, D. E.; White, P. S. *J. Am. Chem. Soc.* **1982**, *104*, 5651. (d) Bottomley, F. *Polyhedron* **1992**, *11*, 1707.

(10) Piro, N. A.; Lichterman, M. F.; Harman, W. H.; Chang, C. J. *J. Am. Chem. Soc.* **2011**, *133*, 2180.

(11) Wang, G.; Jin, X.; Chen, M.; Zhou, M. *Chem. Phys. Lett.* **2006**, *420*, 130.

(12) (a) Kumar, V.; Kalita, A.; Mondal, B. *Dalton Trans.* **2013**, *42*, 16264. (b) Jazdzewski, B. A.; Tolman, W. B. *Coord. Chem. Rev.* **2000**, *200*, 633. (c) Coombes, R. G.; Diggle, A. W.; *Tetrahedon Lett.* **1994**, *35*, 6373.

(13) Sarma, M.; Kalita, A.; Kumar, P.; Singh, A.; Mondal, B. *J. Am. Chem. Soc.* **2010**, *132*, 7846.

(14) Paulat, F.; Kuschel, T.; Nather, C.; Praneeth, V. K. K.; Sander, O.; Lehnert, N. *Inorg. Chem.* **2004**, *43*, 6979.

(15) (a) Mudalige, D. C.; Rettig, S. J.; James, B. R.; Cullen, W. R. *Chem. Commun.* **1993**, 830. (b) Mudalige, D. C.; Ma, E. S.; Rettig, S. J.; James, B. R.; Cullen, W. R. *Inorg. Chem.* **1997**, *36*, 5426. (c) Ma, E. S. F.; Rettig, S. J.; James, B. R. *Chem. Commun.* **1999**, 2463.

(16) (a) Ghosh, S.; Deka, H.; Dangat, Y. B.; Saha, S.; Gogoi, K.; Vanka, K.; Mondal, B. *Dalton Trans.* **2016**, *45*, 10200. (b) MacNeil, J. H.; Berseth, P. A.; Bruner, E. L.; Perkins, T. L.; Wadia, Y.; Westwood, G.; Trogler, W. C. *J. Am. Chem. Soc.* **1997**, *119*, 1668.

(17) Ahlrichs, R.; Baer, M.; Haeser, M.; Horn, H.; Koelmel, C. *Chem. Phys. Lett.* **1989**, *162*, 165.

(18) (a) Chen, P.; Cabrito, I.; Moura, J. J. G.; Moura, I.; Solomon, E. I. *J. Am. Chem. Soc.* **2002**, *124*, 10497. (b) Ghosh, S.; Gorelsky, S. I.; Chen, P.; Cabrito, I.; Moura, J. J. G.; Moura, I.; Solomon, E. I. *J. Am. Chem. Soc.* **2003**, *125*, 15708.

(19) SMART, SAINT and XPREP, Siemens Analytical X-ray Instruments Inc., Madison, Wisconsin, USA, **1995**.

(20) Sheldrick, G. M.; SADABS: software for Empirical Absorption Correction, University of Gottingen, Institut fur Anorganische Chemieder Universitat, Tammanstrasse 4, D-3400 Gottingen, Germany, 1999–2003.

(21) Sheldrick, G. M. SHELXS-97, University of Gottingen, Germany, **1997**.

(22) Farrugia, L. J. J. *Appl. Crystallogr.* **1997**, *30*, 565.

(23) TURBOMOLE GmbH, "TURBOMOLE V6.3 2011, a development of University of Karlsruhe and Forschungszentrum Karlsruhe GmbH, 1989–2007," **2011**.

(24) Ansgar, S.; Christian, H.; Reinhart, A. *J. Chem. Phys.* **1994**, *100*, 5829.

(25) Perdew, J. P.; Burke, K.; Ernzerhof, M. *Phys. Rev. Lett.* **1996**, *77*, 3865.

(26) Grimme, S.; Antony, J.; Ehrlich, S.; Krieg, H. *J. Chem. Phys.* **2010**, *132*, 154104.

(27) (a) Eichkorn, K.; Treutler, O.; Öhm, H.; Häser, M.; Ahlrichs, R. *Chem. Phys. Lett.* **1995**, *240*, 283.

(28) Klamt, A.; Schuurmann, G. *J. Chem. Soc., Perkin Trans.* **1993**, *2*, 799.

(29) Frisch, M. J., et al. "Gaussian 09, revision B. 01." *Gaussian Inc., Wallingford, CT*, **2010**.

(30) Tomasi, J.; Mennucci, B.; Cammi, R. *Chem. Rev.* **2005**, *105*, 2999.

Chapter 3

Nitric oxide reactivity of a Cu(II) complex of an imidazole based ligand: Aromatic C-nitrosation followed by the formation of N-nitrosohydroxylaminato complex

Abstract

A binuclear Cu(II) complex, **3.1,** $[Cu_2(L2)_2(OAc)](OAc)$ of imidazole based ligand **L2H** {**L2H** = 2-(*bis*(2-ethyl-5-methyl-1H-imidazol-4-yl)methyl)phenol} was synthesized and characterized spectroscopically and structurally. Addition of an equivalent amount of nitric oxide (NO) by a gastight syringe to the acetonitrile:methanol (5:1, v/v) solution of complex **3.1** at room temperature resulted in the reduction of Cu(II) center to Cu(I) with concomitant C-nitrosation of the ligand. Spectroscopic characterization of the resulting Cu(I) complex (**3.1a**) of the C-nitrosylated ligand, **L2′** {**L2′** =2-(*bis*(2-ethyl-5-methyl-1H-imidazol-4-yl)methyl)-4-nitroso-phenol} has been done. The Cu(I) complex, **3.1a** further reacted with NO to result in the corresponding N-nitrosohydroxylaminato complex, **3.2,** $[Cu_2(L2\text{-}ONNO)_2](OAc)_2$ through the formation of a Cu(I)-nitrosyl intermediate. A small fraction of the nitrosyl intermediate decomposed to the corresponding Cu(II) complex **3.3,** $[Cu(L2')_2]$, and N_2O in a parallel reaction.

3.1 Introduction

The aromatic C-nitroso compounds are known as the reactive intermediates in the biological systems which form either by the metabolic N-oxidation of arylamines or by the reduction of aromatic nitro compounds.[1-4] These compounds show important reactivity towards biological targets like hemoglobin. In fact, it is known that hemoglobin has a greater affinity toward nitrosoarene over dioxygen.[5] They are also known as the synthetic analogue of another reactive species, nitroxyl (HNO).[6] These observations have stimulated the reactivity study of the C-nitroso compounds with a number of the heme model complexes.[2] In addition, the C-nitroso compounds are reported to serve in various catalytic reactions as well.[1,2] For instance, Cu(I)-nitrosoarene adducts are used as the precursor in catalytic formation of the C-N bond. $[Cu\{\kappa^1\text{-}N(O)Ph\}_3]^+$ is a catalyst involved in the C-H amination of the allylic substrates.[7] These complexes are found to be useful in the asymmetric Diels-Alder reaction of the electron deficient nitrosoarene with dienes as well.[8] On the other hand, the adduct, $[(Me_6tren)Cu(\kappa^1\text{-}O\text{-}(O)NPh)]^+$ [Me_6tren = *Tris*{2-(dimethylamino)ethyl}amine] formed in the reaction of PhNO with $[(Me_6tren)Cu]^+$ was suggested as a model for the end-on superoxide binding to the mononuclear copper-enzymes.[9] Thus, the reactivity of the nitrosoarene compounds with transition metal complexes is an attractive field of research. As a result a number of examples of the metal-nitrosoarene complexes are reported with various binding modes and varying degrees of the RN=O activation. In the recent past, Warren *et al.* reported the reaction of the β-diketiminato Cu(I) and Ni(I) nitrosoarene complexes. These complexes are found to result in the diazeniumdiolates in presence of nitric oxide (NO).[10a-c] Recently, the same group has reported the reaction of nitrosobenzene (PhNO) with the electrondeficient β-diketiminato nickel(I) complex $[^iPr_2NN_{F6}]Ni$ to result in the reduction of the PhNO ligand to a

$(PhNO)^{\bullet 1-}$ species coordinated to a square planar Ni^{II} center in $[^{i}Pr_2NN_{F6}]Ni(\eta^2\text{-}ONPh)$. Structure-reactivity studies revealed that $(PhNO)^{\bullet 1-}$ and $(PhNO)^{2-}$ ligands parallels with superoxo $(O_2)^{\bullet 1-}$ and peroxo $(O_2)^{2-}$ ligands, respectively.[10d]

In our study on the reactivity of NO with Cu(II) complexes, it has been observed that the reduction of Cu(II) center by NO resulted in the aromatic C-nitrosation. For example, when the Cu(II) complex of 4-amino-3-hydroxynaphthalene-1-sulphonic acid was treated with NO in acetonitrile solution, the reduction of the metal centre was observed with concomitant C-nitrosation of the phenol ring present in the ligand framework.[11] This reaction is more like the examples of N-nitrosation of the ligand frameworks in the reaction of Cu(II) complexes with NO (Scheme 3.1).

$$\mathbf{LCu^{II}(X)} \xrightarrow[NO_{(g)}]{CH_3CN \text{ (or } CH_3OH)} \mathbf{Cu^{I}} + \mathbf{L\text{-}NO} + \mathbf{X}$$

[X = CH_3CN or CH_3OH; L = Ligand with amine donor group/s
L-NO = N-nitrosated ligand]

Scheme 3.1

In this context here we report the reaction of a Cu(II) complex of the ligand **L2H** {**L2H** = 2-(*bis*(2-ethyl-5-methyl-1H-imidazol-4-yl)methyl)phenol} (Figure 3.1) in the acetonitrile:methanol (5:1, v/v) solution with NO. Earlier it was found that the Cu(II) complex of the parent *bis*(2-ethyl-4-methyl-imidazol-5yl)methane ligand upon reaction with NO affords the corresponding Cu(II)-nitrosyl complex. In general, phenol ring is susceptible for C-nitrosation. There are not much examples of C-nitrosation through the

reaction of Cu(II) complexes with NO. Thus, the framework was chosen to understand the detail mechanism of the reaction.

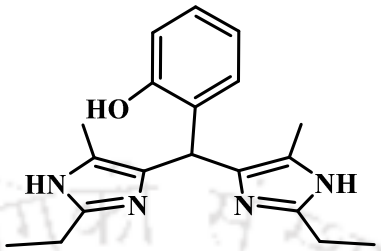

Figure 3.1 Ligand used for the present work.

3.2 Results and Discussion

The ligand **L2H** was prepared from the reaction of 2-ethyl-4-methyl imidazole and salicylaldehyde in presence of potassium hydroxide (Experimental Section). The copper(II) complex **3.1**, **$[Cu_2(L2)_2(OAc)](OAc)$,** was synthesized from the reaction of an equivalent amount of copper(II) acetate monohydrate with **L2H** (Experimental Section). The formation of the complex was confirmed by the elemental and spectroscopic analyses (Experimental Section). The single crystal structure determination of the complex **3.1** revealed the presence of a diphenolato-bridged di-copper(II) moiety in the unit cell (Figure 3.2). The copper centres are in square pyramidal geometry with two phenolato and one acetate bridge. Two nitrogen-donor atoms from the ligand, one oxygen atom from the phenolato group and one oxygen atom from the acetate moiety resulted in a square pyramidal coordination geometry around each copper(II) centre {calculated τ values: Cu(1), 0.018 and Cu(2), 0.020}. The fifth coordination site is occupied by the phenolato group of the other ligand. Thus, the bridging phenolato oxygen occupied the axial position of same copper and the equatorial position of the other centre of the binuclear unit. The

Cu−N distances in the complex **3.1** are within 1.958 - 2.041 Å that are also in the range observed earlier.[12]

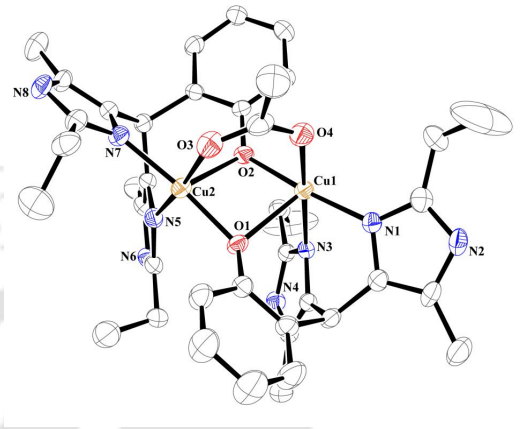

Figure 3.2 ORTEP diagram of complex **3.1** (30% thermal ellipsoid plot, H-atoms and counter anions are not shown for clarity).

The axial Cu-O bond lengths are found to be longer than the equatorial ones as expected. The average Cu-O bond distance of bridging acetate ion is 1.988 Å. The average Cu−$O_{(phenolato)}$−Cu angle is 93.2°. In the earlier reported compounds, it was observed in the range of 91−104°.[13, 14] The two Cu(II) centres are separated by 3.047 Å.

In acetonitrile:methanol (5:1, v/v) solution, the complex **3.1** absorbed at 625 nm (ε/ $M^{-1}cm^{-1}$, 268) and 405 nm (ε/ $M^{-1}cm^{-1}$, 500) along with the other intra-ligand transitions in the lower wavelengths (Appendix II). The 625 nm absorption was attributed to a *d-d* transition and the band centered at 405 nm was assigned to the phenolato→Cu(II) charge transfer. Similar absorption was observed in the other analogous Cu(II) complexes having coordinated phenolato groups.[15] The X-band EPR spectrum of the complex **3.1** in acetonitrile:methanol (5:1, v/v) solution displayed the characteristic signals for a Cu(II) centre with $g_{\parallel}$, 2.43, $g_{\perp}$, 2.07 and A, 204 × 10^{-4} cm^{-1} (Appendix II) having $d_{x^2-y^2}$ ground state in square pyramidal geometry.[16] In ESI mass spectrometry, the molecular ion peak

appeared at 831.12 corresponding to the dinuclear unit $[Cu_2(L2)_2(CH_3COO)]$ (Appendix II). The isotopic distribution pattern was found to be in good agreement with the simulated one.

Nitric oxide reactivity

The purging of NO gas to a dry and degassed acetonitrile:methanol (5:1, v/v) solution of complex **3.1**, resulted in the change of color from green to light yellow. The solution was allowed to stand overnight under an NO atmosphere and resulted in the dark blue crystals of complex **3.2, $[Cu_2(L2\text{-}ONNO)_2](OAc)_2$**. The excess of NO was removed from the reaction vessel by applying several cycles of vacuum and an Ar purging. The crystals of complex **3.2** were separated by filtration. Addition of diethylether to the filtrate afforded the crystalline precipitate of complex **3.3, $[Cu(L2')_2]$** {$L2'$ =2-(*bis*(2-ethyl-5-methyl-1H-imidazol-4-yl)methyl)-4-nitroso-phenol} (Scheme 3.2). Spectral characterization as well as single crystal structure determination confirmed the formulation of the complexes **3.2** and **3.3** (Experimental Section). The single crystal structure of complex **2** (Figure 3.3) revealed the presence of a binuclear unit where two nitrogen atoms of the imidazole moiety binds with one copper centre and two oxygen atoms of N-nitrosohydroxylaminato group binds to the other copper centre. The overall geometry of both the copper centres was square planar {τ values, Cu(1), 0.127 and Cu(2), 0.128}. Crystallographic data are shwon in table 3.1. The average Cu-N and Cu-O bond distance were 1.951 Å and 1.914 Å, respectively.

The ORTEP diagram of complex **3.3** is shown in figure 3.4. It was crystallized out as a mononuclear unit with distorted octahedral geometry. Four nitrogen atoms of imidazole from two ligands are coordinated to the copper centre at equatorial position and two oxygen atoms of phenolato group binds from axial position. The average Cu-N and Cu-O

Table 3.1 Crystallographic data of complexes **3.1**, **3.2** and **3.3**.

	3.1	**3.2**	**3.3**
Formulae	$C_{42}\ H_{52}\ Cu_2\ N_8\ O_7$	$C_{44}\ H_{55}\ Cu_2\ N_{13}\ O_{10}$	$C_{38}\ H_{52}\ Cu\ N_{10}\ O_8$
Mol. wt.	908.02	1053.11	840.44
Crystal system	Monoclinic	Monoclinic	Triclinic
Space group	P21/n	P21/c	P-1
Temperature /K	296	296	150
Wavelength /Å	0.71073	0.71073	0.71073
a /Å	12.4631(4)	17.8022(14)	8.4863(8)
b /Å	30.4969(9)	15.3356(9)	10.9805(10)
c /Å	12.6547(4)	21.883(3)	12.8436(12)
α/°	90	90.00	65.122(9)
β/°	93.733(2)	121.384(7)	76.964(8)
γ/°	90	90.00	78.346(7)
V/ $Å^3$	4799.7(3)	5100.2(9)	1049.98(19)
Z	4	4	1
Density/g cm^{-3}	1.257	1.371	1.329
Abs. Coeff. /mm^{-1}	0.938	0.900	0.581
Abs. correction	Multi-Scan	Multi-Scan	Multi-Scan
F(000)	1896.0	2192.0	443.49
Total no. of reflections	9803	8965	3797
Reflections, $I > 2\sigma(I)$	4693	4444	3141
Max. 2θ/°	26.45	25.00	25.25
Ranges (h, k, l)	-14≤ h ≤15 -38≤ k ≤37 -15≤ l ≤ 15	-21≤ h ≤21 -17≤ k ≤18 -26≤ l ≤ 19	-10≤ h ≤10 -10≤ k ≤13 -10≤ l ≤ 15
Complete to 2θ (%)	99.1	99.8	99.8
Refinement method	Full-matrix least-squares on F^2	Full-matrix least-squares on F^2	Full-matrix least-squares on F^2
Goof (F^2)	1.094	0.943	1.193
R indices [$I > 2\sigma(I)$]	0.0621	0.0769	0.0584
R indices (all data)	0.1217	0.1590	0.0719

bond distance are 2.002 Å and 2.342 Å, respectively. The *para* position of the phenol ring is occupied by a nitroso group. The N-O bond length is 1.297 Å.

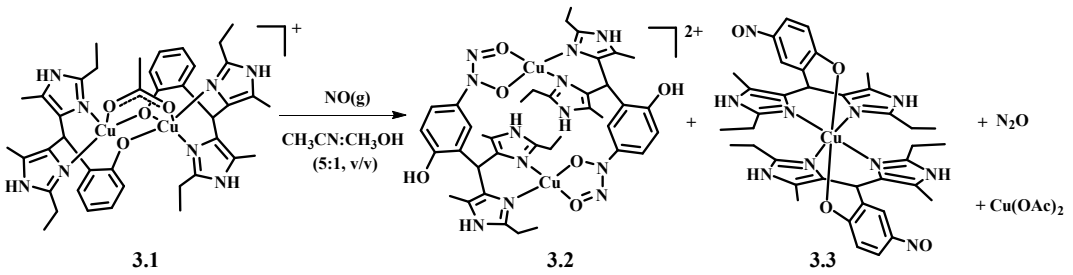

3.1 **3.2** **3.3**

Scheme 3.2

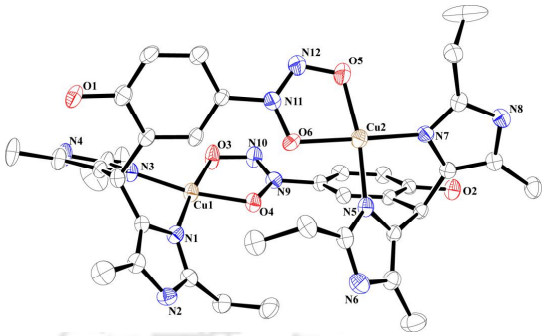

Figure 3.3 ORTEP diagram of complex **3.2** (30% thermal ellipsoid plot, counter anion and H-atoms are not shown for clarity).

In the UV-visible spectrum of complex **3.1** in CH_3CN:CH_3OH (5:1, v/v) solution, the bands at 625 nm and 405 nm disappeared immediately after addition of an equivalent amount of NO (Figure 3.5a). The frozen (at 77K) reaction mixture was found to be silent in X-band EPR (Figure 3.5b) indicating the formation of a diamagnetic species. The appearance of a very less signal intensity in the spectrum was either due to the unreacted complex or a small fraction of the decomposition product present in the EPR tube. The silent nature could be either due to the formation of a $[CuNO]^{10}$ complex which is diamagnetic in nature or because of the reduction of Cu(II) centre to Cu(I).[17] It is to be noted that addition of NO into the acetonitrile solution of Cu(II) complexes of pyridine methylamine, *bis*-aminoethyl amine, N,N-*bis*-(2-aminoethyl)ethane-1-2-diamine and *bis*(2-ethyl-5-methyl-1H-imidazol-4-yl)methane ligands were reported to result in the formation of the $[CuNO]^{10}$ species.[18] In UV-visible spectrum, *d-d* band for the respective $[CuNO]^{10}$ complexes were observed at 660, 595, 812 and 704 nm.[18] In addition in the FT-IR spectrum, characteristic stretching frequencies at 1640, 1635, 1650 and 1662 cm^{-1} were observed.[18] However, this frequency was not observed in the present case; but, a new stretching frequency at 1302 cm^{-1} was observed (Appendix II). This frequency was attributed to the aromatic C-nitroso group. It was observed at 1122, 1113 and 1358 cm^{-1} in

case of complexes [[Me_2NN]Cu(η^2-ONPh)], [[Me_2NN_{F6}]Cu(η^2-ONPh)], [^{iPr2}TpCu(κ^1-N(O)Ph)] {Me_2NN = N-((2Z,4E)-4-((2,6-dimethylphenyl)imino)pent-2-en-2-yl)-2,6-dimethylaniline, Me_2NN_{F6} = N-((2Z,4Z)-4-((2,6-dimethylphenyl)imino)-1,1,1,5,5,5-hexafluoropent-2-en-2-yl)-2,6-dimethylaniline and ^{iPr2}Tp= *tris*(3,5-diisopropyl-1H-pyrazol-1-yl)hydroborate}, respectively.[7,10,19] Thus, the reduction of Cu(II) to Cu(I) by NO with concomitant C-nitrosation of the ligand is more logical to believe. Reduction of

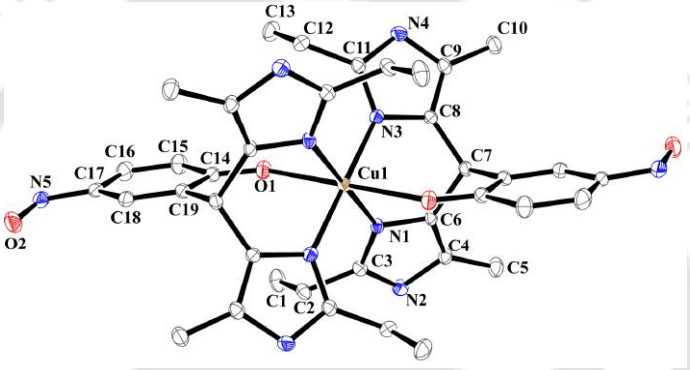

Figure 3.4 ORTEP diagram of complex **3.3** (30% thermal ellipsoid plot, solvent and H-atoms are not shown for clarity).

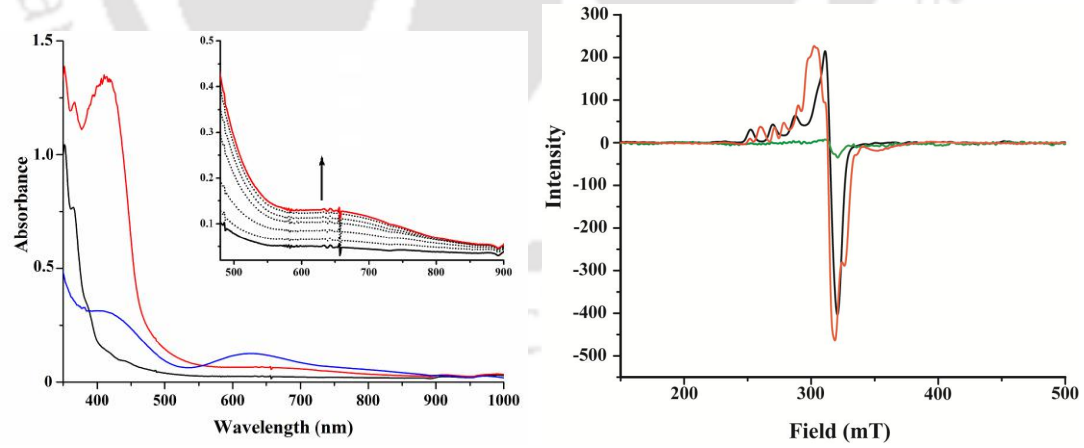

(a) **(b)**

Figure 3.5 (a) UV-visible spectra of complex **3.1** (blue), after 1 minute (black) and 24 hours (red) of addition of NO in acetonitrile:methanol mixture (1:5, v/v) (Inset shows the gradual increase of the d-d band). (b) X-band EPR spectra of complex **3.1** (black), after 1 minute (green) and 24 hours (red) of addition of NO in acetonitrile:methanol mixture (1:5, v/v) at 77 K.

Cu(II) to Cu(I) was also confirmed by ^{1}H-NMR spectroscopy. The broad nature of the NMR signals of complex **3.1** became well resolved after addition of an equivalent amount of NO (Appendix II).

Furthermore, in the ESI Mass spectrum of the reaction mixture the molecular ion peak appeared at 416.03 indicating the formation of L2$^{/}$ by C-nitrosation in the ligand framework (Appendix II). Isolation of L2$^{/}$ followed by spectral characterization confirmed the C-nitrosation unambiguously (Experimental Section). It is to be noted that the aromatic C-nitrosation in the reaction of Cu(II) complexes with NO was observed earlier only in one case, though there are a number of examples of the N-nitrosation.[11,18,20] The formation of the C-nitrosated ligand can be envisaged considering the reduction of Cu(II) centre by NO leading to the simultaneous formation of NO^{+} which is very reactive and unstable.[21] This then reacted with the phenol ring to afford C-nitrosation. The GC-mass analysis of the solution confirmed the presence of MeONO, though in very small quantity (Appendix II). This is attributed to the reaction of NO^{+} with solvent methanol. It would be worth to mention that NO itself did not find to result in MeONO formation in the reaction condition. Thus, the yellow compound was formulated as the corresponding Cu(I) complex having C-nitroso ligand (**3.1a**) (Scheme 3.3). It was found to be air and moisture sensitive and hence attempts were not made to isolate the complex **3.1a**. However, it was isolated as a perchlorate salt which is reasonably stable at room temperature under an Ar atmosphere (Experimental Section). Unfortunately, we could not get the X-ray quality crystals for structure determination.

There are a few examples of Cu(I) complexes with nitrosoarene ligands in literature. Warren and co-worker reported the formation of [{$(Me_2NN)Cu$}$_2$(μ-η^2;η^1-ONAr)] and

[{(Me_2NN)Cu}(η^2-ONAr)] {Ar = Ph or 3,5-$Me_2C_6H_3$} from the reaction of [{(Me_2NN)Cu}(NCMe)] with nitrosoarene.[10b] It was also reported that the addition of nitrosobenzene to copper(I) complexes of β-diketiminato and *tris*(pyrazolyl)borate ligands; [(Me_2NN_{F6})Cu($NCCH_3$)] and [(^{iPr2}Tp)Cu($NCCH_3$)] resulted in the formation of corresponding nitrosobenzene adducts, [(Me_2NN_{F6})Cu(μ^2-ONPh)] and [(^{iPr2}Tp)Cu(κ^1-N(O)Ph)], respectively.[10] It was observed that the back bonding to the nitrosoarene is strongest *via* μ^2-NO binding mode. The strength of this interaction was correlated directly to the N-O bond length and ν_{NO} stretching frequencies. The N-O bond lengths in [(Me_2NN_{F6})Cu(μ^2-ONPh)] and [{(Me_2NN)Cu}$_2$(η^2-ONAr)] were found to be 1.338 and 1.330 Å, respectively. [10] The weak back bonding in electron-poor [Me_2NN_{F6}]Cu moiety

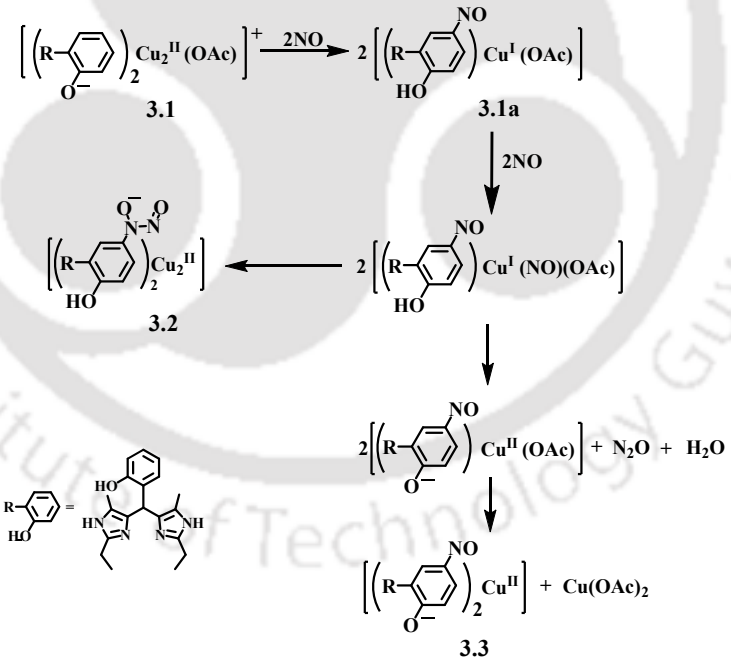

Scheme 3.3

resulted in higher υ_{NO} stretching frequency (1122 cm^{-1}) in [{(Me_2NN_{F6})Cu}2(η^2-ONAr)] compared to that in case of [{(Me_2NN)Cu}$_2$(η^2-ONAr)] (1113 cm^{-1}).[10] In contrast, in the

present case, the ν_{NO} stretching frequency appeared at 1302 cm^{-1}. For free monomeric nitrosobenzene, ν_{NO} stretching frequency appeared at 1506 cm^{-1}.[2, 22]

The reaction mixture was found to afford complexes **3.2** and **3.3** while kept under NO atmosphere at room temperature. It is believed that in the first step of the reaction between complex **3.1** and NO, the Cu(I) intermediate complex, **3.1a** is formed and this reacted with further equivalents of NO to result in the complexes **3.2** and **3.3** (Scheme 3.3). To confirm this, isolated intermediate Cu(I) complex, **3.1a** with perchlorate anion was made to react with NO which resulted in complexes **3.2** and **3.3** as well. In FT-IR spectrum of complex **3.1a**, though no characteristic peak around 1600-2000 cm^{-1} was observed; bubbling of NO into the degassed solution of **3.1a** resulted in a new peak at 1712 cm^{-1}. This frequency was assigned to the Cu(I)-nitrosyl, {CuNO}[11] species which was formed upon reaction of **3.1a** with NO. In earlier reports of Cu(I)-nitrosyls, this frequency was found to appear at 1712, 1720 and 1753 cm^{-1} in case of $[(Tp^{tBu,H})Cu(NO)]$, $[(Tp^{Ph,Ph})Cu(NO)]$ and $[(Tp^{CF_3,CF_3})Cu(NO)]$, respectively.[23] The ESI mass spectrum displayed the appearance of molecular ion peak at 446.80 which corresponds to the mononuclear, Cu(I)-nitrosyl moiety with a C-NO ligand (Appendix II). This nitrosyl complex was unstable and allowing to stand for 5-6 hrs at room temperature resulted in complexes **3.2** and **3.3** (Scheme 3.3). The formation of the complex **3.2** can be envisaged by the attack of coordinated nitrosyl group of the Cu(I)-nitrosyl to the C-nitroso moiety to result in the corresponding diazeniumdiolate with concomitant oxidation of Cu(I) to Cu(II).[10] Formally, Cu(I) gets oxidized to Cu(II) with concomitant reduction of the NO to NO^-. The formation of complex **3.3** is attributed to the decomposition of the Cu(I)-nitrosyl in a parallel reaction resulting in the release of N_2O (Scheme 3.3). This has been observed earlier also.[24] The

GC-mass analyses of the head space of the reaction vessel detected the existence of N_2O (Appendix II). Similar reaction was observed in cases of [{(Me_2NN)Cu}(η^2-ONAr)] {Ar =Ph or 3,5-$Me_2C_6H_3$}, [(Me_2NN_{F6})Cu($NCCH_3$)] and [^{iPr2}TpCu(κ^1-N(O)Ph)].[10] Reaction of these complexes with excess of NO resulted in the formation of corresponding diazeniumdiolates. It was proposed that in these cases the reaction may proceed through a inner-sphere attack of NO on [Cu(η^2-ONAr)] moiety, but there was no evidence. The findings of the present study are also in accord to the earlier observation.

3.3 Experimental Section

3.3.1 Materials and methods

All reagents and solvents of reagent grade were purchased from commercial sources and used as received except specified. Deoxygenation of the solvent and solutions was effected by repeated vacuum/purge cycles or bubbling with nitrogen or argon gas. NO gas was used from a cylinder after purification using standard procedure.[25] UV-visible spectra were recorded on a Agilent HP 8454 series Diode Array UV-visible spectrophotometer. FT-IR spectra were taken on a Perkin Elmer spectrophotometer with samples prepared either as KBr pellets or in KBr cell for solution. NMR spectra were recorded in a 400 MHz Varian FT spectrometer. The X-band Electron Paramagnetic Resonance (EPR) spectra were recorded on a JES-FA200 ESR spectrometer, at room temperature or at 77 K. Elemental analyses were obtained from a Perkin Elmer Series II Analyzer. Mass spectra were recorded on a Waters, Model: Q-Tof Premier instrument with ESI mode of ionization. Solution electrical conductivity was checked using a Systronic 305 conductivity bridge. The magnetic moment of complexes are measured on a Cambridge Magnetic Balance.

Single crystals were grown by slow evaporation technique. The intensity data were collected using a Bruker SMART APEX-II CCD diffractometer, equipped with a fine focus 1.75 kW sealed tube MoK_α radiation (λ = 0.71073 Å) at 273(3) K, with increasing ω (width of 0.3° per frame) at a scan speed of 3 s/frame. The SMART software was used for data acquisition. Data integration and reduction were undertaken with SAINT and XPREP software.[26] Multi-scan empirical absorption corrections were applied to the data using the program SADABS.[27] Structures were solved by direct methods using SHELXS-97 and refined with full-matrix least squares on F^2 using SHELXL-97.[28] Structural illustrations have been drawn with ORTEP-3 for Windows.[29]

3.3.2 Synthesis of ligand L2H

2-ethyl-4-methyl imidazole (2.2 g, 20 mmol) was taken in a round bottom flask in methanol (10 ml). To this salicylaldehyde (1.22 g, 10 mmol) and aqueous solution of potassium hydroxide (3.36 g, 60 mmol) were added. The reaction mixture was stirred for 3 days at room temperature. The color of the solution changed from yellow to dark red. Methanol was removed *via* vacuum. Dilute HCl was added dropwise to this solution till the precipitation of ligand was completed. The precipitate was filtered and washed thoroughly with water to give light yellow mass. It was then dried in oven at 80 ℃ for 20 hours to obtain ligand **L2H**. Yield: 2 g (60%). Elemental analyses for $C_{19}H_{24}N_4O$, Calcd(%): C, 70.34; H, 7.46; N, 17.27. Found (%): C, 70.31; H, 7.48; N, 17.37. FT-IR (in KBr): 3380, 2964, 2842, 1614, 1529, 1455, 1252, 1071, 884, 753 cm^{-1}. ^{1}H-NMR (400 MHz, $CDCl_3$) δ_{ppm}: 1.22(t, 6H), 2.17(s, 6H) 2.61(q, 4H), 4.98(s, 1H), 6.82(t, 1H), 7.00(d, 1H) and 7.17(m, 2H). ^{13}C-NMR (100 MHz, $CDCl_3$) δ_{ppm}: 10.7, 12.4, 21.5, 29.8, 120.2, 120.6, 125.0, 128.9, 129.9, 130.8, 131.4, 147.1, and 156.2. Mass (m/z): Calcd: 324.19, found: 325.12 (M+1).

3.3.3 Synthesis of Complexes

(a) Complex 3.1, $[Cu_2(L2)_2(OAc)](OAc)$

Copper(II) acetate monohydrate (1.99 g, 10 mmol) was taken in a 250 ml round bottom flask, and dissolve in 200 ml of MeOH. The ligand, **L2H** (3.24 g, 10 mmol) was added to this solution and stirred for 1 hr. The volume of the resulting solution was reduced to 50 ml by using rotary evaporator. To it, 150 ml of diethylether was added and kept overnight to give green precipitate of complex **3.1**. Single crystal of X-ray quality was obtained by slow evaporation of an acetonitrile:methanol (5:1, v/v) solution of complex **3.1**. Yield: 3.0 g (67%). Elemental analyses for $C_{42}H_{52}N_8O_6Cu_2$, Calcd(%): C, 56.55; H, 5.88; N, 12.56. Found (%): C, 56.48; H, 5.89; N, 12.68, FT-IR (in KBr): 3283, 2966, 1656, 1448, 1268, 1088, 797, 626 cm^{-1}. UV-visible (methanol:acetonitrile, 1:5 (v/v)): 625 nm (ε/ M^{-1} cm^{-1}, 268), 405 nm (ε/ M^{-1} cm^{-1}, 500); $\mu_{obs.}$: 2.09 BM. Molar conductivity: 120 S cm^2 mol^{-1}. X-band EPR: $g_{\parallel}$, 2.43; $g_{\perp}$, 2.07 and A = 204 $\times 10^{-4}$ cm^{-1}. Mass (m/z): Calcd: 831.25 for $[Cu_2(L2)_2(OAc)]^+$, found: 831.12.

(b) Complex 3.2, $[Cu_2(L2\text{-}ONNO)_2](OAc)_2$

To 10 ml of dry and degassed acetonitrile:methanol (5:1, v/v) solution of complex **3.1** (200 mg, 0.24 mmol), NO was bubbled for 2 minutes. The reaction mixture was kept overnight in an NO atmosphere to result in the blue crystals of complex **3.2**. The excess NO was removed by applying vacuum/Ar cycles. The crystals were filtered and washed with cold acetonitrile. Yield: 90 mg (60%). Elemental analyses for $C_{42}H_{52}N_{12}O_{10}Cu_2$, Calcd(%): C, 49.85; H, 5.18; N, 16.61. Found (%): C, 49.69; H, 5.11; N, 16.78, FT-IR (in KBr): 3440, 2975, 2925, 1632, 1440, 1280, 1238, 1155, 1104, 960, 646 cm^{-1}. UV-visible (Methanol):

605 nm (ε/ M^{-1} cm^{-1}, 150), Molar conductivity: 220 S cm^2 mol^{-1}. X-band EPR: $g_{av,}$ 2. 27. Mass (m/z): Calcd: 446.11 for $[Cu_2(L2\text{-}ONNO)_2]^{2+}/2$, found: 446.26.

(c) Complex 3.3, $[Cu(L2')_2]$

The filtrate obtained from synthesis of complex **3.2** was dried in vacuum. It was then dissolved in 10 ml of methanol. To it, 30 ml of diethyl ether was added and kept in freezer for a week which gave red crystals of X-ray quality. Yield: 30 mg (30%). Elemental analyses for $C_{38}H_{45}N_{10}O_4Cu$, Calcd(%): C, 59.32; H, 5.90; N, 18.21. Found (%): C, 59.23; H, 5.92; N, 18.29, FT-IR (in KBr): 2970, 2920, 1610, 1460, 1415, 1348, 1310, 1215, 1120, 866, 825, 635 cm^{-1}. UV-visible (Methanol): 685 nm (ε/$M^{-1}cm^{-1}$, 157) and 405 nm (ε/$M^{-1}cm^{-1}$, 4260). $\mu_{obs.}$: 1.62 BM. Molar conductivity: 40 S cm^2 mol^{-1}. Mass (m/z): Calcd: 768.28 for $[Cu(L2')]^+$, found: 768.29.

3.3.4 Isolation of modified ligand L2′

In a 50 ml round bottom flask, 0.768 g of complex **3.3** was dissolved in minimum volume of methanol. To it 5 ml of saturated aqueous solution of Na_2S was added to give black precipitate of CuS. The precipitate was filtered off and to the filtrate dilute HCl was added drop wise to obtain yellow precipitate of modified ligand **L2′** along with **L2H**. **L2′** was separated by using preparative thin layer chromatography in methanol. Elemental analyses for $C_{19}H_{23}N_5O_2$, calcd(%):C, 64.57; H, 6.56; N, 19.82; found (%): C, 64.50; H, 6.55; N, 19.90: FT-IR (in KBr): 2925, 1652, 1600, 1490, 1450, 1312, 1285, 1165, 1110, 1075, 1000 cm^{-1}. ^{1}H-NMR (400 MHz, CD_3OD) δ_{ppm}: 1.21 (t, 6H), 1.91 (s, 6H), 2.61 (q, 4H), 5.57 (s, 1H), 6.78 (d, 1H), 7.52 (d, 1H), 7.55 (s, 1H). ^{13}C-NMR (100 MHz, CD_3OD) δ_{ppm}: 11.7, 14.2, 22.9, 25.1, 117.8, 121.3, 123.4, 128.7, 131.1, 137.8, 181.5. Mass (m/z): Calcd: 353.18, found: 354.20 (M+1).

3.3.5 Synthesis of complex 3.1a

$[Cu(CH_3CN)_4]ClO_4$ (326 mg, 1 mmol) was taken in a 25 ml round bottom flask and dissolved in 10 ml of acetonitrile. The solution was degassed by purging argon for 30 minute. To it, degassed methanol solution of 353 mg of ligand **L2′** was added drop wise and stirred for 1hour. To it, dry and degassed diethyl ether was added to get precipitate of brown solid. The filtrate was removed by syringe in degassed condition and solid part was dried by purging argon and stored in argon atmosphere. FT-IR (in KBr): 2930, 2255, 1630, 1505, 1456, 1375, 1285, 1128, 624 cm^{-1}. Mass (m/z): Calcd: 416.11, found: 416.20.

3.4 Conclusion

The reaction of NO with a Cu(II) complex, **3.1** in acetonitrile:methanol (5:1, v/v) solution was studied. Spectroscopic evidence suggest that the reduction of Cu(II) center by NO with concomitant C-nitrosation of the ligand took place at the initial stage of reaction. This resulted in the formation of corresponding Cu(I) complex of the C-nitroso ligand. In the presence of NO, the Cu(I) complex afforded a binuclear N-nitrosohydroxylaminato complex, **3.2** through the formation of corresponding Cu(I)-nitrosyl intermediate. A small fraction of the nitrosyl intermediate decomposed to the corresponding Cu(II) complex **3.3,** $[Cu(L2^{/})_2]$, and N_2O in a parallel reaction.

3.5 References

(1) Zuman, P.; Shah, B. *Chem. Rev.* **1994**, *94*, 1621.

(2) Lee, J.; Chen, L.; West, A. H.; Richter-Addo, G. B. *Chem. Rev.* **2002**, *102*, 1019.

(3) Maples, K. R.; Eyer, P.; Mason, R. P. *Mol. Pharmacol.* **1990**, *37*, 311.

(4) Becker, A. R.; Sternson, L. A. *Bioorg. Chem.* **1980**, *9*, 305.

(5) Eyer, P.; Ascherl, M. *Biol. Chem. Hoppe-Seyler* **1987**, *368*, 285.

(6) (a) Fukuto, J. M.; Bartberger, M. D.; Dutton, A. S.; Paolocci, N.; Wink, D. A.; Houk, K. N. *Chem. Res. Toxicol* **2005**, *18*, 790. (b) Paolocci, N.; Jackson, M. I.; Lopez, B. E.; Miranda, K.; Tocchetti, C. G.; Wink, D. A.; Hobbs, A. J.; Fukuto, J. M. *Pharmacol. Ther.* **2007**, *113*, 442.

(7) Srivastava, R. S.; Khan, M. A.; Nicholas, K. M. *J. Am. Chem. Soc.* **2005**, *127*, 7278.

(8) Yamamoto, Y.; Yamamoto, H. *J. Am. Chem. Soc*. **2004**, *126*, 4128.

(9) Askari, M. S.; Girard, B.; Murugesu, M.; Ottenwaelder, X. *Chem. Commun*. **2011**, *47*, 8055.

(10) (a) Williams, K. D.; Cardenas, A. J. P.; Oliva, J. D.; Warren, T. H. *Eur. J. Inorg. Chem*. **2013**, 3812. (b) Wiese, S.; Kapoor, P.; Williams, K. D.; Warren, T. H. *J. Am. Chem. Soc*. **2009**, *131*, 18105.

(11) Rout, K. C.; Mondal, B. *Dalton Trans*. **2015**, *44*, 1829.

(12) (a) Rajendiran, T. M.; Kannappan, R.; Venkatesan, R.; Rao, P. S.; Kandaswami, M. *Polyhedron* **1999**, *18*, 3085. (b) O'Connor, C. J. *Prog. Inorg. Chem.* **1982**, *29*, 203.

(13) (a) Thakurta, S.; Chakraborty, J.; Rosair, G.; Tercero, J.; Fallah, M. S. E.; Garribba, E.; Mitra, S. *Inorg. Chem*. **2008**, *47*, 6227.

(14) (a) Massoud, S. S.; Junk, T.; Louka, F. R.; Herchel, R.; Travnicek, Z.; Fischerc, R. C.; Mautner, F. A. *RSC Adv.* **2015**, *5*, 87139.

(15) Kalita, A.; Deka, R. C.; Mondal, B. *Inorg. Chem*. **2013**, *52*, 10897.

(16) (a) Holz, R. C.; Bradshaw, J. M.; Bennett, B. *Inorg. Chem*. **1998**, *37*, 1219; (b) Sikdar, Y.; Modak, R.; Bose, D.; Banerjee, S.; Bienko, D.; Zierkiewich, W.; Bienko, A.; Saha, K. D.; Goswami, S. *Dalton Trans.* **2015**, *44*, 8876.

(17) (c) Sarma, M.; Kalita, A.; Kumar, P.; Singh, A.; Mondal, B. *J. Am. Chem. Soc*. **2010**, *132*, 7846.

(18) (a) Sarma, M.; Mondal, B. *Inorg. Chem*. **2011**, *50*, 3206. (b) Sarma, M.; Singh, A.; Gupta, G. S.; Das, G.; Mondal, B. *Inorg. Chim. Acta* **2010**, *363*, 63.

(19) Srivastava, R. S.; Traver, N. R.; Nicholas, K. M. J. *Am. Chem. Soc*. **2007**, *129*, 15250.

(20) Tsuge, K.; DeRosa, F.; Lim, M. D.; Ford, P. C. *J. Am. Chem. Soc*. **2004**, *126*, 6564.

(21) Tran, D.; Ford, P. C. *Inorg. Chem*. **1996**, *35*, 2411.

(22) Calligaris, M.; Yoshida, T.; Otsuka, S. *Inorg. Chim. Acta* **1974**, *11*, L15–L16.

(23) (a) Carrier, S. M.; Ruggiero, C. E.; Tolman, W. B.; Jameson, G. B. *J. Am. Chem. Soc*. **1992**, *114*, 4407. (b) Ruggiero, C. E.; Carrier, S. M.; Antholine, W. E.; Whittaker, J. W.; Cramer, C. J.; Tolman, W. B. *J. Am. Chem. Soc*. **1993**, *115*, 11285.

(24) Shafirovich, V.; Lymar, S. V. *Proc. Natl. Acad. Sci. U.S.A.* **2002**, *99*, 7340.

(25) Hughes, E. E. *J. Chem. Phy*. **1961**, *35*, 1531.

(26) *SMART, SAINT and XPREP*, Siemens Analytical X-ray Instruments Inc., Madison, Wisconsin, USA, **1995**.

(27) Sheldrick, G. M. *SADABS*: *software for Empirical Absorption Correction*, University of Gottingen, Institut fur Anorganische Chemieder Universitat, Tammanstrasse 4, D-3400 Gottingen, Germany, **1999**.

(28) Sheldrick, G. M. *SHELXS-97*, University of Gottingen, Germany, **1997**.

(29) Farrugia, L. J. *J. Appl. Crystallogr*. **1997**, *30*, 565.

Chapter 4

Effect of ligand denticity on the nitric oxide reactivity of its cobalt(II) complexes

Abstract

The activation of nitric oxide (NO) by transition metal complexes has attracted a wide range of research activity. To study the role of ligand denticity on the NO reactivity of Co(II) complexes, three complexes (**4.1**, **4.2** and **4.3**) were prepared with ligands **L3**, **L4** and **L5** {**L3** = N^1,N^2-*bis*(2,4,6-trimethylbenzyl)ethane-1,2-diamine; **L4** = N^1-(2,4,6 trimethylbenzyl)-N^2-(2-((2,4,6-trimethylbenzyl)amino)ethyl)ethane-1,2-diamine and **L5** = N^1-(2,4,6-trimethylbenzyl)-N^2,N^2-*bis*(2-((2,4,6-trimethylbenzyl)amino)ethyl)ethane-1,2-diamine}, respectively. The complexes differ from each other in terms of denticity and flexibility of the ligand frameworks. In degassed methanol solution, they were exposed to NO gas and their reactivity was studied using various spectroscopic techniques. In the case of complex **4.1** with a bidentate ligand, reductive nitrosylation of the metal ion with concomitant dinitrosation of the ligand framework was observed. Complex **4.2** with a tridentate ligand did not undergo reductive nitrosylation; rather, the formation of [Co(III)(NO^-)] was observed. The nitrosyl complexes were isolated and structurally characterized. On the other hand, complex **4.3** with a tetradentate tripodal ligand did not react with NO. This can be attributed to the geometry of the complex as well as due to the accessibility of the corresponding redox potential.

4.1 Introduction

Nitric oxide (NO) plays diverse roles in biological processes such as neurotransmission, immune responses, regulation of blood pressure etc.[1-4] Most of these reactivity are attributed to the interaction of NO with the metallo-proteins.[1-5] The biological roles of NO inspire a wide range of studies of its coordination and interaction with transition metal centers.[6-9] NO chemistry of cobalt has not been studied as extensively as that of iron, perhaps because of less significance of cobalt in biological systems. However, cobalt nitrosyls are interesting for it's several unique reactions. For instance, cobalt dinitrosyls nitrosylate alkene double bonds to result in corresponding *bis*-nitroso compounds.[10] Cobalt is also known to mediate the disproportionation of NO which is industrially important.[10] Like iron nitrosyls, a variety of cobalt nitrosyls are known; however, cobalt mononitrosyls having $\{Co(NO)\}^7$ and $\{Co(NO)\}^9$ configurations are rare and only a few examples are there in literature.[11] On the other hand, recently Harrop *et al.* reported an example where cobalt nitrosyl complex in a pyrrole/imine ligand frame having $\{CoNO\}^8$ configuration could serve as potential HNO donor.[12] The reported $\{CoNO\}^8$ complex in the presence of stoichiometric amount of H^+ behaves as an HNO donor. In the absence of an HNO target, the $\{Co(NO)_2\}^{10}$ dinitrosyl was found as the end product. Thus the NO reactivity of cobalt complexes is a field of ongoing current research.

It has been reported recently that the ligand denticity and geometry plays a considerable role in controlling the reactivity of NO with transition metal complexes. For instance, Cu(II) complex of macrocyclic 5,5,7,12,12,14-hexamethyl-1,4,8,11-tetraazacyclotetra decane ligand does not react with NO in pure acetonitrile solvent; whereas the same with analogous 5,5,7-trimethyl-[1,4]-diazepane ligand in acetonitrile solution reacts with NO to afford $\{CuNO\}^{10}$ intermediate followed by the reduction of the metal center.[13] Recently,

Lippard's group demonstrated the influence of tetraazamacrocyclic tropocoronand (TC) ligands on the NO reactivity of their Co(II) complexes. [Co(TC-3,3)] , [Co(TC-4,4)] and [Co(TC-5,5)] were found to result in the formation of corresponding mononitrosyls, which were then isolated and structurally characterized. On the other hand, [Co(TC-6,6)] upon reaction with NO, results in $\{Co(NO)_2\}^{10}$ species which was further decomposes to $[Co(NO_2)(TC\text{-}6,6)]$ complex.[14] Thus, the increasing length of the polymethylene linker of the ligand framework was found to control the reactivity of the complexes.

This chapter we demonstrates the difference of NO reactivity of three Co(II) complexes based on their ligand denticity and geometry. For the present study mesityl derivatives of ethylene diamine {**L3** = N^1, N^2-*bis*(2,4,6-trimethylbenzyl)ethane-1,2-diamine}, BAEA {**L4**= N^1-(2,4,6-trimethylbenzyl)-N^2-(2-((2,4,6-trimethylbenzyl)amino) ethyl)ethane-1,2-diamine} and TAEA {**L5** =N^1-(2,4,6-trimethylbenzyl)-N^2,N^2-*bis*(2-((2,4,6 trimethylbenzyl) amino)ethyl)ethane-1,2-diamine} have been used (Figure 4.1).

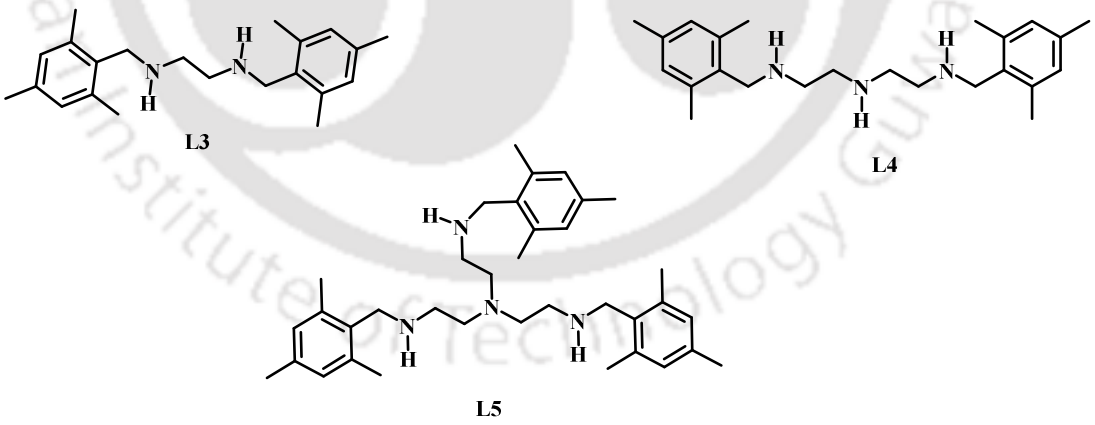

Figure 4.1 Ligands used for the present study.

4.2 Results and Discussion

The ligands were prepared by the general reaction of mesitylaldehyde with corresponding amine followed by the reduction of the imine with $NaBH_4$ following an earlier reported procedure.[15] All the ligands were characterized by spectroscopic analyses as well as elemental analyses (Experimental Section).

Metallation was achived by stirring the ligand with equivalent amount of cobalt(II) chloride hexahydrate in methanol (Experimental Section). The complexes were isolated as solid and characterized by spectral analyses (Experimental Section and Appendix III) and by their single crystal structure determination. The ORTEP views of the complexes are given in figure 4.2. The crystallographic data, selected bond distances and angles are listed in tables 4.1, 4.2 and 4.3 respectively. The crystal structure reveals that in complex **4.1**, the metal ion, Co(II) is hexa-coordinated. Four N-atoms from two ligand moieties and two Cl are coordinated to Co(II) in an octahedral geometry. The N-atoms form a square plane and the Cl atoms are coordinated from the axial positions in *trans* fashion. In complex **4.2**, Co(II) is hexa-coordinated. Three N-atoms from the ligand, two Cl and one solvent water molecule is coordinated to the central metal ion in a distorted octahedral geometry. The Cl atoms are coordinated from the axial positions. However, in complex **4.3**, the metal ion is five-coordinated in trigonal bipyramidal geometry. Three secondary N-atoms from the ligand form the trigonal plane; tertiary N-atom of the ligand and the one Cl atom are coordinated from the axial positions to complete the geometry. The charge of metal ion is satisfied by the presence of a second Cl ion in the unit cell. The order of average Co(II)-N bond length of the complexes is **4.1** > **4.2** > **4.3** (2.224, 2.141 and 2.123 Å, respectively). However, all these bond lengths are in a normal range when compared to those in analogous reported complexes.[16]

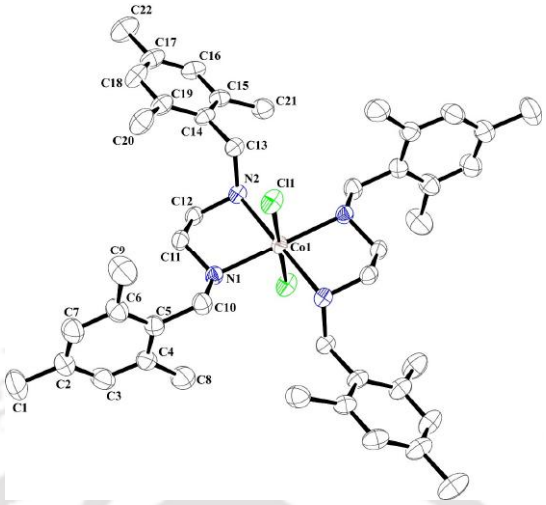

(a)

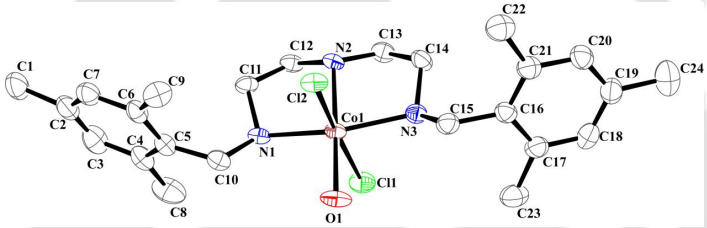

(b)

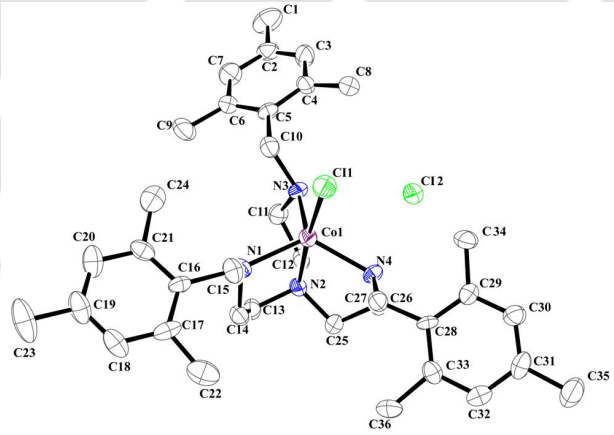

(c)

Figure 4.2 ORTEP diagrams of complexes (a) **4.1**, (b) **4.2** and (c) **4.3** (30% thermal ellipsoid plot, H-atoms are omitted for clarity).

In the UV-visible spectroscopy, complexes **4.1** and **4.2** in methanol solution show *d-d* transition band at 560 nm ($\varepsilon/M^{-1}cm^{-1}$, 237) and 525 nm ($\varepsilon/M^{-1}cm^{-1}$, 300), respectively. Complex **4.3**, in methanol solution absorbs at 480 nm ($\varepsilon/M^{-1}cm^{-1}$, 357), 594 nm ($\varepsilon/M^{-1}cm^{-1}$, 222), 760 nm ($\varepsilon/M^{-1}cm^{-1}$, 85). The difference in absorption band is attributed to the trigonal bipyramidal geometry of complex **4.3**.[17] The all the three complexes are EPR active in X-band EPR spectroscopy confirming the presence of Co(II) centre (Appendix III).[18] The cyclic volatmmogram of the complexes are recorded in methanol using tetrabutylammonium perchlorate supporting electrolyte in a three electrode configuration with Ag/Ag^{+} reference, glassy carbon working and Pt auxiliary electrodes. The voltammogram shows the presence of irreversible reductions at -0.468 and -0.318 V in cases of complexes **4.1** and **4.2**, respectively (Appendix III). These are attributed to the Co(II)/Co(I) reduction.[19] However, complex **4.3**, does not show any electrode process in this range suggesting a relatively high reduction potential for Co(II)/Co(I) couple. On the positive side, the Co(II)/Co(III) irreversible couple for complexes **4.1**, **4.2** and **4.3** appears at 0.304, 0.585 and 0.429 V, respectively.

Nitric oxide reactivity

NO was added into the dry and degassed methanol solution of complex **4.1** and the mixture was allowed to stand overnight, resulting in the formation of complex **4.4a** as brown precipitate. Elemental and spectral analyses confirm the formation of the complex (Experimental Section). However, the X-ray quality crystals were not grown. To get X-ray quality crystals, the counter anion has been replaced by perchlorate anion (**4.4b**) (Experimental Section). Single crystal structure of complex **4.4b** (Figure 4.4) reveals the presence of Co(I)-dinitronsyl, $\{Co(NO)_2\}^{10}$ moiety where Co(I) is tetrahedrally coordinated by two N-atoms from the ligand and two NO groups. The Co-N_{NO} distances

Table 4.1 Crystallographic data for complex **4.1, 4.2, 4.3, 4.4b, 4.5** and modified ligand **L3′**.

	4.1	**4.2**	**4.3**	**4.4b**	**4.5**	**L3′**
Formulae	$C_{44}H_{64}Cl_2CoN_4O_5$	$C_{24}H_{39}Cl_2N_3O_2$	$C_{36}H_{54}Cl_2CoN_4O$	$C_{23}H_{36}ClCoN_4O_7$	$C_{25}H_{41}Cl_2CoN_4O_2$	$C_{22}H_{30}N_4O_2$
Molecular weight	858.82	531.41	688.66	574.94	559.45	382.50
Crystal system	Monoclinic	Orthorhombic	Monoclinic	Triclinic	Monoclinic	Monoclinic
Space group	P 2/c	P 21 21 21	P 21/n	P -1	P 21/n	P 21/c
Temperature/K	293	293	296	293	293	293
Wavelength	0.71073	0.71073	0.71073	0.71073	0.71073	0.71073
a/Å	14.2041 (6)	27.9485 (17)	14.7068 (15)	9.0274 (8)	11.0311 (13)	4.9480 (4)
b/Å	10.6502 (4)	11.5046 (5)	15.7398 (16)	12.0143 (10)	12.658 (2)	17.236 (2)
c/Å	16.5585 (6)	8.5689 (2)	17.2246	14.0393 (10)	20.544 (3)	12.605 (8)
α/°	90	90	90	70.559 (7)	90	90
β/°	95.337 (4)	90	105.099 (7)	76.564 (7)	96.626 (13)	91.761 (7)
γ/°	90	90	90	87.579 (10)	90	90
V/ Å^3	2494.05 (17)	2755.2 (2)	3769.7(4)	1395.5 (2)	2849.3 (7)	1074.47(16)
Z	2	4	4	2	4	2
Density/gcm^{-1}	1.144	1.281	1.213	1.368	1.297	1.182
Absorption Coefficient	0.493	0.841	0.616	0.757	0.817	0.077
Absorption Correction	Multi-scan	Multi-scan	Multi-scan	Multi-scan	Multi-scan	Multi-scan
F(000)	914.0	1124.0	1468.0	604.0	1184.0	412.0
Total no of reflections	4396	4668	6824	5040	5147	1936
Reflections, *I>2σ(I)*	3371	3614	4912	3833	1928	1091
Max. 2θ/°	25.00	25.25	25.25	25.25	25.25	25.25
Ranges (h, k, l)	-16≤ h ≤15 -12≤ k ≤9 -19≤ l ≤12	-21≤ h ≤33 -8≤ k ≤13 -9≤ l ≤10	-15≤ h ≤17 -18≤ k ≤18 -15≤ l ≤20	-10≤ h ≤10 -14≤ k ≤14 -16≤ l ≤12	-13≤ h ≤13 -11≤ k ≤15 -15≤ l ≤24	-5≤ h ≤5 -20≤ k ≤20 -15≤ l ≤14
Complete to 2θ(%)	99.8	99.7	99.8	99.8	99.7	99.8
Refinement method	Full-matrix least-squares on F^2	Full-matrix least-squares on F^2	Full-matrix least-squares on F^2	Full-matrix least-squares on F^2	Full-matrix least-squares on F^2	Full-matrix least-squares on F^2
Goof (F^2)	1.154	1.083	1.296	1.188	1.043	1.230
R indices [*I>2σ(I)*]	0.0654	0.0581	0.0430	0.0615	0.0918	0.0774
R Indices (all data)	0.0832	0.0783	0.0681	0.0796	0.2328	0.1370

Table 4.2 List of selected bond lengths (Å) of complex **4.1, 4.2, 4.3, 4.4b, 4.5** and modified ligand **L3′**.

Atoms	**4.1**	**4.2**	**4.3**	**4.4b**	**4.5**	**L3′**
Co(1)-N(1)	2.150 (3)	2.169 (5)	2.095 (19)	2.033 (3)	1.990 (6)	-
Co(1)-N(2)	2.298 (3)	2.122 (5)	2.119 (18)	2.022 (2)	1.936 (7)	-
Co(1)-N(3)	-	2.153 (5)	2.081 (19)	1.654 (5)	2.022 (6)	-
Co(1)-O(1)		2.036 (4)				
Co(1)-N(4)	-		2.218 (18)	1.659 (4)	1.765 (10)	-
Co(1)-Cl(1)	2.459 (10)	2.641 (17)	2.310 (7)	-	2.243 (3)	-
Co(1)-Cl(2)		2.459 (16)				
N(1)-C(11)	1.484 (5)	1.490 (7)	1.477 (3)	1.487 (5)	1.484 (10)	1.453 (4)
N(2)-C(12)	1.480 (5)	1.464 (7)		1.487 (5)	1.472 (9)	-
N(2)-C(13)	1.486 (5)	1.464 (8)		1.511 (5)	1.481 (9)	-
N(3)-O(1)	-			1.150 (7)		-
N(4)-O(1)					1.103 (9)	
N(2)-O(1)	-			-		1.222 (3)
N(4)-O(2)	-			1.150 (6)		-
C(5)-C(6)	1.405 (5)	1.409 (9)	1.393 (3)	1.396 (5)	1.423 (12)	1.387 (5)
C(4)-C(8)	1.495 (5)	1.490 (9)	1.526 (10)	1.513 (5)		1.508 (5)
N(1)-N(2)	-			-		1.338 (4)

Table 4.3 List of selected bond angles (°) of complex **4.1, 4.2, 4.3, 4.4b, 4.5** and modified ligand **L3′**.

Atoms	4.1	4.2	4.3	4.4b	4.5	L3′
N(2)-Co(1)-N(1)	81.38 (11)	81.19 (19)	120.34 (7)	84.80 (1)	84.30 (4)	-
N(2)-Co(1)-N(3)	-	81.05 (19)	109.82 (8)	109.00 (2)	85.90 (3)	-
N(2)-Co(1)-N(4)	-		80.29 (7)	114.50 (2)	96.80 (4)	-
N(1)-Co(1)-N(3)	-	157.52 (13)	121.76 (8)	115.90 (2)	162.60 (3)	-
N(1)-Co(1)-N(4)	-		79.65 (7)	109.40 (2)	103.00 (4)	-
O(1)-Co(1)-N(2)		177.14 (18)				
O(1)-Co(1)-N(3)		99.70 (2)				
N(3)-Co(1)-N(4)	-		79.65 (8)	118.60 (2)	92.50 (4)	-
Co(1)-N(3)-O(1)	-			170.80 (4)		-
Co(1)-N(4)-O(2)	-			169.70 (4)		-
Co(1)-N(4)-O(1)					124.57 (10)	
Co(1)-N(1)-C(10)	120.60 (3)	116.60 (14)	100.75 (5)	116.80 (2)	120.90 (5)	-
C(10)-N(1)-C(11)	112.30 (2)	114.50 (13)	115.53 (19)	114.30 (3)	111.90 (7)	122.20 (3)
C(13)-C(14)-C(15)	120.70 (4)			121.50 (3)		-
O(3)-Cl(1)-O(6)				103.40 (5)		-
N(1)-Co(1)-Cl(1)	88.04 (10)	86.05 (14)	95.65 (6)	-	95.00 (5)	-
N(2)-Co(1)-Cl(1)	88.05 (10)	94.07 (14)	102.55 (6)	-	168.20 (2)	-
O(1)-N(2)-N(1)	-			-		112.80 (3)
N(2)-N(1)-C(10)	-			-		114.30 (3)

were 1.654(5) and 1.659(4) Å, respectively. This distance is within the range of linear nitrosyls.[10a,20] The Co-N-O angles were found to be 169.8(4)° and 170.4(4)°. The N-O distances of the coordinated NO were 1.150 Å. In complex **4.1**, there are two **L3** units coordinated to the central metal. In complex **4.4b**, only one **L3** is present. Analysis of complex **4.4a** also supports this formulation. In UV-visible spectroscopy, the *d-d* transition of complex **4.1** centred on 560 nm was found to shifted to 600 nm upon addition of NO (Figure 4.3). When the filtrate part of the reaction mixture was analyzed, the presence of un-reacted **L3** and dinitrosation product (**L3′**) was observed in roughly equal proportions (Experimental Section). The dinitrosated product was isolated and purified using column chromatography and crystallographic characterization has been done (Experimental Section). The ORTEP diagram is shown in figure 4.5. It is to be noted that the free ligand, **L3** does not react with NO under the reaction condition to afford dinitrosation. However, it reacts with $NOClO_4$ leading to dinitrosation.

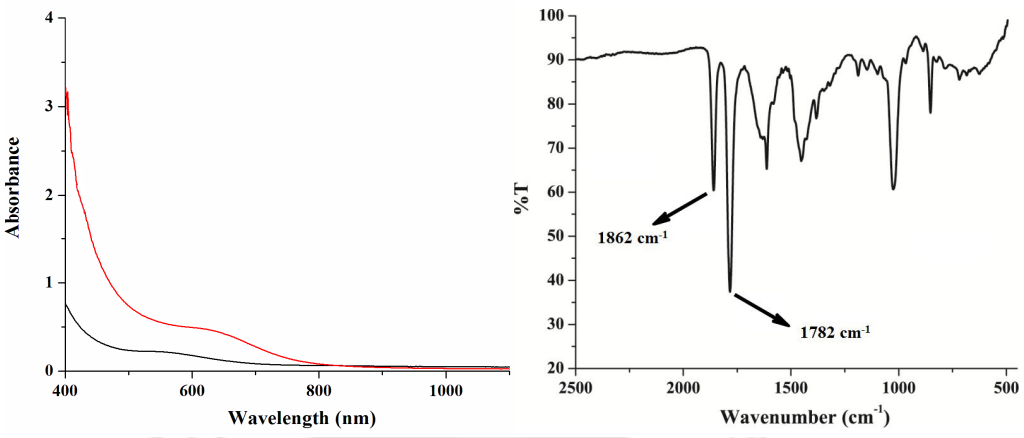

Figure 4.3 (a) UV-visible spectra of complex **4.1** (black) and upon addition of excess NO (red) in methanol. (b) FT-IR spectrum of complex **4.4a** in KBr pellet.

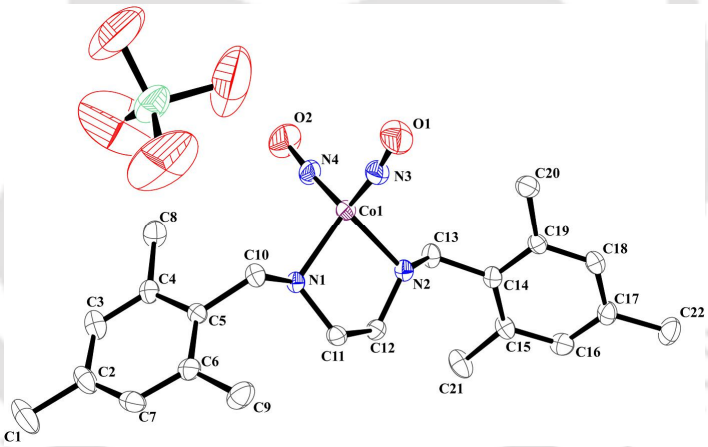

Figure 4.4 ORTEP diagram of complex **4.4b** (30% thermal ellipsoid plot, H-atoms are omitted for clarity).

In the FT-IR spectroscopy, complexes **4.4a** showed NO stretching frequencies at 1862 and 1782 cm^{-1} (Figure 4.3) which are assignable to the $\{Co(NO)_2\}^{10}$ unit.[20] In case of dinitrosyl of [Co(TC-6,6)], the NO stretching were observed at 1807 and 1730 cm^{-1} in CH_2Cl_2. These stretching of $[Co_2(NO)_4(TC\text{-}6,6)]$ were observed at 1799 and 1720 cm^{-1} in CH_2Cl_2 solution.[14a] In general, tertrahedral $\{Co(NO)_2\}^{10}$ complexes exhibit symmetric and

asymmetric NO stretching bands between 1820-1876 cm^{-1} and between 1755-1798 cm^{-1}, respectively.[21]

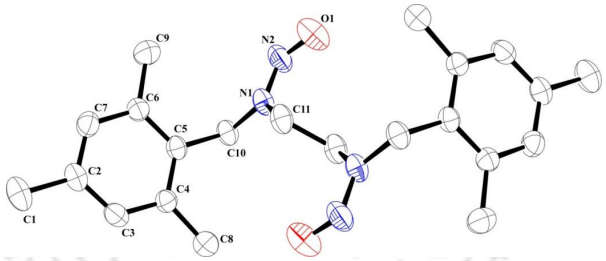

Figure 4.5 ORTEP diagram of modified ligand **L3′** (30% thermal ellipsoid plot, H-atoms are omitted for clarity).

It has been reported earlier that addition of excess NO to CH_2Cl_2 solution of Co(II) complex, $[Co(^{i}PrDATI)_2]$, results in the formation of corresponding Co(I)-dinitrosyl adducts.[18,22] FT-IR spectrum shows the appearance of two bands at ~1838 and ~1760 cm^{-1} indicating the presence of dinitrosyl complexes. In ^{1}H-NMR spectrum after the reaction, two sets of resonances for diamagnetic compounds corresponding to the free ligand H^{i}PrDATI and the $\{Co(NO)_2\}^{10}$ species $[Co(NO)_2(^{i}PrDATI)]$ were observed.[22] It is believed that the reaction proceeds by a reductive nitrosylation mechanism (Scheme 4.1). Similarly, the reactions of $[Co(^{t}BuDATI)_2]$, $[Co(BzDATI)_2]$, and [Co(DATI-4)] in CH_2Cl_2 solutions with NO are slow, but after several hours of exposure to an NO atmosphere, the formation of corresponding dinitrosyl complexes were observed.[18,22]

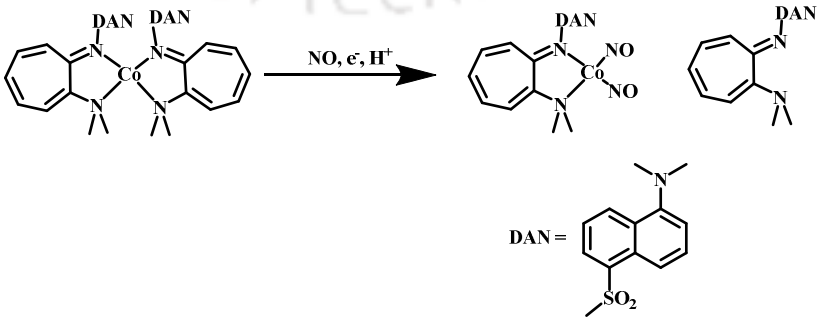

Scheme 4.1

Cobalt dinitrosyl complexes are known as 4-coordinated, pseudotetrahedral species having $\{Co(NO)_2\}^{10}$ configuration in the Enemark-Feltham notation for metal nitrosyls.[23] In some examples, the formation of $\{Co(NO)_2\}^{10}$ from Co^{2+} complexes were reported to proceed through the disproportionation of $[Co^{II}(L)_2]$ to give $[Co^{I}(NO)_2L]$ and $[Co^{III}(L)_3]$ {L = bidented ligands}. [24] In the present case, the formation of *tris*(chelate)Co^{3+} was not evidenced at any stage of reaction. The formation of dinitrosated **L3′** in almost quantitative amount suggests the quantitative formation of nitrosonium ion. This suggests NO act as the reductant in this reductive nitrosylation mechanism. [25]

On the other hand, addition of excess NO gas into the dry and degassed methanol solution of complex **4.2** led to the formation of complex **4.5** (Scheme 4.2). In UV-visible study, complex **4.2** and **4.5** exhibit characteristic absorption bands at 525 nm ($\varepsilon/M^{-1}cm^{-1}$, 300) and 475 nm ($\varepsilon/M^{-1}cm^{-1}$, 521), respectively (Figure 4.6). FT-IR spectrum of complex **4.5** in KBr pellet exhibit a strong stretching band at 1659 cm^{-1} assignable to the coordinated NO (Figure 4.6). This low energy stretching band for metal-nitrosyl is consistent with $Co^{III}(NO^{-})$ or $\{Co(NO)\}^8$ formulation.[26] In the case of recently reported Co^{III}-nitrosyl complexes bearing 12- and 13- membered N-tetramethylated cyclam (TMC) ligands, $[(12\text{-TMC})Co^{III}(NO)]^{2+}$ (12-TMC = 1,4,7,10-tetramethyl-1,4,7,10-tetraazacy clododecane) and $[(13\text{-TMC})Co^{III}(NO)]^{2+}$ (13-TMC = 1,4,7,10-tetramethyl-1,4,7,10-tetraazacyclotridecane), this frequency was observed at 1712 and 1716 cm^{-1}, respectively.[27] In electron paramagnetic resonance (EPR) studies, though complex **4.2** showed characteristic signals, complex **4.5** is silent (Appendix III). This is also suggesting the trivalency of the cobalt centre and thus formally $Co^{III}(NO^{-})$ or $\{Co(NO)\}^8$ descriptions.[26, 27] Electrospray ionization mass spectrometry (ESI-MS) of complex **4.5** exhibits a prominent ion peak at m/z 491.17 (Appendix III). The mass and isotope distribution patterns of this ion peak

match well with **4.5** (Calculated m/z for $[Co(L4)(NO)Cl]^+$, 491.19). In addition, complex **4.5** was structurally characterized by single-crystal X-ray crystallography. The NO group is coordinated to the central metal ion, cobalt from the apical position in an end-on fashion having a distorted square pyramidal geometry (Figure 4.7). The three corners of the square plane are occupied by the nitrogen atoms from the ligand and a chloride ion fulfils the fourth site. The Co-N_{NO} distance is 1.765 Å and the Co-N-O angle of 124.57(5)° suggest the bent fashion of nitrosyl binding.[26, 27]

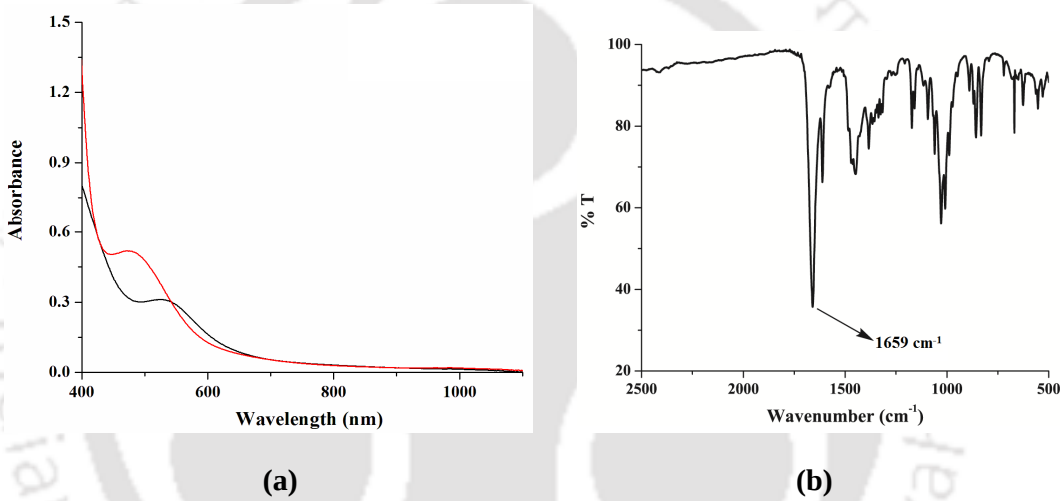

Figure 4.6 (a) UV-visible spectrum of complex **4.2** (black) and upon addition of excess NO (red) in methanol. (b) FT-IR spectrum of complex **4.5** in KBr pellet.

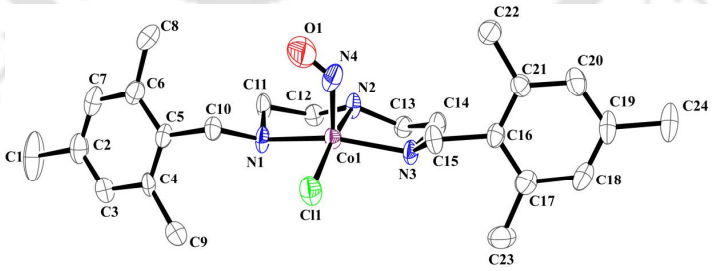

Figure 4.7 ORTEP diagram of complex **4.5** (30% thermal ellipsoid plot, H-atoms are omitted for clarity).

Thus the crystal structure also supports the [$Co^{III}(NO^{-})$] formulation having {Co(NO)}^{8} description. Complex **4.3**, in the similar reaction condition was not found to react with NO even after several days.

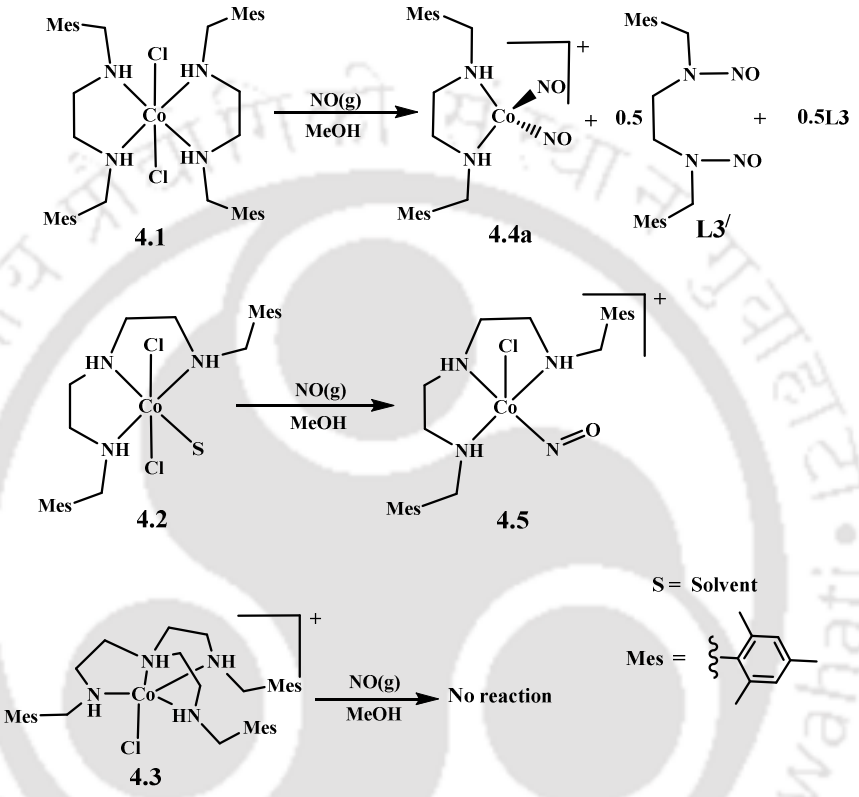

Scheme 4.2

Thus, while moving from complexes **4.1** to **4.3**, the reactivity of the complexes towards NO changes. In case of complex **4.1**, reductive nitrosylation of the metal ion takes place resulting in the corresponding cobalt(I)-dinitrosyl, while in **4.2**, addition of NO resulted in the formation of [$Co^{III}(NO^{-})$] and complex **4.3** does not react with NO (Scheme 4.2). The ligand framework including denticity has a considerable effect on dictating the NO reactivity of a complex. In case of Co(II) complexes of tropocoronand ligands, it has been reported that the ring size of the ligand controls the reactivity by controlling the

tetrahedral character of the cobalt dinitrosyls over square planar one. In case of complex **4.1**, the formation of tetrahedral $\{Co(NO)_2\}^{10}$ is favourable from the structural as well as redox potential point of views. In complexes **4.2** and **4.3**, the ligand frameworks do not prefer tetrahedral geometry as such.

4.3 Experimental Section

4.3.1 Materials and methods

All reagents and solvents were purchased from commercial sources and were of reagent grade. Deoxygenation of the solvent and solutions were effected by repeated vacuum/purge cycles or bubbling with nitrogen for 30 minutes. NO gas was purified by passing through KOH and P_2O_5 column. UV-visible spectra were recorded on a HP/Agilent 8453 UV-visible spectrophotometer. FT-IR spectra of the solid samples were taken on a Perkin Elmer spectrophotometer with samples prepared as KBr pellets. Solution electrical conductivity was checked using a Systronic 305 conductivity bridge. ^{1}H-NMR spectra were obtained with a 400 MHz Varian FT spectrometer. Chemical shifts (ppm) were referenced either with an internal standard (Me_4Si) or to the residual solvent peaks. The X-band Electron Paramagnetic Resonance (EPR) spectra were recorded on a JES-FA200 ESR spectrometer, at room temperature. Elemental analyses were obtained from a Perkin Elmer Series II Analyzer. The magnetic moment of complexes is measured on a Cambridge Magnetic Balance.

Single crystals were grown by slow diffusion followed by slow evaporation technique. The intensity data were collected using a Bruker SMART APEX-II CCD diffractometer, equipped with a fine focus 1.75 kW sealed tube MoK_α radiation (λ = 0.71073 Å) at 273(3) K, with increasing ω (width of 0.3° per frame) at a scan speed of 3 s/frame. The SMART

software was used for data acquisition. Data integration and reduction were undertaken with SAINT and XPREP software.[28] Multi-scan empirical absorption corrections were applied to the data using the program SADABS.[29] Structures were solved by direct methods using SHELXS-97 and refined with full-matrix least squares on F^2 using SHELXL-97.[30] Structural illustrations have been drawn with ORTEP-3 for Windows.[31]

4.3.2 Synthesis of ligands

(a) Ligand L3

Ethylene diamine (0.60 g, 10 mmol) was taken in a round bottom flask in 50 ml of ethanol. To this, 2.96 g (20 mmol) of mesitaldehyde was added dropwise. The reaction mixture was stirred for 1 hour to give light yellow precipitate of Schiff base. The Schiff base was reduced by 2.5 equivalent of $NaBH_4$ in ethanol to give **L3** (yield, 2.50g, 78%). Elemental analyses for $C_{22}H_{32}N_2$, calcd(%): C, 81.43; H, 9.94; N, 8.63; found (%): C, 81.48; H, 9.95; N, 8.77. FT-IR (in KBr): 3314, 3200, 2922, 2787, 1611, 1459, 1089, 849, 805, 772 cm^{-1}. ^{1}H-NMR (400 MHz, $CDCl_3$) δ_{ppm}: 2.21 (s, 6H), 2.32 (s, 12H), 2.82 (s, 2H), 3.71 (s, 4H), 6.82 (s, 4H),. ^{13}C-NMR (100 MHz, $CDCl_3$) δ_{ppm}: 19.7, 21.0, 47.7, 49.9, 129.1, 134.0, 136.4, and 137.0. Mass (m/z): Calcd: 324.25, found: 325.20 (M+1).

(b) Ligand L4

N-(2-aminoethyl)ethane-1,2-diamine (1.03 g, 10 mmol) was taken in a round bottom flask in 50 ml of ethanol. To this, 2.96 g (20 mmol) of mesitaldehyde was added dropwise. The reaction mixture was stirred for 1 hour to give a yellow solution of Schiff base. The Schiff base was reduced by 3 equivalent of $NaBH_4$ in ethanol. The solution was dried and ligand **L4** was extracted with chloroform (yield, 2.75g, 75%). Elemental analyses for $C_{24}H_{37}N_3$,

calcd(%): C, 78.42; H, 10.15; N, 11.43; found (%): C, 78.34; H, 10.14; N, 11.58. FT-IR (in KBr): 3430, 2925, 2848, 1611, 1485, 1450 1105, 1031, 849, 716 cm^{-1}. ^{1}H-NMR (400 MHz, $CDCl_3$) δ_{ppm}: 2.25 (s, 6H), 2.33 (s, 12H), 2.72 (t, 4H), 2.79 (t, 4H), 3.72 (s, 4H), 6.83 (s, 4H),. ^{13}C-NMR (100 MHz, $CDCl_3$) δ_{ppm}: 19.6, 21.0, 47.6, 49.5, 49.6, 129.1, 133.8, 136.5, 137.0, and. Mass (m/z): Calcd: 367.30, found: 368.31 (M+1).

(c) Ligand L5

Tris-(2-aminoethyl)amine (1.46 g, 10 mmol) was taken in a round bottom flask in 50 ml of ethanol. To it 4.44 g (30 mmol) mesitaldehyde was added drop wise. The reaction mixture was stirred for 1 hour at 60 °C. The color of the solution becomes dark yellow. It was reduced by 4.5 equivalent of $NaBH_4$ in ethanol. The solution was dried and ligand **L5** was extracted with chloroform (yield, 4.5g, 82 %). Elemental analyses for $C_{36}H_{54}N_4$, calcd(%): C, 79.65; H, 10.03; N, 10.32; found (%): C, 79.72; H, 10.05; N, 10.43. FT-IR (in KBr): 3428, 2915, 1612, 1448, 1378, 1111, 1050, 850, 716 cm^{-1}. ^{1}H-NMR (400 MHz, $CDCl_3$) δ_{ppm}: 2.22 (s, 9H), 2.25 (s, 18H), 2.55 (t, 6H), 2.67(t, 6H), 6.77 (s, 6H). ^{13}C-NMR (100 MHz, $CDCl_3$) δ_{ppm}: 19.7, 21.0, 47.7, 47.9, 54.8, 129.1, 133.9, 136.4, 137.0, and. Mass (m/z): Calcd: 542.42, found: 543.44 (M+1).

4.3.3 Synthesis of the complexes

(a) Complex 4.1, [$Co(L3)_2Cl_2$]

Cobalt(II) chloride hexahydrate, $CoCl_2.6H_2O$ (0.237 g, 1 mmol) was dissolved in 10 ml distilled methanol. To this solution, 0.648 g (2 mmol) of the ligand **L3** was added slowly with constant stirring. After ½ hour, a light pink colored precipitate of complex **4.1** was obtained. It was filtered off and washed with diethyl ether and vacuum dried (yield, 0.70g

(90%). Elemental analyses for $C_{44}H_{64}N_4CoCl_2$, calcd (%): C, 67.85; H, 8.28; N, 7.19; found (%): C, 67.91; H, 8.27; N, 7.26. FT-IR (in KBr): 3270, 2960, 1613, 1450, 1380, 1000, 928, 887, 850 cm^{-1}. UV-visible (in methanol): 560 nm (ε/ M^{-1} cm^{-1}, 237), g_{av} = 2.01. Mass (m/z): Calcd: 777.38, found: 778.51(M+1). Molar conductivity: 50 S cm^2 mol^{-1}.

(b) Complex 4.2, [Co(L4)Cl_2(H_2O)]

Cobalt(II) chloride hexahydrate, $CoCl_2.6H_2O$ (0.237 g, 1 mmol) was dissolved in 10 ml distilled methanol. To this solution, 0.367 g (1 mmol) of the ligand **L4** was added slowly with constant stirring. Complex **4.2** was precipitated out from the reaction mixture. It was filtered and washed with diethyl ether to get the pure crystalline complex **4.2** (yield, 0.40 g, 77%). Elemental analyses for $C_{24}H_{39}N_3CoCl_2O$, calcd (%): C, 55.93; H, 7.63; N, 8.15; found (%): C, 55.84; H, 7.61; N, 8.21. FT-IR (in KBr): 3429, 3250, 2915, 1611, 1456, 1380, 1170, 970, 850 cm^{-1}. UV-visible (in methanol): 525 nm (ε/ M^{-1} cm^{-1}, 300), g_{av} = 2.01. Mass (m/z): Calcd: 537.20 for [Co(L4)Cl_2(CH_3CN)], found: 537.21. Molar conductivity: 60 S cm^2 mol^{-1}.

(c) Complex 4.3, [Co(L5)Cl]Cl

Cobalt(II) chloride hexahydrate, $CoCl_2.6H_2O$ (0.474 g, 2 mmol) was dissolved in 10 ml distilled methanol. To this solution, 1.084 g (2 mmol) of the ligand **L5** was added slowly with constant stirring till a light blue colored complex **4.3** precipitated out. It was filtered off and washed with diethyl ether to obtain pure crystalline complex **4.3** (yield, 1g, 75%). Elemental analyses for $C_{36}H_{54}N_4CoCl_2$, calcd (%): C, 64.28; H, 8.09; N, 8.33; found (%): C, 64.21; H, 8.08; N, 8.45. FT-IR (in KBr): 3176, 2966, 1612, 1469, 1384, 1163, 1081, 989, 852, 816 cm^{-1}. UV-Visible (in methanol): 480 nm (ε/ M^{-1} cm^{-1}, 357), 594 nm (ε/ M^{-1}

cm^{-1}, 222), 760 nm (ε/ M^{-1} cm^{-1}, 85). g_{av}= 2.22. Mass (m/z): Calcd: 636.31, found: 636.31. Molar conductivity: 120 S cm^2 mol^{-1}.

(d) Complex 4.4a, [Co(L3)$(NO)_2$]Cl

In a 50 ml round bottom flask, 1 g of complex **4.1** was dissolved in dry methanol. The solution was degassed by purging argon for 30 minutes. To this solution, NO was purged for 2 minutes. The solution was kept overnight to result in brown precipitate of complex **4.4a** (yield, 0.60g ;~50%). Elemental analyses for $C_{22}H_{32}N_4CoO_2Cl$, calcd(%):C, 55.18; H,6.74; N, 11.70; found (%): C, 55.12; H, 6.71; N, 11.73. FT-IR (in KBr): 3409, 2960, 1860, 1782, 1612, 1456, 1380, 1030 and 852 cm^{-1}. UV-visible (in methanol): 600 nm (ε/M^{-1} cm^{-1}, 500). Mass (m/z): Calcd: 443.44, found: 443.12.

(e) Complex 4.4b, [Co(L3)$(NO)_2$](ClO_4)

In a 50 ml round bottom flask, 0.478 g of complex **4.4a** was dissolved in dry methanol. To it, 0.122 g of sodium perchlorate was added stirred for 1 hour under argon atmosphere. The solution was then kept in freeze for 4-5 days to result in dark brown crystal of complex **4.4b** (yield, 0.25g; ~45 %). Elemental analyses for $C_{22}H_{32}N_4CoO_6Cl$, calcd(%):C, 48.67; H, 5.94; N, 10.32; found (%): C, 48.70; H, 6.01; N, 10.35 . FT-IR (in KBr): 3463, 3245, 2919, 1860, 1782, 1612, 1456, 1380, 1095, 623 cm^{-1}. UV-visible (in methanol): 600 nm (ε/ M^{-1} cm^{-1}, 410). Mass (m/z): Calcd: 443.44, found: 443.13.

(f) Isolation of modified ligand L3′

In a 50 ml round bottom flask, 0.777 g of complex **4.1** was dissolved in dry methanol. The solution was degassed by purging argon for 30 minutes. To this solution, NO was purged for 2 minutes. The solution was kept overnight. The precipitate was filtered out and the

filtrate was dried and washed with acetonitrile to remove complex **4.4a**. The crude white solid was subjected to column chromatography using silica gel column to yield dinitrosation product, **L3′** and unreacted **L3**.

L3′ (yield, 0.18g, ~25 %). Elemental analyses for $C_{22}H_{30}N_4O_2$, calcd (%):C, 69.08; H, 7.91; N, 14.65; found (%): C, 69.10; H, 7.95; N, 14.70. FT-IR (in KBr): 2970, 2990, 1610, 1450, 1423, 1345, 1094, 1044, 856 cm^{-1}. ^{1}H-NMR (400 MHz, $CDCl_3$) δ_{ppm}: 2.26 (s, 6H), 2.32 (s, 12H), 3.20 (s, 4H), 5.30 (s, 4H), 6.86 (m, 4H),. ^{13}C-NMR (100 MHz, $CDCl_3$) δ_{ppm}: 20.1, 21.1, 38.8, 50.7, 126.7, 129.7, 130.0 and 138.2. Mass (m/z): Calcd: 382.24, found: 383.24 (M+1).

(g) Complex 4.5, [Co(L4)(NO)Cl]Cl

In a 50 ml round bottom flask, 0.514 g of complex **4.2** was dissolved in dry methanol. The solution was degassed by purging argon for 30 minutes. To this solution, NO was purged for 2 minutes. The solution was kept overnight to result in red crystals of complex **4.5** (yield, 0.50g, 90 %). Elemental analyses for $C_{24}H_{37}N4CoOCl_2$, calcd(%):C, 54.65; H, 7.07; N, 10.62; found (%): C, 54.68; H, 7.09; N, 10.35, FT-IR (in KBr): 3388, 3055, 2870, 1659, 1611, 1450, 1170, 1026, 856, 829, 665 cm^{-1}. UV-visible (MeOH): 475 nm ($\varepsilon/M^{-1}cm^{-1}$, 521). Mass (m/z): Calcd: 491.19, found: 491.17.

4.4 Conclusion

The NO reactivity of three Co(II) complexes, **4.1**, **4.2** and **4.3** have been studied in degassed methanol solution. The complexes differ from each other from denticity and flexibility of the ligand fameworks. In case of complex **4.1** with bidentate ligand, reductive nitrosylation of the metal ion with concomitant dinitrosation of the ligand framework was

observed. Complex **4.2** with tridentate ligand does not undergo reductive nitrosylation; rather formation of [$Co^{III}(NO^{-})$] was observed. The nitrosyl complexes were isolated and structurally characterized. On the other hand, complex **4.3** with tetradentate tripodal ligand, does not react with NO. This can be attributed to geometry of the complex as well as the accessibility of the corresponding redox potential.

4.5 References

(1) (a) Ignarro, L. J. *Nitric Oxide, Biology and Pathobiology* Ed. Academic Press; San Diego, CA, **2000**. (b) Richter-Addo, G. B.; Legzdins, P. *Metal Nitrosyls*, Oxford University Press, New York, **1992**. (c) Moncada, S.; Palmer, R. M. J.; Higgs, E. A. *Phermacol. Rev*. **1991**, *43*, 109. (d) Bredt, D. S.; Snyder, S. H. *Annu Rev. Biochem.* **1994**, *63*, 175. (e) Butler, A. R.; Williams, D. L. *Chem. Soc. Rev*. **1993**, *233*. (f) Hunt, A. P.; Lehnert, N. *Acc. Chem. Res.* **2015**, *48*, 2117.

(2) (a) *Methods in Nitric Oxide Research*, Feelisch, M.; Stamler, J. S.; Ed. John Wiley and Sons, Chichester, England, **1996**. (b) Jia, L.; Bonaventura, C.; Bonaventura, J.; Stamler, J. S. *Nature* **1996**, *380*, 221. (c) Galdwin, M. T.; Lancaster Jr., J. R.; Freeman, B. A.; Schechter, A. N. *Nat. Med*. **2003**, *9*, 496.

(3) (a) Ye, R. W.; Toro-Suarez, I.; Tiedje, J. M.; Averill, B. A. *J. Biol. Chem.* **1991**, *266*, 12848. (b) Hulse, C. L.; Averill, B. A.; Tiedje, J. M. *J. Am. Chem. Soc*. **1989**, *111*, 232. (c) Jackson, M. A.; Tiedje, J. M.; Averill, B. A. *FEBS Lett.* **1991**, *291*, 41.

(4) (a) Godden, J. W.; Turley, S.; Teller, D. C.; Adman, E. T.; Liu, M. Y.; Payne, W. J.; LeGall, J. *Science* **1991**, *153*, 438. (b) Adman, E. T.; Turley, S. *Bioinorganic Chemistry of Copper;* Karlin, K.D.; Tyekllr, Z. Ed., Chapman & Hall, Inc.: New York, **1993**, 397. (c) Ferguson, S. J. *Curr. Opin. Chem. Biol.* **1998**, *2*, 182.

(5) (a) Richardson, D. J.; Watmough, N. J. *Curr. Opin. Chem. Biol.* **1999**, *3*, 207. (b) Moura, I.; Moura, J. J. G. *Curr. Opin. Chem. Biol.* **2001**, *5*, 168. (c) Tocheva, E. I.; Rosell, F. I.; Mauk, A. G.; Murphy, M. E. P. *Biochem.* **2007**, *46*, 12366. (d) Zhou, X.; Espey, M. G.; Chen, J. X.; Hofseth, L. J.; Miranda, K. M.; Hussain, S. P.; Winks, D. A.; Harris, C. C. *J. Biol. Chem.* **2000**, *275*, 21241.

(6) (a) Tonzetich, Z. J.; McQuade, L. E.; Lippard, S. J. *Inorg. Chem*. **2010**, *49*, 6338. (b) McCleverty, J. A. *Chem. Rev*. **2004**, *104*, 403. (c) Tennyson, A. G.; Lippard, S. J. *Chem Biol*. **2011**, *18*, 1211. (d) Rose, M. J.; Butterley, N. M.; Mascharak, P. K. *J. Am. Chem. Soc*. **2009**, *131*, 8340. (e) Sun, N.; Liu, L. V.; Dey, A.; Villar-Acevedo, A. G.; Kovacs, J. A.; Darensbourg, M. Y.; Hodgson, K. O.; Hedman, B.; Solomon, E. I. *Inorg. Chem.* **2010**, *50*, 427.

(7) (a) Lu, T.-T.; Lai, S.-H.; Li, Y.-W.; Hsu, I.-J.; Jang, L.-Y.; Lee, J.-F.; Chen, I.-C.; Liaw, W.-F. *Inorg. Chem*. **2011**, *50*, 5396. (b) Pellegrino, J.; Bari, S. E.; Bikiel, D. E.; Doctorovich, F. *J. Am. Chem. Soc*. **2009**, *132*, 989. (c) Berto, T. C.; Praneeth, V. K. K.; Goodrich, L. E.; Lehnert, N. *J. Am. Chem. Soc*. **2009**, *131*, 17116. (d) Goodrich, L. E.; Paulat, F.; Praneeth, V. K. K.; Lehnert, N. *Inorg. Chem*. **2010**, *49*, 6293. (e) Dudle, B.; Rajesh, K.; Blacque, O.; Berke, H. *Organometallics* **2011**, *30*, 2986.

(8) (a) Hess, J.; Hsieh, C.-H.; Reibenspies, J. H.; Darensbourg, M. Y. *Inorg. Chem*. **2011**, *50*, 8541. (b) Hsieh, C.-H.; Darensbourg, M.Y. *J. Am. Chem. Soc*. **2010**, *132*, 14118. (c) Tsai, F.-T.; Chen, P.-L.; Liaw, W.-F. *J. Am. Chem. Soc*. **2010**, *132*, 5290. (d) Fry, N. L.; Mascharak, P. K. *Acc. Chem. Res*. **2011**, *44*, 289.

(9) Hess, J. L.; Hsieh, C.-H.; Brothers, S. M.; Hall, M. B.; Darensbourg, M. Y. *J. Am. Chem. Soc*. **2011**, *133*, 20426. (b) Lehnert, N.; Scheidt, W. R.; Wolf, M. W. *Struct.*

Bond. **2014**, *154*, 155. (c) Mariela, F. R.; Slep, V. L. D.; Olabe, J. A. *Coord. Chem. Rev*. **2007**, *251*, 1903. (d) Wright, A. M.; Hayton, T. W. *Comments Inorg. Chem.* **2012**, *33*, 207. (e) Wasser, I. M.; De Vries, S.; Loccoz, P. M.; Schroeder, I.; Karlin, K. D. *Chem. Rev*. **2002**, *102*, 1201.

(10) (a) Brunner, H. *J. Organomet. Chem.* **1968**, *12*, 517. (b) Brunner, H.; Loskot, S. *Angew. Chem. Int. Ed*. **1971**, *10*, 515. (c) Weiner, W. P.; White, M. A.; Bergman, R. G. *J. Am. Chem. Soc*. **1981**, *103*, 3612. (d) Becker, N. P.; Bergman, R. G. *J. Am. Chem. Soc*. **1983**, *105*, 2985. (e) Becker, P. N.; Bergman, R. G. *Organometallics* **1983**, *2*, 787. (f) Weiner, W. P.; Hollander, F. J.; Bergman, R. G. *J. Am. Chem. Soc*. **1984**, *106*, 7462.

(11) (a) Richter-Addo, G. B.; Hodge, S. J.; Yi, G.-B.; Khan, M. A.; Ma, T.; Van Caemelbecke, E.; Guo, N.; Kadish, K. M. *Inorg. Chem*. **1996**, *35*, 6530. (b) Di Vaira, M.; Ghilardi, C. A.; Sacconi, L. *Inorg. Chem*. **1976**, *15*, 1555. (c) Thyagarajan, S.; Incarvito, C. D.; Rheingold, A. L.; Theopold, K. H. *Inorg. Chim. Acta* **2003**, *345*, 333.

(12) Rhine, M. A.; Rodrigues, A. V.; Urbauer, R. L. B.; Urbauer, J. L.; Stemmler, T. L.; Harrop, T. C. *J. Am. Chem. Soc*. **2014**, *136*, 12560.

(13) Kalita, A.; Kumar, P.; Deka, R. C.; Mondal, B. *Inorg. Chem*. **2011**, *50*, 11868.

(14) (a) Kozhukh, J.; Lippard, S. J. *J. Am. Chem. Soc*. **2012**, *134*, 11120. (b) Franz, K. J.; Doerrer, L. H.; Springler, B.; Lippard, S. J. *Inorg. Chem*. **2001**, *40*, 3774. (c) Scott, M. J.; Lippard, S. J. *J. Am. Chem. Soc*. **1997**, *119*, 341. (d) Villacorta, G. M.; Lippard, S. J. *Pure Appl. Chem*. **1986**, *58*, 1474. (e) Zask, A.; Gonnella, N.; Nakanishi, K.; Turner, C. J.; Imajo, S.; Nozoe, T. *Inorg. Chem*. **1986**, *25*, 3400. (f) Jaynes, B. S.; Doerrer, L. H.; Liu, S.; Lippard, S. J. *Inorg. Chem*. **1995**, *34*, 5735.

(15) Costa, A. M.; Jimeno, C.; Gavenonis, J.; Carroll, P. J.; Walsh, P. J. *J. Am. Chem. Soc*. **2002**, *124*, 6929.

(16) Solanki, A.; Patil, Y. P.; Kumar, S. B. *J. Coord. Chem*. **2015**, *68*, 4017.

(17) Massoud, S. S.; Broussard, K. T.; Mautner, F. A.; Vicente, R.; Saha, M. K.; Bernal, I. *Inorg. Chim. Acta*. **2008**, *361*, 123.

(18) Tomson, N. C.; Crimmin, M. R.; Petrenko, T.; Rosebrugh, L. E.; Sproules, S.; Boyd, W. C.; Bergman, R. G.; DeBeer, S.; Toste, F. D.; Wieghardt, K. *J. Am. Chem. Soc.* **2011**, *133*, 18785.

(19) Franz, K. J.; Singh, N.; Spingler, B.; Lippard S. J. *Inorg. Chem*. **2000**, *39*, 4081.

(20) (a) Franz, K. J.; Lippard, S. J. *J. Am. Chem. Soc*. **1999**, *121*, 10504. (b) Siladke, N.; Meihaus, K. R.; Ziller, J. W.; Fang, M.; Furche, F.; Long, J. R.; Evans, W. J. *J. Am. Chem. Soc*. **2011**, *134*, 1234.

(21) (a) Sarma, M.; Kalita, A.; Kumar, P.; Singh, A.; Mondal, B. *J. Am. Chem. Soc.* **2010**, *132*, 7846. (b) Sarma, M.; Mondal, B. *Inorg. Chem*. **2011**, *50*, 3206. (c) Sarma, M.; Mondal, B. *Dalton Trans.* **2012**, *41*, 2927. (d) Haymore, B. L.; Huffman, J. C.; Butler, N. E. *Inorg. Chem*. **1983**, *22*, 168.

(22) (a) Hilderbrand, S. A.; Lippard, S. J. *Inorg. Chem.* **2004**, *43*, 5294 (b) Lim, M. H.; Lippard, S. J. *Acc. Chem. Res.* **2007**, *40*, 41.

(23) Enemark, J. H.; Feltham, R. D. *Coord. Chem. Rev.* **1974**, *13*, 339.

(24) (a) Hendrickson, A. R.; Ho, R. K. Y.; Martin, R. L. *Inorg. Chem.* **1974**, *13*, 1279. (b) Martin, R. L.; Taylor, D. *Inorg. Chem.* **1976**, *15*, 2970. (c) Del Zotto, A.; Mezzetti, A.; Rigo, P. *Inorg. Chim. Acta* **1990**, *171*, 61.

(25) Scheidt, W. R.; Ellison, M. K. *Acc. Chem. Res.* **1999**, *32*, 350.

(26) (a) Enemark, J. H.; Feltham, R. D. *Coord. Chem. Rev.* **1974**, *5*, 686. (b) Richter-Addo, G. B.; Legzdins, P. *Metal Nitrosyls*, Oxford University Press: New York, **1992**. (c) McCleverty, J. A. *Chem. Rev*. **2004**, *104*, 403. (d) Berto, T. C.; Speelman, A. L.; Zheng, S.; Lehnert, N. *Coord. Chem. Rev.* **2013**, *257*, 244.

(27) Kumar, P.; Lee, Y. M.; Park, Y. J.; Siegler, M. A.; Karlin, K. D.; Nam, W. *J. Am. Chem. Soc.* **2015**, *137*, 4284.

(28) *SMART*, *SAINT and XPREP*, Siemens Analytical X-ray Instruments Inc., Madison, Wisconsin, USA, **1995**.

(29) Sheldrick, G. M. *SADABS*: *software for Empirical Absorption Correction*, University of Gottingen, Institut fur Anorganische Chemieder Universitat, Tammanstrasse 4, D-3400 Gottingen, Germany, **1999**.

(30) Sheldrick, G. M. *SHELXS-97*, University of Gottingen, Germany, **1997**.

(31) Farrugia, L. J. *J. Appl. Crystallogr.* **1997**, *30*, 565.

Chapter 5

Reaction of a Co(II)-superoxo complex with nitric oxide: Formation of Co(III)-nitrite complex *via* putative Co(II)-peroxynitrite intermediate

Abstract

The reaction of a cobalt(II) complex [Co(L5)Cl]Cl (**4.3**) of tetradentate amine ligand **L5** {**L5** = N^1-(2,4,6-trimethylbenzyl)-N^2,N^2-*bis*(2-((2,4,6-trimethylbenzyl) amino)ethyl)ethane -1,2-diamine}, with KO_2 in $CHCl_3$ resulted in the formation of corresponding cobalt(II) superoxo complex, **5.1**. Reaction of this superoxo complex with NO led to the formation of $[Co(L5)(NO_2)_2]Cl$ (**5.2**). Complex **5.2** was structurally characterized. Spectroscopic and analytical evidence suggest that the reaction proceeds through a putative cobalt(II) peroxynitrite intermediate.

5.1 Introduction

Nitric oxide (NO) is a ubiquitous signal transduction molecule found in various physiological processes; for example cellular signalling, platelet disaggregation, neurotransmission and in the immune response to bacterial infection. However, as NO is a radical, it is highly reactive and toxic.[1] It forms other secondary reactive species such as nitrogen dioxide (NO_2) and peroxynitrite (PN, oxoperoxonitrate, $^{-}OONO$), in the presence of oxidizing agents (O_2, O_2^{-}, O_2^{2-} etc) and transition metals.[2] Peroxynitrite, which is formed by the diffusion controlled reaction of NO and O_2^{-} is highly toxic and its spontaneous decay to radical-decomposition products results in the damage of cellular molecules such as DNA, peptides, proteins, sugars, and lipids.[3] Hence, the study of the formation and decomposition of peroxynitrite to biologically benign products like NO_3^{-} or NO_2^{-} has a great interest from bioinorganic point of view.

In this regard example of heme and non-heme model assisted formation and decomposition of peroxynitrite intermediate have been reported.[4] However, the study involving other transition metal ions in generation and reactivity of $ONOO^{-}$ are limited. Clarkson and Basolo reported the reaction of cobalt nitrosyl complex with O_2 to result in the corresponding nitrite product.[5] Reactivity of Cu-NO complex with O_2 leading to nitrite product *via* putative peroxynitrite intermediate was reported by the Karlin's group.[6] Recently non-heme Cr(IV)-peroxo and Cr(III)-superoxo complexes were exemplified to result in presumed Cr(III)- PN upon reaction with NO.[7] We reported the reaction of Cu-NO complexes with H_2O_2 to form Cu-nitrato complex *via* thermal decomposition of presumed Cu-PN intermediate.[8] Co(III)-nitrosyl complex of 12 and 13 membered N-tetramethylated cyclam ligand have been found to react with superoxide ion to afford corresponding Co(II)-nitrite and O_2 *via* a presumed Co(II)-PN intermediate.[9]

This chapter describes the reaction of a cobalt superoxo complex with NO to form a Co-PN species. Thermal decomposition of this Co-PN intermediate resulted in the formation of Co(III)-nitrite complex.

5.2 Results and Discussion

It is observed in Chapter 4 that complex **4.3** doesn't react with NO. However, addition of KO_2 to the chloroform solution of complex **4.3** at -40°C gave a dark green solution of complex **5.1** (Scheme 5.1). Complex **5.1** is stable for a couple of days at bellow 0 °C. It was isolated as a solid by applying high vacuum to evaporate chloroform at 0 °C. Complex **5.1** exhibits a band around 420 nm which is assignable as charge transfer band of metal superoxo species. In the reported Co-superoxo complex $Tp^{t\text{-}Bu,Me}Co(O_2)$, it shows a peak at 365 nm.[10] In case of Cu-superoxo complex $[(^{DMA}N_3S)\text{-}Cu(II)(O_2^{\cdot-})]^+$ {3,3'-(2-(2-(o-tolylthio)ethyl)propane-1,3-diyl)bis(N,N-dimethylaniline)}, this band was reported around 418 nm.[11] In FT-IR spectrum, a new peak appeared around 1067 cm^{-1} (Appendix IV). It was found to gradually diminish with time at room temperature (Appendix IV). The reaction of Na[Fe(III)(TAML)] (TAML = tetraamido marcrocyclic ligand, 3,3,6,6,9,9-hexamethyl- 2,5,7,10-tetraoxo-3,5,6,7,9,10-hexahydro-*2H*-benzo[*e*][1,4,7,10] tetraaza cyclo-tridecine-1,4, 8,11-tetraide) with KO_2 was to yield corresponding superoxo complex $[Fe(III)(TAML)(O_2)]^{2-}$. The complex was structurally characterised and found to be side on binding of the superoxo moiety. This complex was found to be stable for several days at -20 ºC. In FT-IR spectroscopy, this complex shows the O-O stretching frequency around 1260 cm^{-1}.[12] Another superoxo complex of cobalt with tris-pyrazolyl borate, $Tp^{t\text{-}Bu,Me}Co(O_2)$ was synthesized and characterized structurally by Theopold and co-worker. In FT-IR spectroscopy, the peak around 961 cm^{-1} was assigned as O-O stretching frequency.[10] ESI-mass spectrum of complex **5.1** gives a peak at m/z = 633.51 which

corresponds to the cobalt(II) superoxo complex (Figure 5.1). The observed isotopic distribution pattern was also found good agreement with the simulated one.

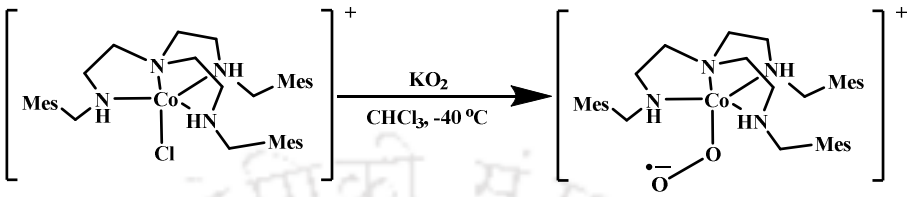

4.3 **5.1**

Scheme 5.1

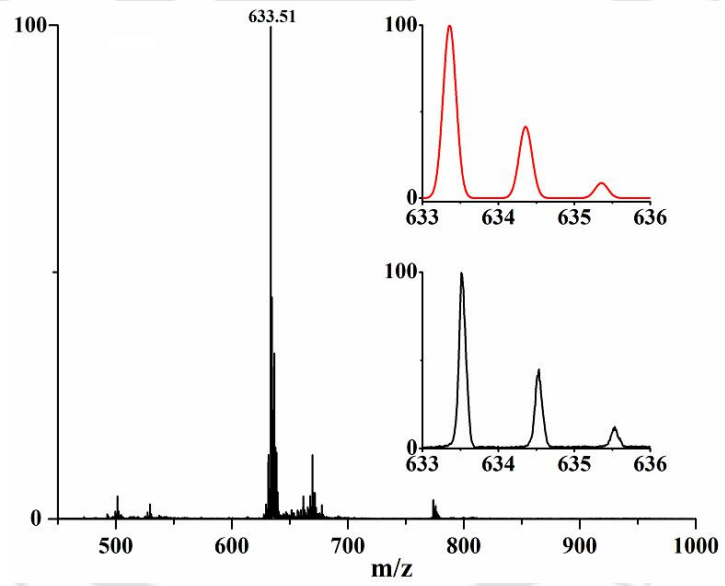

Figure 5.1 ESI mass spectrum of complex **5.1** in acetonitrile. Inset shows the simulated (red) and experimental (black) isotopic distribution pattern.

Purging NO to the chloroform solution of complex **5.1** at -40 °C, the green solution immediately turned to pink. The pink solution was stirred for 30 minutes to give red precipitate of complex **5.2**. Complex **5.2** was characterized by various spectroscopic techniques. The electrospray ionization mass spectrum of **5.2** exhibits a prominent ion peak at a mass-to-charge (m/z) ratio of 693.65, whose mass and isotope distribution pattern

correspond to $[Co(L5)(NO_2)_2]^+$ (calculated m/z 693.35) (Figure 5.2). In FT-IR spectrum, the two peaks around 1336 and 1305 cm^{-1} are assignable for nitrite stretching frequency (Appendix IV). Direct evidence for the formation of complex **5.2** unambiguously was provided by the X-ray crystal structure. The perspective ORTEP view of the complex is given in figure 5.3. The crystallographic data, selected bond distances and angles are listed in tables 5.1, 5.2 and 5.3 respectively. The cobalt atom is in a distorted octahedral environment. It is bounded to four nitrogen atoms from ligand and two nitrogen atoms from two nitrite anions. One chloride ion is outside the coordination sphere to balance the charge of the metal centre. The average bond distance between Co-N is 2.03Å. However, all these bond lengths and angles are in a normal range when compared to those in analogous reported complexes.[13]

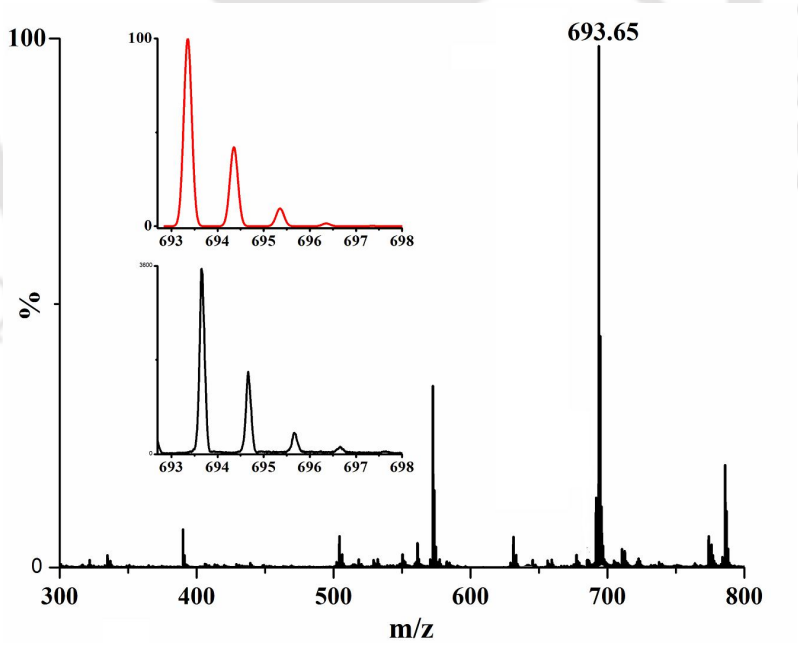

Figure 5.2 ESI mass spectrum of complex **5.2** in acetonitrile. Inset shows the simulated (red) and experimental (black) isotopic distribution pattern.

In UV-visible spectroscopy (Figure 5.4), addition of KO_2 at -40 ºC to complex **4.3**, a new band appeared at around 420 nm along with 510 and 620 nm. Upon addition of NO, these bands immediately disappeared with concomitant formation of a new band around 560 nm. This band was found to be unstable and gradually shifted to 535 nm. This band corresponds to complex **5.2**. The blue line with λ_{max} = 535 nm is attributed to formation of

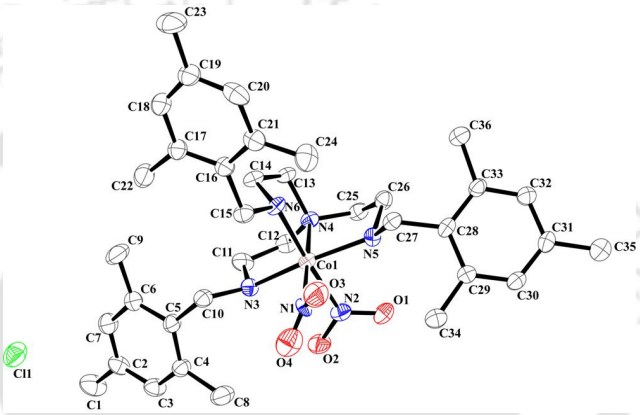

Figure 5.3 ORTEP diagram of complex **5.2**. (30% thermal ellipsoid plot, H-atoms are omitted for clarity).

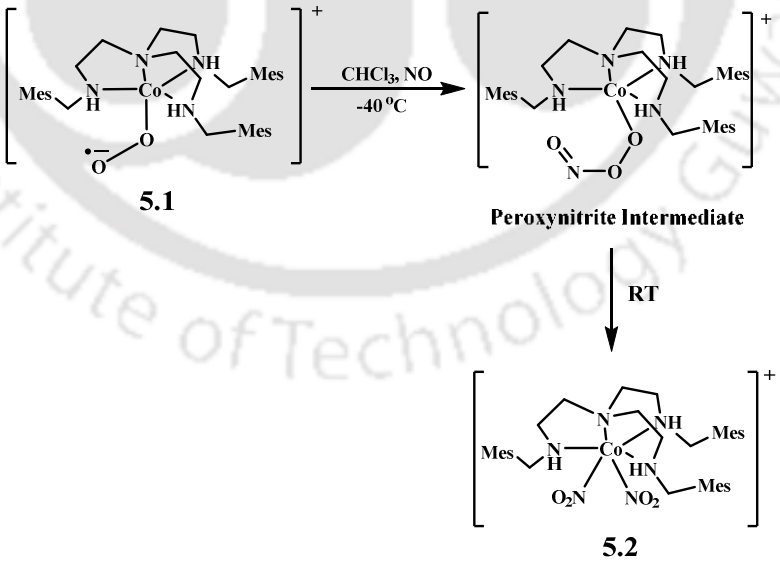

Scheme 5.2

unstable peroxynitrite intermediate which was formed by the reaction of superoxo species with NO (Scheme 5.2). Similar type of reaction was also observed in the case $[(NC)_5Co(O_2)]^{3-}$ when it reacts with NO. The corresponding peroxynitrite complex $[NEt_4]_3[(NC)_5Co(ONOO)]$ was found to stable at room temperature.[14] Theopold and co-worker reported the formation peroxynitrite intermediate from the reaction of $[Tp^{t\text{-}Bu,Me}Co(O_2)]$ with NO at -60 ºC which decomposes to nitrite and nitrate.[15] Catalytic

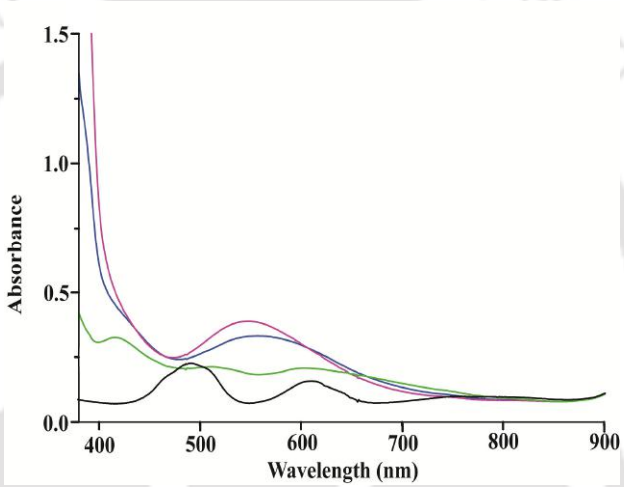

Figure 5.4 UV-visible spectra of complex **4.3** (black), upon addition of 1 equiv of KO_2 (green), after 1 minute (blue) and 30 minute (pink) of purging NO chloroform at -40 °C.

decomposition of peroxynitric acid was investigated by Groves and co-worker. They reported Mn(III) complex of substituted corrole catalytically decomposes the peroxynitrite ion to nitrite with concomitant oxidation of Mn(III) to Mn(IV)=O.[16] Recently Nam and co-worker reported the decomposition of Mn(III)-peroxynitrite of TAML (TAML= tetraamido macrocyclic ligand) to nitrite and formation of $(TAML)Mn^{V}=O$. The formation of peroxynitrite intermediate was evidenced by DFT calculation.[17] They also reported the formation of Cr(IV)=O complex from peroxynitrite which further reacts with NO to give Cr(III)-NO_2 complex.[7] In present case, the intermediate decomposes to nitrite to form complex **5.2**.

Table 5.1 Crystallographic data of complex **5.2**.

Formula	$C_{74}H_{110}ClCo_2N_{12}O_{12}$
Molecular weight	1513.05
Crystal system	Triclinic
Space group	P-1
Temperature/K	293
Wavelength	0.71073
a/Å	11.0410 (4)
b/Å	12.0519 (5)
c/Å	16.1873 (7)
α/°	103.547 (3)
β/°	109.886 (2)
γ/°	97.335 (3)
V/ Å^3	1917.86(14)
Z	1
Density/gcm^{-1}	1.310
Absorption Coefficient	0.534
Absorption Correction	Multi-scan
F(000)	805.0
Total no of reflections	9212
Reflections, $I>2\sigma(I)$	3803
Max. 2θ/°	28.360
Ranges (h, k, l)	$-14\leq h\leq 14$ $-15\leq k\leq 16$ $-21\leq l\leq 21$
Complete to 2θ(%)	96.0
Refinement method	Full-matrix least-squares on F^2
Goof (F^2)	0.630
R indices [$I>2\sigma(I)$]	0.0668
R Indices (all data)	0.1425

We sought more support for our proposal of formation of peroxynitrite intermediate along with the formation of **5.2** from **5.1**. In this regard, we carried out trapping experiments using 2,4-di-*tert*-butylphenol (DTBP). After addition of NO to chloroform solution of complex **5.1** at -40°C, DTBP was added. Oxidatively dimerized DTBP (2,2′-dihydroxy-3,3′,5,5′-tetra-*tert*-butylbiphenol, DTBP-dimer) was produced with 28% yield.

Table 5.2 List of selected bond lengths (Å) of complex **5.2**.

Co(1)-N(1)	2.033 (5)
Co(1)-N(2)	2.026 (4)
Co(1)-N(3)	2.058 (4)
Co(1)-N(4)	1.983 (4)
Co(1)-N(6)	2.021 (4)
N(3)-C(10)	1.507 (6)
N(6)-C(15)	1.503 (6)
N(6)-C(14)	1.487 (6)
N(2)-O(1)	1.244 (5)
N(1)-O(4)	1.094 (6)
N(2)-O(2)	1.234 (5)
N(1)-O(3)	1.186 (5)

Table 5.3 List of selected bond angles (°) of complex **5.2**.

N(1)-Co(1)-N(2)	85.17 (16)
N(1)-Co(1)-N(3)	92.88 (18)
N(1)-Co(1)-N(4)	177.24 (18)
N(2)-Co(1)-N(3)	85.28 (18)
N(2)-Co(1)-N(4)	92.98 (16)
N(3)-Co(1)-N(4)	84.91 (14)
O(1)-N(2)-O(2)	117.8 (4)
O(2)-N(2)-Co(1)	120.7 (7)
O(3)-N(1)-O(4)	126.5 (4)
O(3)-N(1)-Co(1)	116.9 (4)

5.3 Experimental Section

5.3.1 Materials and methods

All reagents and solvents were purchased from commercial sources and were of reagent grade. Deoxygenation of the solvent and solutions were effected by repeated vacuum/purge cycles or bubbling with nitrogen for 30 min. NO gas was purified by passing through KOH and P_2O_5 column. UV−visible spectra were recorded on an either Perkin-Elmer lambda 25 UV−visible spectrophotometer or Agilent Technologies Cary

8454 UV-visible spectrometer equipped with Unisoku temperature controller. FT-IR spectra were taken on a Perkin-Elmer spectrophotometer with either sample prepared as KBr pellets or in solution in a potassium bromide cell. Solution electrical conductivity was checked using a Systronic 305 conductivity bridge. ^{1}H- NMR spectra were obtained with a 400 MHz Varian FT-spectrometer. Chemical shifts (ppm) were referenced either with an internal standard (Me_4Si) for organic compounds or to the residual solvent peaks. The X-band Electron Paramagnetic Resonance (EPR) spectra of the complexes and of the reaction mixtures were on a JES-FA200 ESR spectrometer. Elemental analyses were obtained from a Perkin-Elmer Series II Analyzer. The magnetic moment of complexes were measured on a Cambridge Magnetic Balance. Mass spectra of the compounds in acetonitrile were recorded in a Waters Q-Tof Premier and Aquity instrument.

Single crystals were grown by slow diffusion followed by slow evaporation technique. The intensity data were collected using a Bruker SMART APEX-II CCD diffractometer, equipped with a fine focus 1.75 kW sealed tube MoKα radiation (λ = 0.71073 Å) at 273(3) K, with increasing ω (width of 0.3° per frame) at a scan speed of 3 s/ frame. The SMART software was used for data acquisition. Data integration and reduction were undertaken with the SAINT and XPREP software.[18] For complex **5.2**, empirical absorption corrections were applied to the data using the program SADABS.[19] Structures were solved by direct methods using SHELXS-97 and refined with full-matrix least-squares on F^2 using SHELXL-97.[20] All non-hydrogen atoms were refined anisotropically. Structural illustrations have been drawn with ORTEP-3 for Windows.[21] The disorder present in the crystal structure has been tried to be minimized by use of SHELXL.

5.3.2 Syntheses of the complexes

(a) Complex 5.1, $[Co(L5)(O_2)]Cl$

Complex **4.3** (0.671 g, 1 mmol) was taken in a 50 mL round bottom flask and dissolved in 25 mL of chloroform and cooled to -40 ^{0}C. To it, KO_2 (0.07 g, 1 mmol) was added and stirred for 30 minute. Then the solvent was dried under vacuum at 0 ºC to obtain the green powder of complex **5.1**. Complex **5.1** is stable at 0 ^{0}C for a week. FT-IR (in KBr): 3415, 2937, 2678, 1610, 1469, 1191, 1167, 1037, 990, 852 and 825 cm^{-1}. Elemental analysis could not be done owing to the thermal instability of the complex. UV-visible (in chloroform): 420 nm (ε/435 $M^{-1}cm^{-1}$), 500 nm (ε/370 $M^{-1}cm^{-1}$), 610 nm (ε/285 $M^{-1}cm^{-1}$). Mass (m/z): Calcd: 633.36 for $[Co(L5)(O_2)]^+$, found: 633.36.

(b) Complex 5.2, $[Co(L5)(NO_2)_2]Cl$

In a 50 ml round bottom flask, 30 ml of dry chloroform is taken and kept in -40 ºC for 30 minutes. To it 0.500 g of complex **5.1** was dissolved and degassed by purging argon. Then NO was purged to it under cold condition. The color of the solution changed from green to pink and within five minute and afforded complex **5.2** as red precipitate. Excess NO was removed from the reaction mixture by purging argon. The red precipitate was filtered out and washed with cold methanol. Slow evaporation of methanol solution of the precipitate gives X-ray quality crystal of complex **5.2**. Yield 0.375g (72%). Elemental analyses for $C_{36}H_{54}N_6O_4CoCl$, Calcd(%): C, 59.29; H, 7.46; N, 11.52. Found (%): C, 59.48; H, 7.89; N, 11.68,FT-IR (in KBr): 3388, 3135, 2964, 1611, 1414, 1336, 1305, 853, 825 cm^{-1}. UV-visible (in chloroform): 535 nm ((ε/370 $M^{-1}cm^{-1}$). Mass (m/z): Calcd: 693.35 for $[Co(L5)(NO_2)_2]^+$, found: 693.35.

5.3.3 Isolation 2,2′-dihydroxy-3,3′,5,5′-tetra-*tert*-butylbiphenol (DTBP dimer)

Complex **5.1** (0.668 g, 1 mmol) was dissolved in 20 ml of pre-cooled chloroform. To it, 2, 4-di-*tert*-butyl phenol (1.03 g, 5 mmol), was added and the mixture was cooled to -40 ºC. The solution was degassed by purging Ar. To this degassed solution, NO was purged and stirred for 20 minute. The reaction mixture was then warmed to room temperature and dried under reduce pressure. The solid mass was then subjected to column chromatography using silica gel column to obtain pure 2,2′-dihydroxy-3,3′,5,5′-tetra-*tert*-butylbiphenol. Yield: 0.069 g (~28%). ^{1}H-NMR (400 MHz, $CDCl_3$) δ_{ppm}: 1.32 (s, 9H), 1.45 (s, 9H), 5.23 (1 H), 7.12 (1 H), and 7.39 (1 H). ^{13}C-NMR (100 MHz, $CDCl_3$) δ_{ppm}: 29.8, 31.8, 34.6, 35.4, 122.5, 125.0, 125.5, 136.4, 143.2, and 150.0. Mass (m/z): Calcd: 410.32, found: 409.32 (M-1).

5.4 Conclusion

In summary, we have investigated the NO reactions of metal–O_2 complex to provide further insight into fundamental aspects of NOD (Nitric oxide dioxygenage) chemistry. Such reactions are important in the biological regulation of NO and they involve transition-metal complexes and species derived from molecular oxygen and nitric oxide. We have shown that the reaction of the cobalt(II)–superoxo complex **5.1** with NO yields the [Co(III)–$(NO_2)_2$] product complex **5.2**, which is most likely formed through an Co(II)–PN intermediate.

5.5 References

(1) (a) Ignarro, L. J. *Nitric Oxide, Biology and Pathobiology* Ed. Academic Press; San Diego, CA, **2000**. (b) Richter-Addo, G. B.; Legzdins, P. *Metal Nitrosyls* Oxford University Press, New York, **1992**. (c) Moncada, S.; Palmer, R. M. J.; Higgs, E. A. *Phermacol. Rev*. **1991**, *43*, 109. (d) Bredt, D. S.; Snyder, S. H. *Annu Rev. Biochem.* **1994**, *63*, 175. (e) Butler, A. R.; Williams, D. L. *Chem. Soc. Rev*. **1993**, *233*. (f) Hunt, A. P.; Lehnert, N. *Acc. Chem. Res.* **2015**, *48*, 2117. (g) Feelisch, M.; Stamler, J. S.; Ed. *Methods in Nitric Oxide Research*, John Wiley and Sons, Chichester, England, **1996**. (h) Ye, R. W.; Toro-Suarez, I.; Tiedje, J. M.; Averill, B. A. *J. Biol. Chem.* **1991**, *266*, 12848.

(2) (a) Ford, P. C.; Fernandez, B. O.; Lim, M. D. *Chem. Rev*. **2005**, *105*, 2439. (b) Schopfer, M. P.; Wang, J.; Karlin, K. D. *Inorg. Chem.* **2010**, *49*, 6267. (c) Fry, N. L.; Mascharak, P. K. *Acc. Chem. Res*. **2011**, *44*, 289. (d) Heilman, B. J.; St. John, J.; Oliver, S. R. J.; Mascharak, P. K. *J. Am. Chem. Soc*. **2012**, *134*, 11573. (e) Radi, R. *Proc. Natl. Acad. Sci. U.S.A* **2004**, *101*, 4003. (f) Kalyanaraman, B. *Proc. Natl. Acad. Sci. U.S.A.* **2004**, *101*, 11527. (g) Goldstein, S.; Lind, J.; Mernyi, G. *Chem. Rev*. **2005**, *105*, 2457.

(3) (a) Bryk, R.; Griffin, P.; Nathan, C. *Nature* **2000**, *407*, 211. (b) Szabo, C. *Toxicol. Lett.* **2003**, *105*, 140. (c) Merenyl, G.; Lind, J.; Goldstein, S.; Czapski, G. *Chem. Res. Toxicol.* **1998**, *11*, 712. (d) Beckman, J. S. *Chem. Res. Toxicol*. **1996**, *9*, 836.

(4) (a) Ford, P. C.; Wink, D. A.; Stanbury, D. M. *FEBS Lett*. **1993**, *326*, 1. (b) Thomas, D. D.; Liu, X.; Kantrow, S. P.; Lancaster, J. R. Jr.; *Proc. Natl. Acad. Sci., U.S.A.* **2001**, *98*, 355. (a) Doyle, M. P.; Hoekstra, J. W. *J. Inorg. Biochem.* **1981**, *14*, 351. (b) Feelisch, M. *Cardiovas. Pharmacol.* **1991**, *17*, S25.

(5) Clarkson, S. G.; Basolo, F. *Inorg. Chem.* **1973**, *12*, 1529.

(6) Schopfer, M. P.; Mondal. B.; Lee, D.-H.; Sarjeant, A. A. N.; Karlin, K. D. *J. Am. Chem. Soc.* **2009**, *131*, 11304.

(7) Yokoyama, A.; Cho, K. B.; Karlin, K. D.; Nam, W. *J. Am. Chem. Soc.* **2013**, *135*, 14900.

(8) Kalita, A.; Kumar, P.; Mondal, B. *Chem. Commun.* **2012**, *48*, 4636.

(9) Kumar, P.; Lee, Y. M.; Park, Y. J.; Siegler, M. A.; Karlin, K. D.; Nam, W. *J. Am. Chem. Soc*. **2015**, *137*, 4284.

(10) Egan, J. W.; Haggerty, B. S.; Rheingold, A. L.; Theopold, K. H. *J . Am. Chem. Soc*. **1990**, *112*, 2446.

(11) Kim, S.; Lee, J. Y.;. Cowley, R. E.; Ginsbach, J. W.; Siegler, M. A.; Solomon, E. I.; Karlin, K. D. *J . Am. Chem. Soc*. **2015**, *137*, 2796.

(12) Hong, S.; Sutherlin, K. D.; Park, J.; Kwon, E.; Siegler, M. A.; Solomon, E. I.; Nam, W. *Nat. Commun.* **2014**, *5*, 5440.

(13) (a) Ishida, T.; Suzuki, T.; Kaizaki, S. *Inorg. Chim. Acta* **2004**, *357*, 3134. (b) Ali, B. B.; Belkhiria, M. S.; Giorgi, M.; Nasri, H. *Open. J. Inor. Chem.* **2011**, *1*, 39. (c) Chun, H.; Bernal, I. *Crys. Growth. Des.* **2001**, *1*, 67.

(14) (a) Wick. P. K.; Kissner, R.; Koppenol, W. H. *Helv. Chim. Acta* **2000**, *83*, 748. (b) Wick. P. K., Kissner; R.; Koppenol, W. H. *Helv. Chim. Acta* **2001**, *84*, 3057.

(15) Thyagarajan, S.; Incarvito, C. D.; Rheingold, A. L.; Theopold, K. H. *Inor. Chim. Acta* **2003**, *345*, 333.

(16) Lee, J.; Hunt, J. A.; Groves, J. T. *J. Am. Chem. Soc.* **1998**, *120*, 7493.

(17) Hong, S.; Kumar, P.; Cho, K.-B.; Lee, Y.-M.; Karlin, K. D.; Nam, W. *Angew. Chem. Int. Ed.* DOI: 10.1002/anie.201605705

(18) *SMART*, *SAINT and XPREP*, Siemens Analytical X-ray Instruments Inc., Madison, Wisconsin, USA, **1995**.

(19) Sheldrick, G. M. *SADABS*: *software for Empirical Absorption Correction*, University of Gottingen, Institut fur Anorganische Chemieder Universitat, Tammanstrasse 4, D-3400 Gottingen, Germany, **1999**.

(20) Sheldrick, G. M. *SHELXS-97*, University of Gottingen, Germany, **1997**.

(21) Farrugia, L. J. *J. Appl. Crystallogr.* **1997**, *30*, 565.

Appendix I

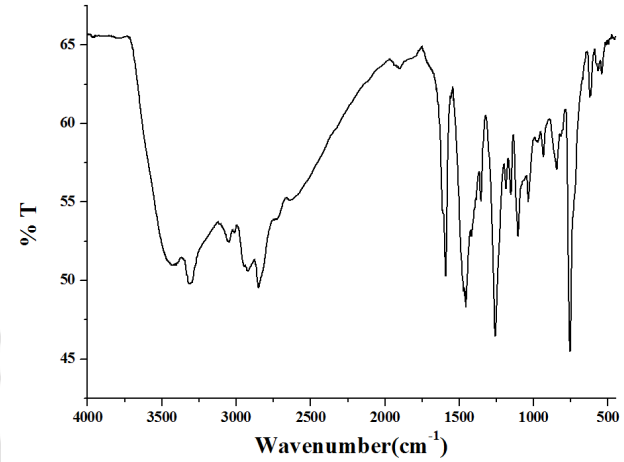

Figure A1.1 FT-IR spectrum of **L1H$_3$** in KBr pellet.

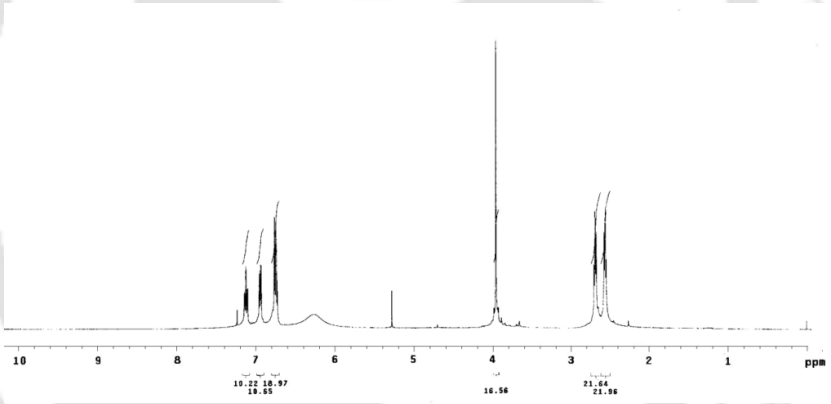

Figure A1.2 ^{1}H-NMR spectrum of **L1H$_3$** in $CDCl_3$.

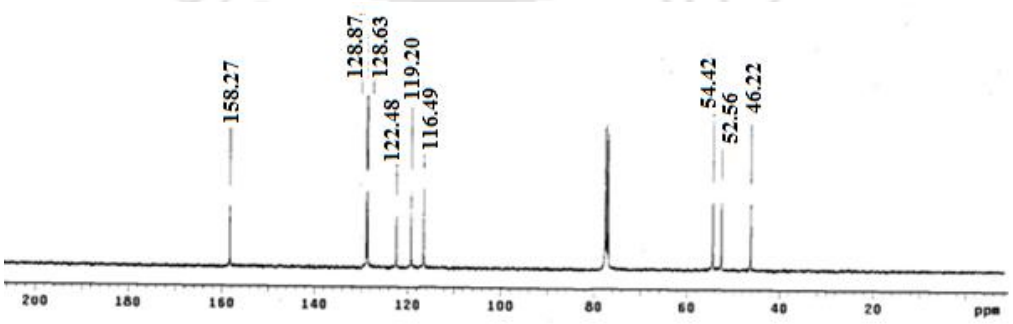

Figure A1.3 ^{13}C-NMR spectrum of **L1H$_3$** in $CDCl_3$.

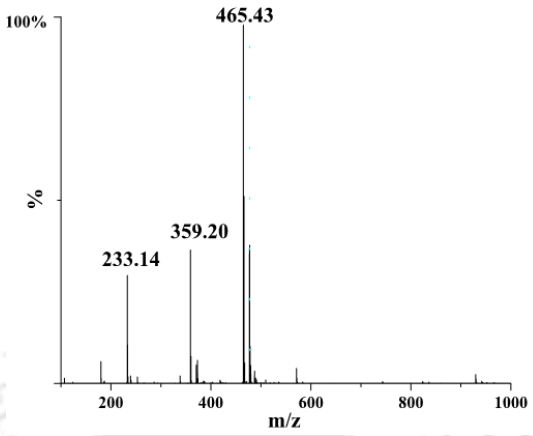

Figure A1.4 ESI mass spectrum of **L1H$_3$** in acetonitrile.

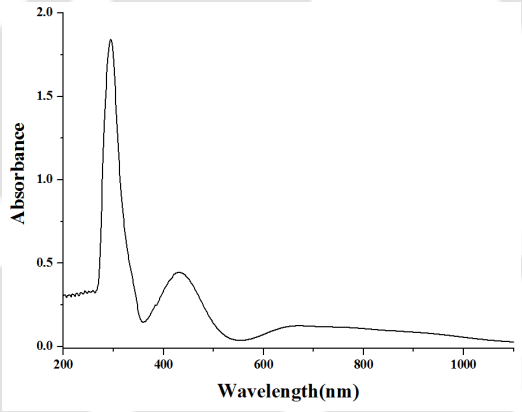

Figure A1.5 UV-visible spectrum of complex **2.1** in acetonitrile.

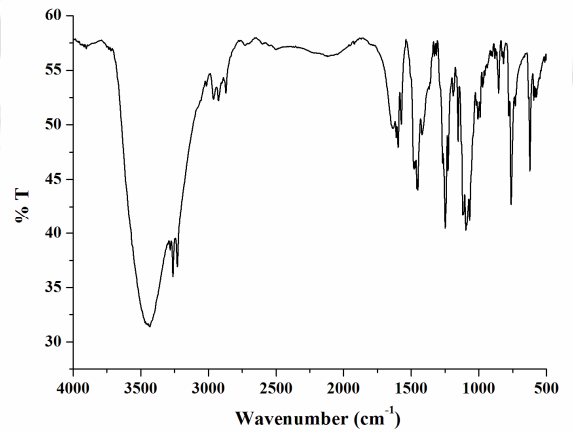

Figure A1.6 FT-IR spectrum of complex **2.1** in KBr pellet.

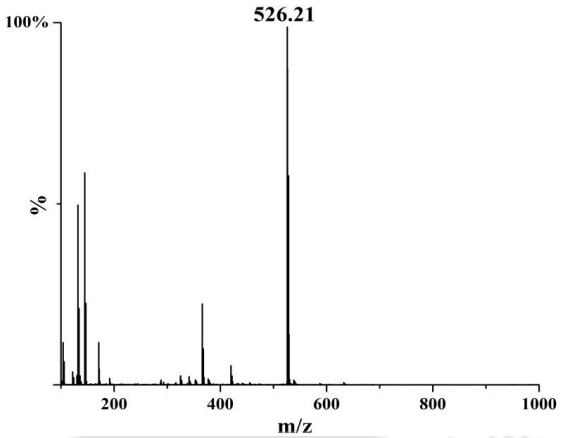

Figure A1.7 ESI-mass spectrum of complex **2.1** in acetonitrile.

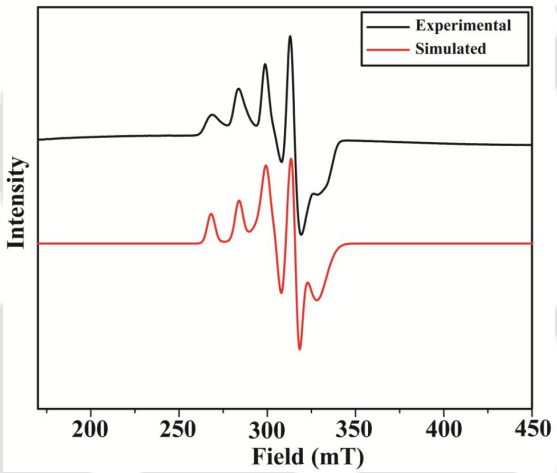

Figure A1.8 X-band EPR of complex **2.1** in acetonitrile at 77 K.

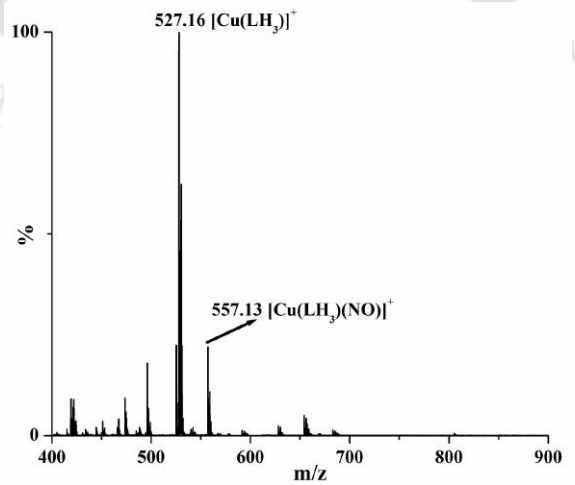

Figure A1.9 ESI mass spectrum of complex **2.1** after purging NO in acetonitrile.

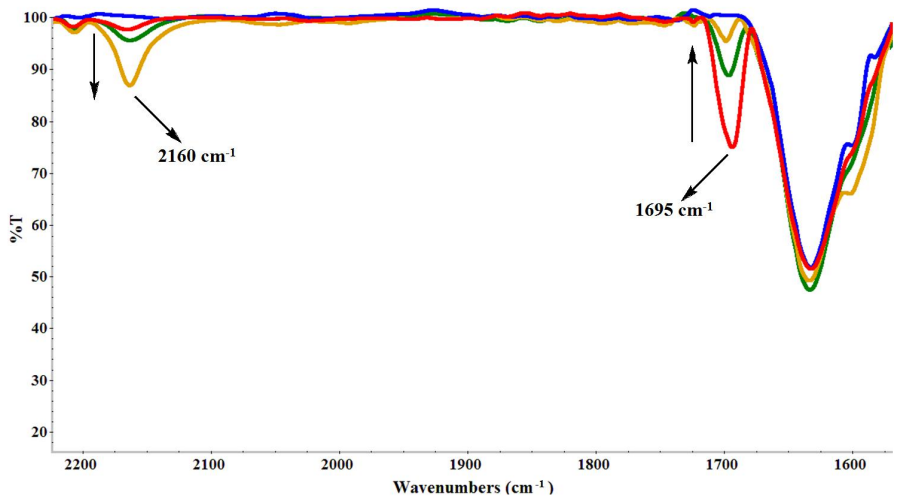

Figure A1.10 Solution FT-IR spectra of complex **2.1** (blue), after 1 (blue), 2 (red) and 3 (green) and 10 (yellow) minutes of addition of NO in acetonitrile in NaCl cell.

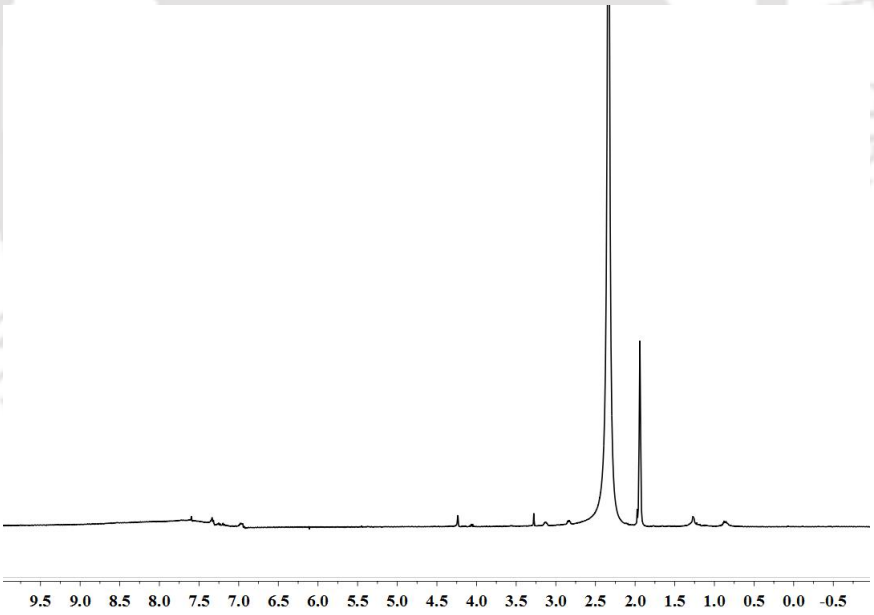

Figure A1.11 ^{1}H-NMR spectrum of complex **2.1** in CD_3CN.

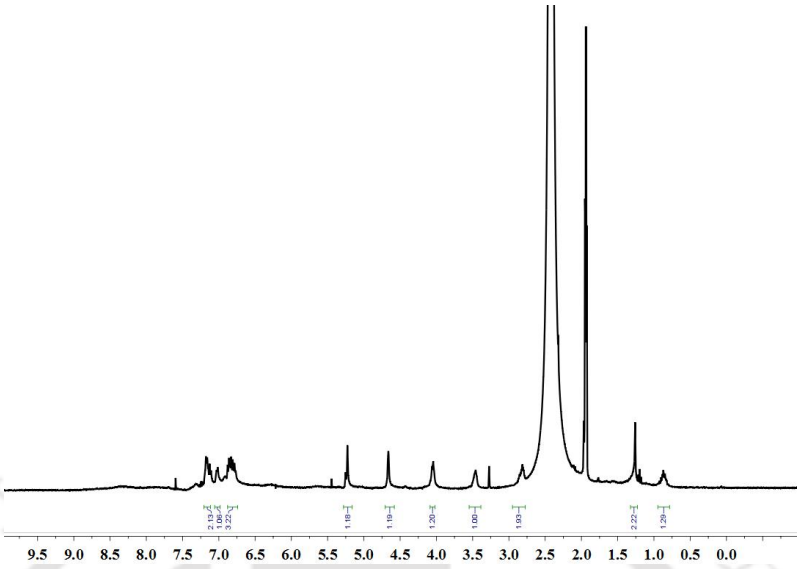

Figure A1.12 ^{1}H-NMR spectrum of complex **2.1** after purging 1 equivalent of NO in CD_3CN.

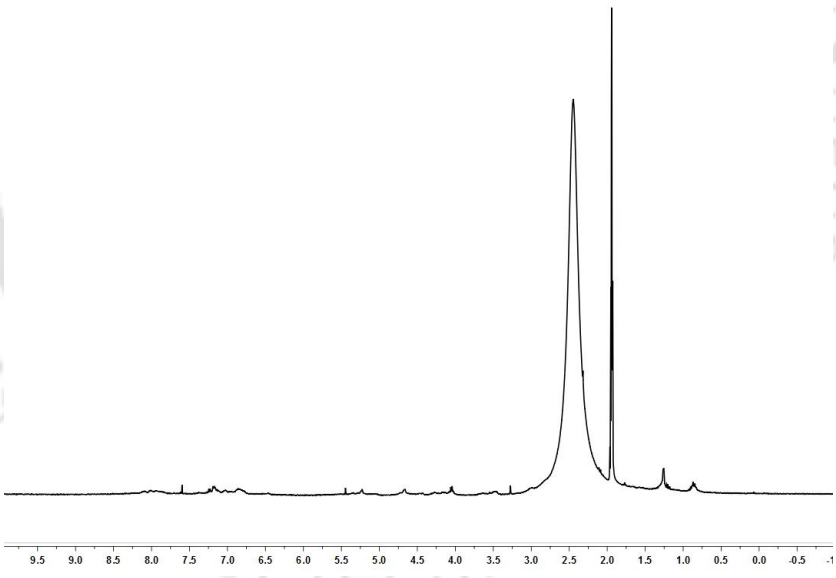

Figure A1.13 ^{1}H-NMR spectrum of complex **2.1** after purging excess of NO in CD_3CN.

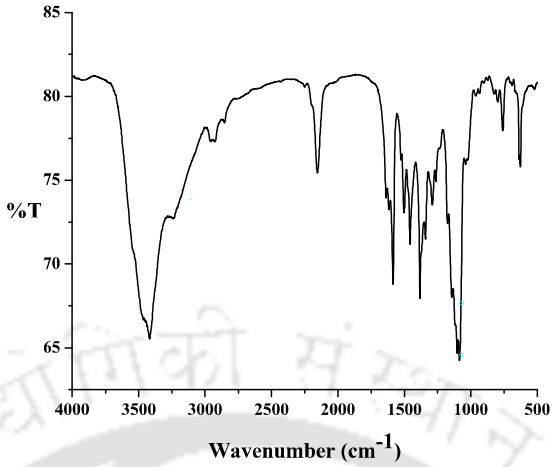

Figure A1.14 FT-IR spectrum of complex **2.2** in KBr pellet.

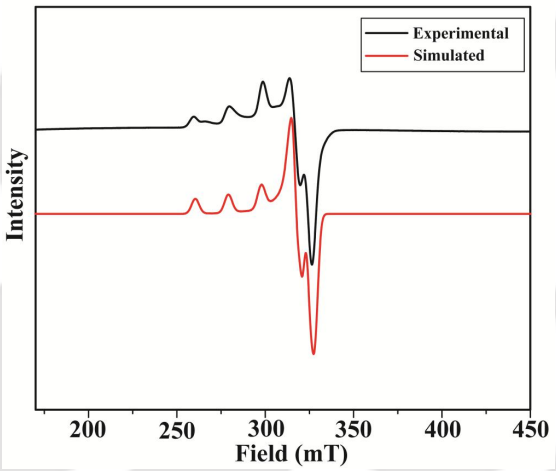

Figure A1.15 X-band EPR of complex **2.2** at 77 k in acetonitrile.

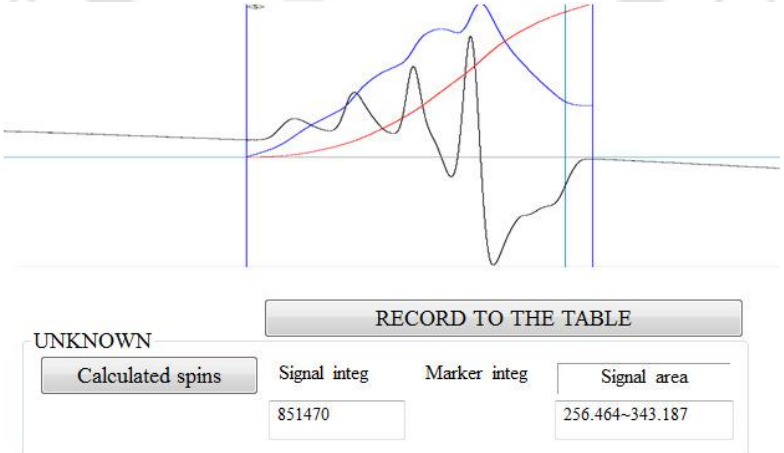

Figure A1.16 Double integration of EPR spectrum of complex **2.1** (concentration 0.5 M) in acetonitrile at 77 K.

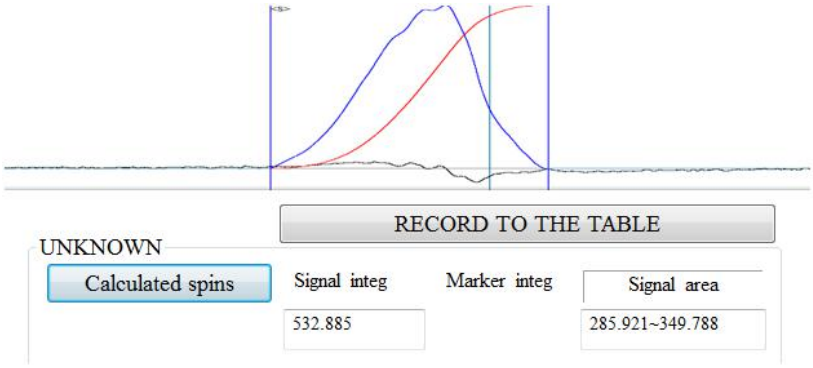

Figure A1.17 Double integration of EPR spectrum of complex **2.1** (concentration 0.5 M) after adding 1 equivalent of NO in acetonitrile at 77 K.

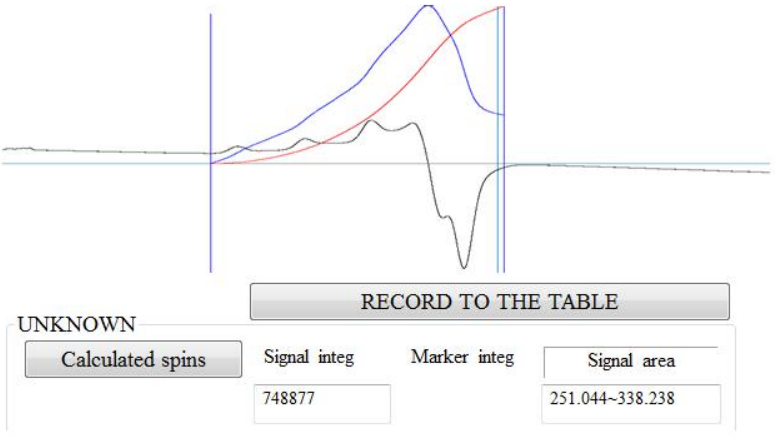

Figure A1.18 Double integration of EPR spectrum of complex **2.1** (concentration 0.5 M) after adding excess of NO in acetonitrile at 77 K.

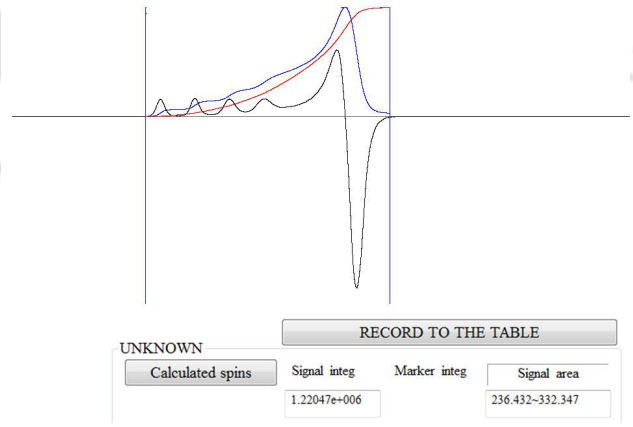

Figure A1.19 Double integration of EPR spectrum of $Cu(ClO_4).6H_2O$ (concentration 0.5 M) in acetonitrile at 77 K.

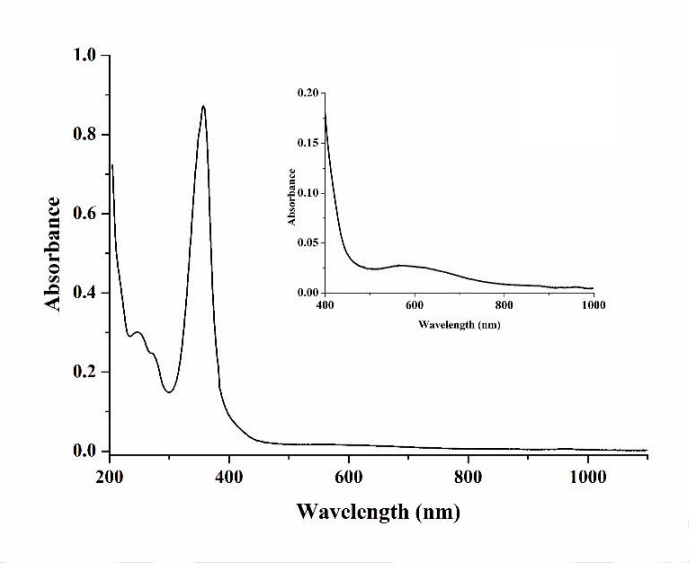

Figure A1.20 UV-visible spectrum of complex **2.2** in methanol.

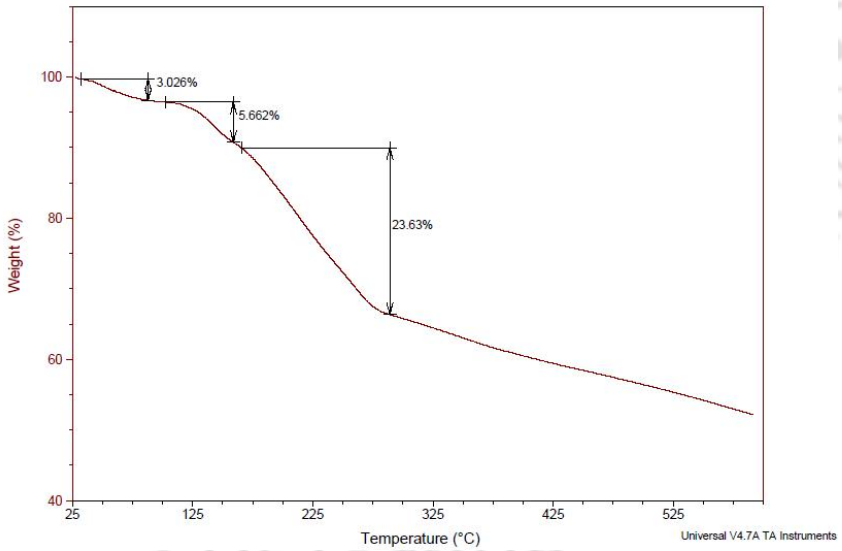

Figure A1.21 TGA of complex **2.2.**

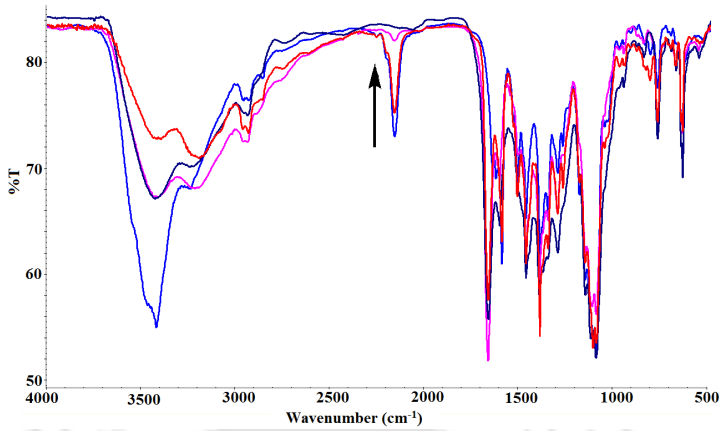

Figure A1.22 FT-IR spectrum of complex **2.2** upon application of vacuum in DMF.

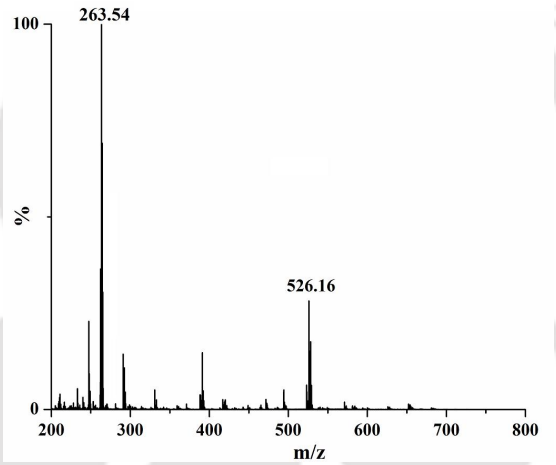

Figure A1.23 ESI mass spectrum of methanol solution of complex **2.2** upon application of vacuum.

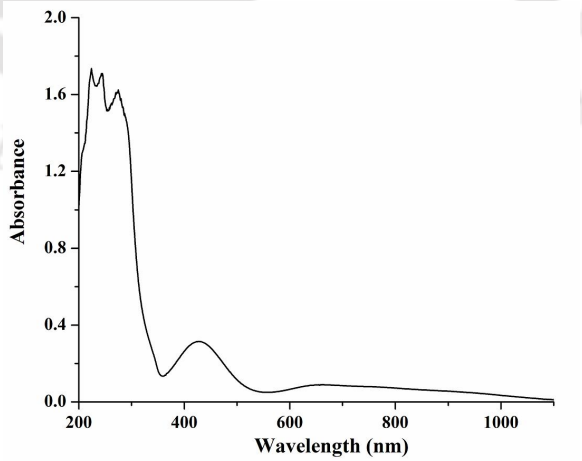

Figure A1.24 UV-visible spectrum of methanol solution of complex **2.2** after applying vacuum.

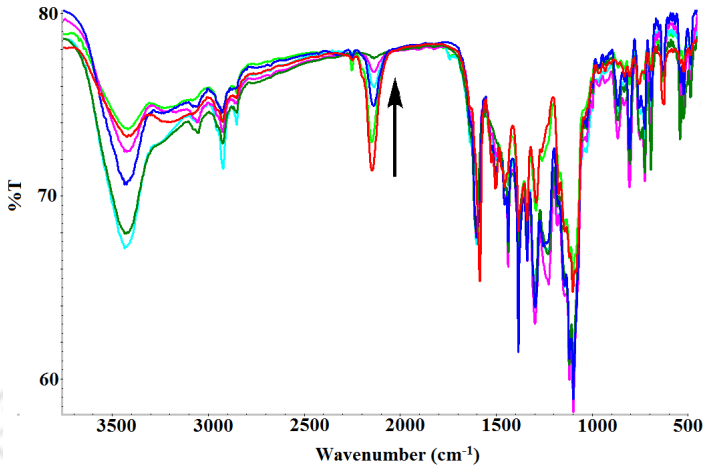

Figure A1.25 FT-IR monitoring of the reaction of complex **2.2** with PPh_3. Decay of intensity of the band at 2153 cm^{-1} is due to the reaction of coordinated N_2O with PPh_3.

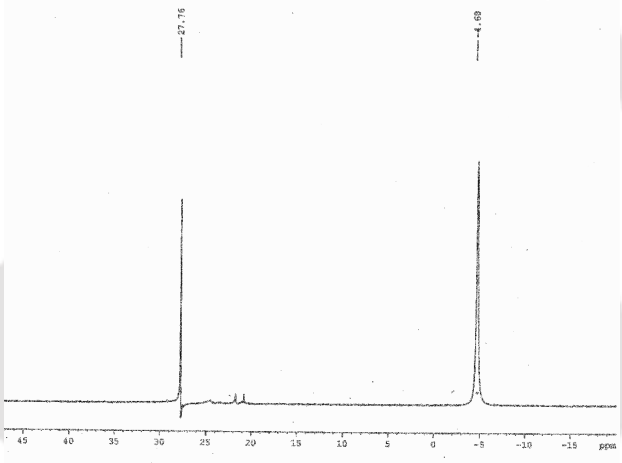

Figure A1.26 ^{31}P-NMR spectrum of reaction mixture of complex **2.2** and PPh_3 in CD_3CN.

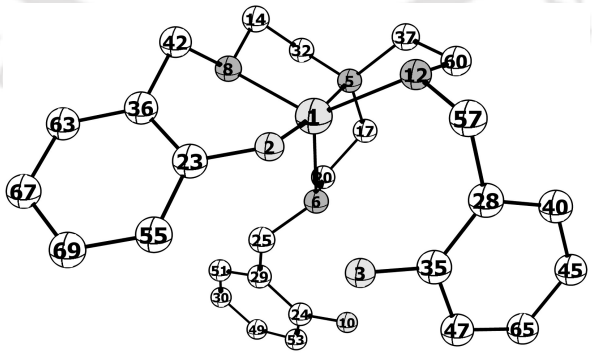

Figure A1.27 Complex **2.2**. The bond distances (Å) : Cu(1)-O(2) = 1.99 Cu(1)-N(5) = 2.08 Cu(1)-N(6) = 2.18 Cu(1)-N(8) = 2.10 Cu(1)-N(12) = 2.10.

Table A1.1 Coordinates of DFT optimized complex **2.1**.

Cu	6.364898	5.232501	18.481661
O	5.381970	4.115081	19.796469
O	6.304116	5.101210	22.008457
H	5.860899	4.792263	21.140845
N	7.143166	6.455444	16.983025
N	8.412076	5.157241	19.227193
H	8.530810	5.806804	20.013458
N	6.166956	3.817098	16.948950
H	7.009005	3.236874	16.859679
O	10.250194	5.343180	21.546582
H	10.827008	5.849577	22.148181
N	5.174646	6.889711	18.975560
H	4.290252	6.656028	18.508600
C	6.028821	4.640597	15.725682
H	5.045985	5.133383	15.763720
H	6.062316	4.029289	14.808903
C	8.512725	6.831609	17.429377
H	8.420689	7.648941	18.158248
H	9.100649	7.214259	16.578639
C	9.215005	5.648882	18.082600
H	9.326309	4.818014	17.369343
H	10.232270	5.948840	18.381138
C	5.469294	2.776734	19.715460

C	10.995427	4.418055	20.858425
C	8.819448	3.808856	19.708574
H	8.465993	3.067302	18.976242
H	8.259958	3.635542	20.639489
C	6.011856	7.431466	21.293643
C	10.302877	3.622583	19.923030
C	12.405567	2.502959	19.383174
H	12.950406	1.754576	18.805819
C	7.155805	5.662777	15.717474
H	8.119412	5.139449	15.649979
H	7.083821	6.331881	14.845457
C	6.665780	6.412303	22.030353
C	5.286963	2.107429	18.471937
C	6.222719	7.622759	16.891033
H	5.352742	7.312506	16.293866
H	6.709311	8.457793	16.360225
C	6.453054	8.757409	21.458166
H	5.926183	9.550735	20.921113
C	5.019229	2.914130	17.231032
H	4.831024	2.245087	16.374637
H	4.136241	3.559853	17.363972
C	7.515659	9.089595	22.298210
H	7.834687	10.128180	22.398889
C	7.724249	6.753184	22.893815

H	8.210230	5.948958	23.447970
C	13.073889	3.303492	20.315165
H	14.148238	3.187091	20.471192
C	11.029944	2.673754	19.194211
H	10.500399	2.056676	18.463103
C	12.373112	4.262531	21.052787
H	12.890828	4.890035	21.783134
C	5.715454	2.003001	20.871773
H	5.851244	2.514554	21.826787
C	4.825495	7.149378	20.407756
H	4.277179	6.262430	20.753801
H	4.131641	8.006361	20.451225
C	5.764691	8.054471	18.274368
H	6.612755	8.413261	18.871884
H	5.045392	8.885862	18.189795
C	5.380029	0.712504	18.420591
H	5.250272	0.212339	17.456745
C	8.151571	8.072021	23.020945
H	8.980452	8.307953	23.692053
C	5.622273	-0.045191	19.571877
H	5.687375	-1.132814	19.511427
C	5.784887	0.611497	20.797542
H	5.974629	0.035525	21.706222

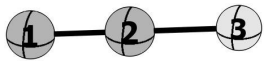

Figure A1.28 The bond distances in (Å) : N(1)-N(2) = 1.14 N(2)-O(3) = 1.19

Table A1.2 Coordinates of DFT optimized nitrous oxide (N_2O).

N	0.137103	1.444952	0.000000
N	1.274173	1.438043	0.000000
O	2.462723	1.430005	0.000000

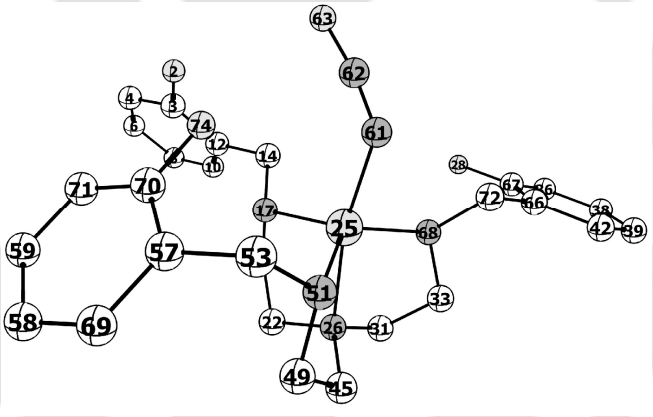

Figure A1.29 Complex **2.2**. The bond distances (Å) : Cu(25)-N(17) = 2.13 Cu(25)-N(26) = 2.24 Cu(25)-N(51) = 2.19 Cu(25)-N(68) = 2.19 Cu(25)-N(61) = 2.05 N(61)-N(62) = 1.16 N(62)-O(63) = 1.20. The hydrogen atoms are removed for clarity.

Table A1.3 Coordinates of DFT optimized complex **2.2**.

H	5.907922	2.388591	-3.401722
O	5.153245	2.213602	-2.807810
C	5.228904	3.059961	-1.711273
C	6.379428	3.820312	-1.476694
H	7.229575	3.739386	-2.159333

C	6.429654	4.683084	-0.379979
H	7.329783	5.274575	-0.203133
C	5.331136	4.789841	0.479046
H	5.360106	5.471437	1.330570
C	4.188294	4.026466	0.230021
H	3.318916	4.125886	0.884590
C	4.113315	3.138838	-0.855057
H	-6.538956	2.243858	-0.805704
C	2.882199	2.295765	-1.094697
H	2.791862	2.066237	-2.162404
H	1.981113	2.853331	-0.800753
N	2.850683	1.000039	-0.352409
H	3.736813	0.511750	-0.526118
C	2.698779	1.164950	1.114919
H	3.595333	1.608421	1.579154
H	1.870255	1.870585	1.278060
C	2.401343	-0.173832	1.788541
H	2.302941	-0.019953	2.880057
H	3.258853	-0.844910	1.638006
Cu	1.372076	-0.404493	-0.980692
N	1.205290	-0.816516	1.213051
H	-0.583166	1.332398	-0.495121
O	-2.024887	2.872958	-1.278673
H	-2.252965	3.800123	-1.078094

H	0.126543	0.850260	1.894022
C	-0.058974	-0.210747	1.670305
H	-0.418533	-0.675384	2.607550
C	-1.139578	-0.303860	0.598004
H	-2.063848	0.165548	0.976509
H	-1.379371	-1.354578	0.372319
C	-4.430957	2.646204	-1.008074
H	-4.531859	3.718149	-0.817621
C	-5.555095	1.814247	-1.003908
C	-5.418410	0.444006	-1.247912
H	-6.293622	-0.207552	-1.243668
H	-4.029674	-1.156208	-1.684057
C	-4.147113	-0.085646	-1.496625
H	0.187225	-2.633191	1.068480
H	-1.704819	-0.915317	-2.002522
C	1.195213	-2.285295	1.337109
H	1.383979	-2.610853	2.379081
H	-1.180875	0.643418	-2.656470
H	2.133381	-4.038363	0.501898
C	2.218282	-2.940469	0.415201
H	3.232023	-2.675198	0.740099
N	2.064519	-2.485408	-0.985576
H	1.228742	-2.940188	-1.369304
C	3.198830	-2.925455	-1.862794

H	3.242644	-4.028779	-1.885583
H	2.965653	-2.573587	-2.876170
H	4.986163	-4.151446	-0.244029
C	4.541820	-2.401787	-1.411865
C	6.558802	-2.689179	-0.047457
C	7.007028	-1.423386	-0.436463
H	6.619656	0.316550	-1.659947
N	1.201659	-0.337692	-3.021525
N	1.716500	0.255552	-3.868634
O	2.365713	0.963678	-4.595149
H	7.952343	-1.029973	-0.057308
H	4.691511	0.467271	-2.853259
C	-3.005730	0.724973	-1.513883
C	-3.166519	2.103525	-1.264026
N	-0.668040	0.321932	-0.657899
C	5.341000	-3.161935	-0.543450
C	5.035439	-1.146716	-1.830833
C	6.253823	-0.657469	-1.327849
C	-1.630094	0.158332	-1.778015
H	7.150794	-3.303101	0.633108
O	4.299303	-0.434341	-2.738279

Details of NBO analysis

In order to gain insights into the interaction of nitrous oxide(N_2O) ligand with the central Cu system, the intramolecular charge transfer in the complex has been analysed with the natural bond orbital (NBO) analysis. The energetic estimate of donor (i) – acceptor (j) orbital interactions can be obtained by the second order perturbation theory analysis of the Fock matrix in the NBO basis. The donor–acceptor interaction energy E(2) is given by,

$$E(2) = \Delta E(i,j) = [q(i,j)F(i,j)^2]/\varepsilon(i)-\varepsilon(j)$$

where q(i) is the donor orbital occupancy, ε(i) and ε(j) are the diagonal elements (orbital energies), and F(i,j) is the off-diagonal NBO Fock matrix element. In the present investigation, the important interaction is between central copper(Cu) and the N_2O unit has been carefully analysed.

Table A1.4 The energy due to orbital interaction.

Orbitals involved	Interaction Energy(kcal/mol)
LP (N) ➞ LP* (Cu)	36.0

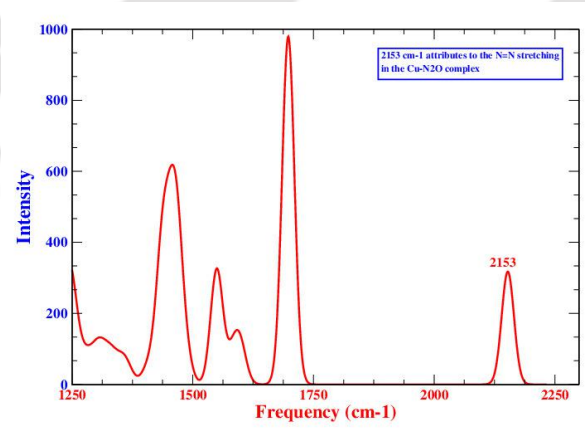

Figure A1.30 Theoretical calculated Infrared (IR) Spectrum of the Cu-N_2O complex.

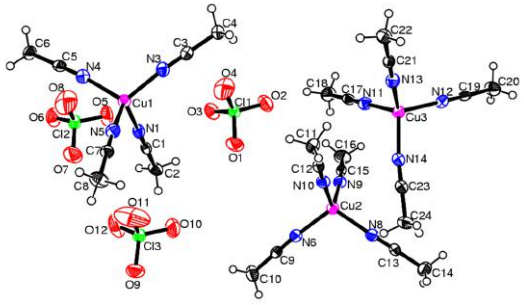

Figure A1.31 ORTEP diagram of $[Cu(CH_3CN)_4]ClO_4$ (50% thermal ellipsoid plot).

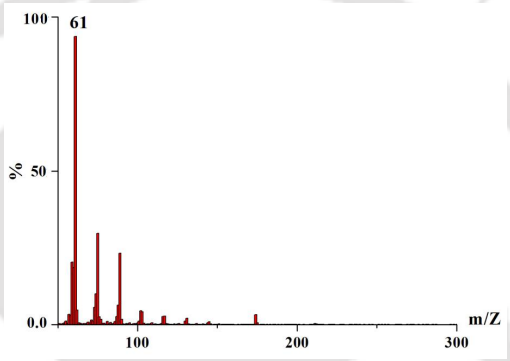

Figure A1.32 GC-mass spectrum of methyl nitrite.

Isolation of $[(CH_3CN)_4Cu](ClO_4)$: To 20 ml of distilled and degassed acetonitrile solution of complex **2.1** (500 mg), equivalent amount of freshly purified $NO_{(g)}$ was added. The solution became colorless. It was then kept in freezer. After 10-12 days, $[(CH_3CN)_4Cu](ClO_4)$ was precipitated out as colorless crystals (yield, ~ 70%). It was confirmed by the single crystal X-ray structure determination. Since, it has been reported earlier, the data are not given. However, the ORTEP diagram is shown in the supporting information. The crystals were filtered out and the resulting solution was dried under reduced pressure. The light green crude mass was dissolved in minimum volume of acetonitrile. To this saturated aqueous solution of Na_2S (1 ml) was added and stirred for 5 mints. 20 ml of water was added to the reaction mixture and the back precipitate was filtered. The filtrate was neutralized using dilute acetic acid and then the organic part was extracted using CH_2Cl. Then it was dried under vacuum. Characterization of the isolated product matches well with $L1H_3$.

Appendix II

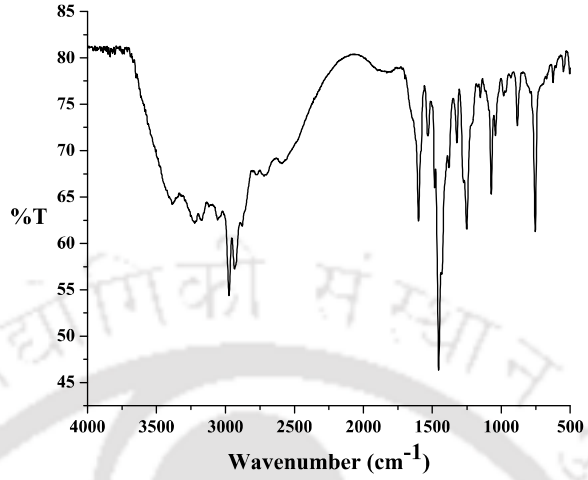

Figure A2.1 FT-IR spectrum of **L2H** in KBr pellet.

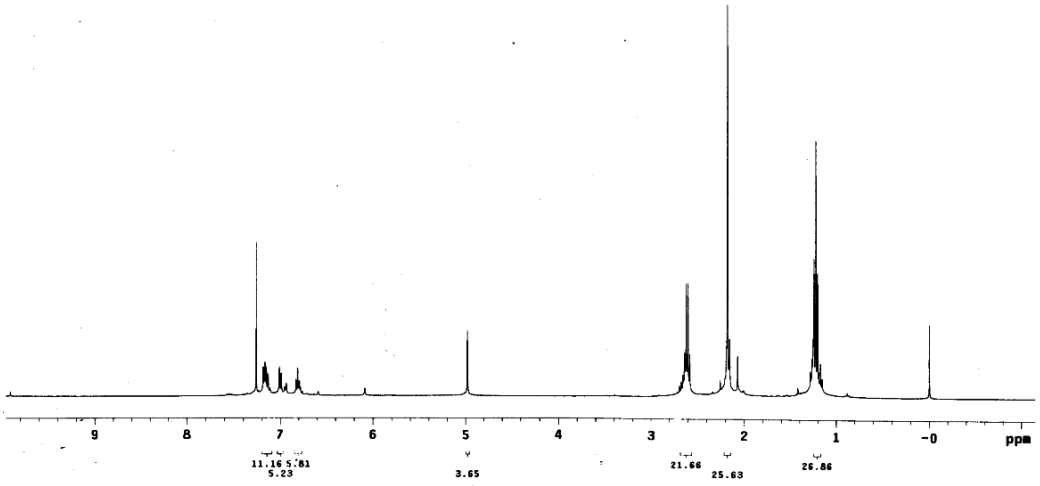

Figure A2.2 ^{1}H-NMR spectrum of **L2H** in $CDCl_3$.

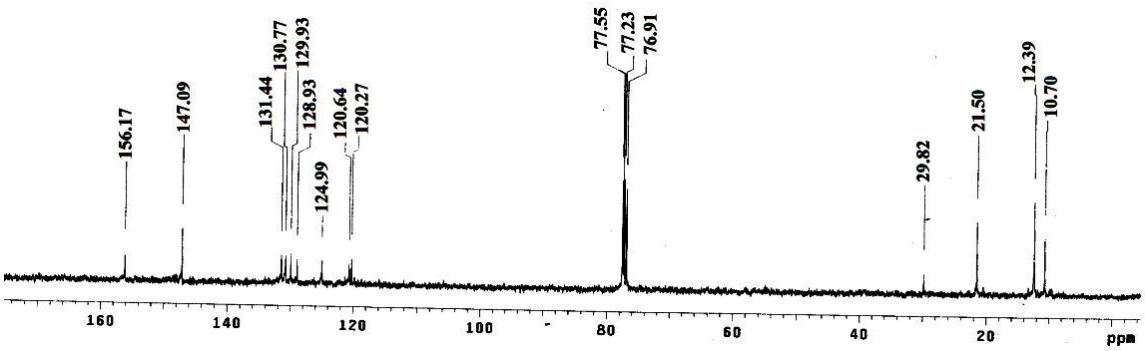

Figure A2.3 ^{13}C-NMR spectrum of **L2H** in $CDCl_3$.

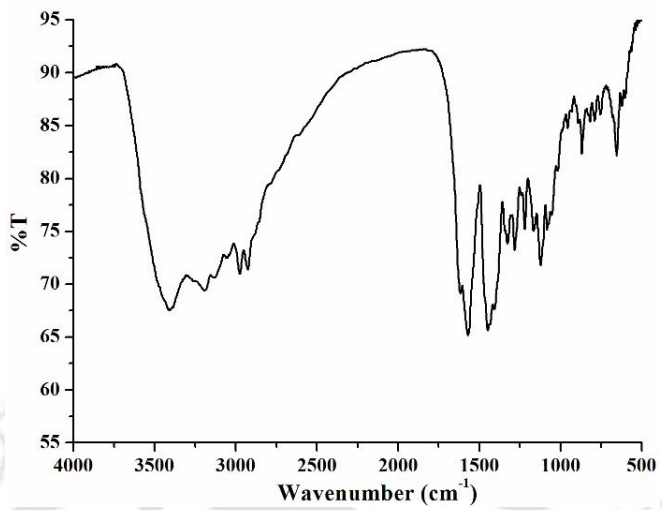

Figure A2.4 FT-IR spectrum of complex **3.1** in KBr pellet.

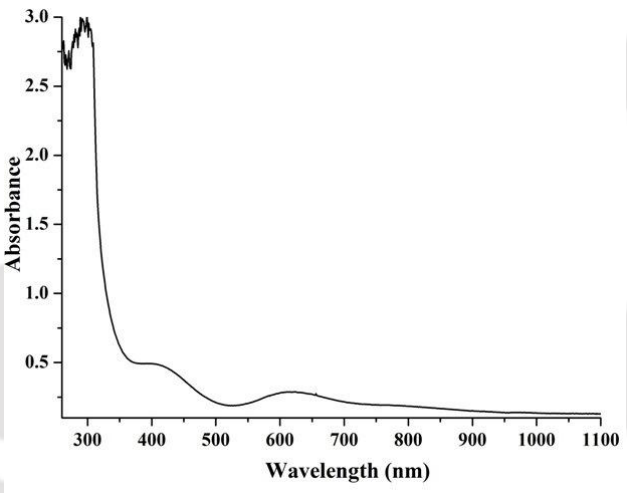

Figure A2.5 UV-visible spectrum of complex **3.1** in methanol.

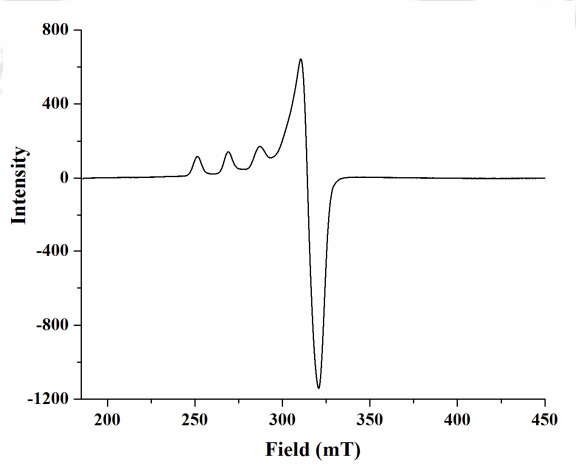

Figure A2.6 X-band EPR spectrum of complex **3.1** in methanol.

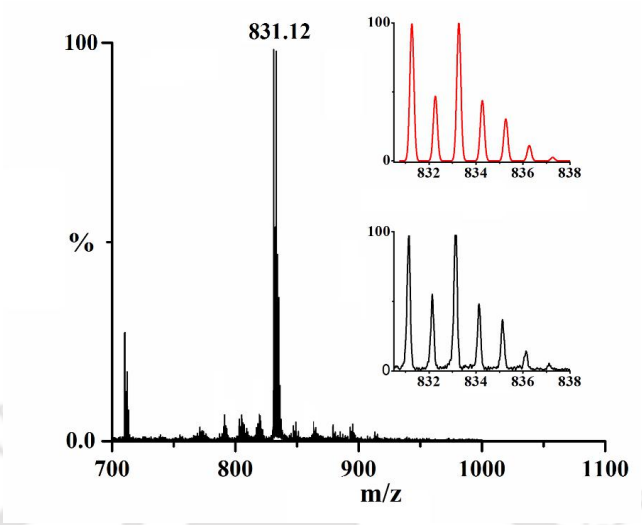

Figure A2.7 ESI-mass spectrum of complex **3.1** in methanol. Inset shows the simulated (red) and experimental (balck) isotopic distribution pattern.

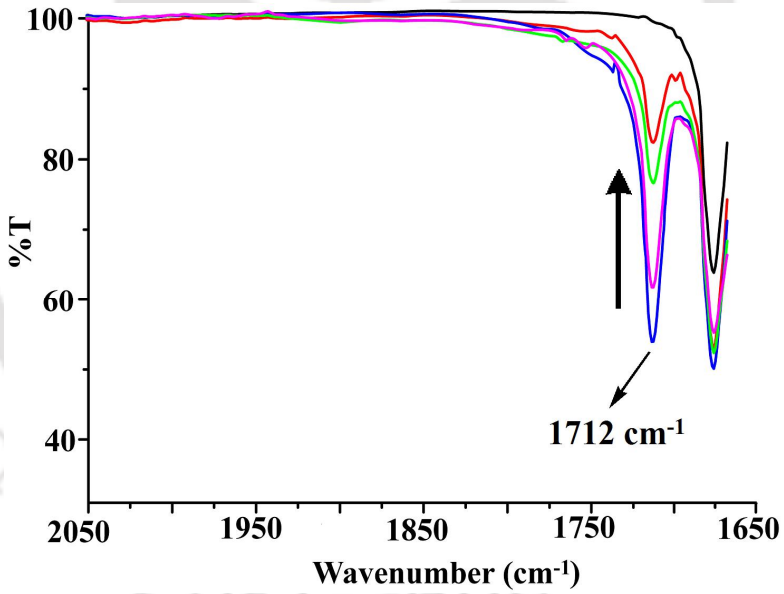

Figure A2.8 Solution FT-IR spectra of complex **3.1** (black), complex **3.1** with excess amount of NO purged (blue; formation of metal nitrosyl,1712cm^{-1}). Pink, green and red traces are after 5, 10 and 20 hours of purging NO respectively in 1:5 methanol acetonitrile mixture in KBr cell.

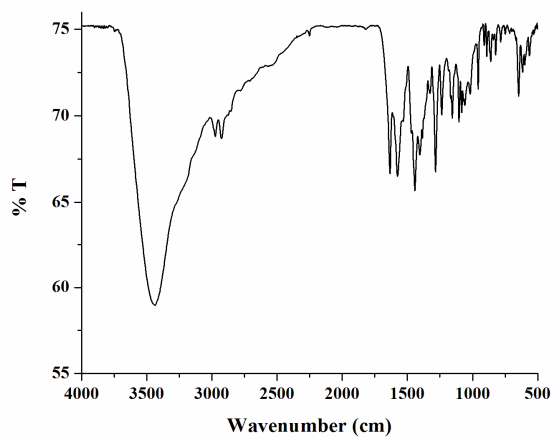

Figure A2.9 FT-IR spectrum of complex **3.2** in KBr pellet.

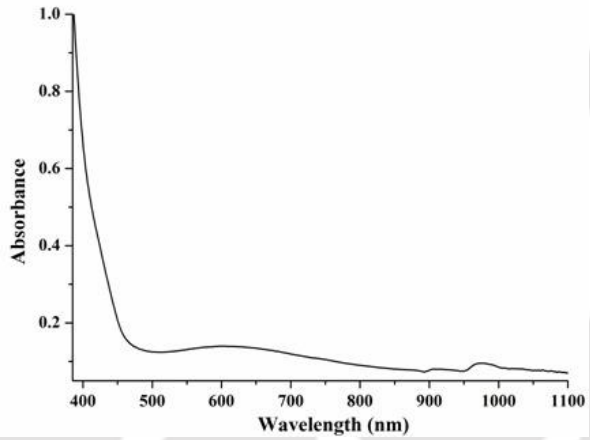

Figure A2.10 UV-visible spectrum of complex **3.2** in methanol.

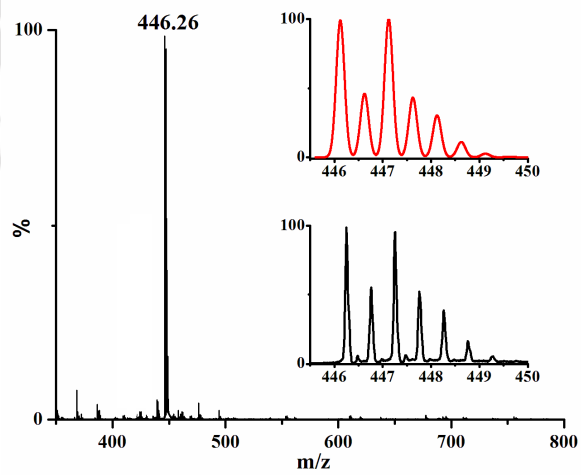

Figure A2.11 ESI-mass spectrum of complex **3.2** in methanol. Inset shows the simulated (red) and experimental (balck) isotopic distribution pattern.

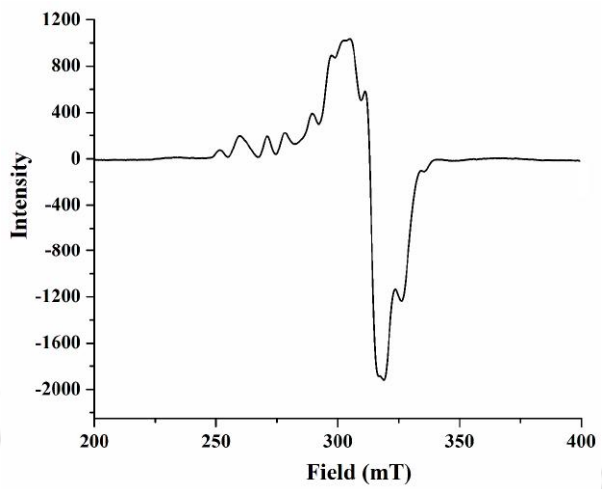

Figure A2.12 X-band EPR spectrum of complex **3.2** in methanol.

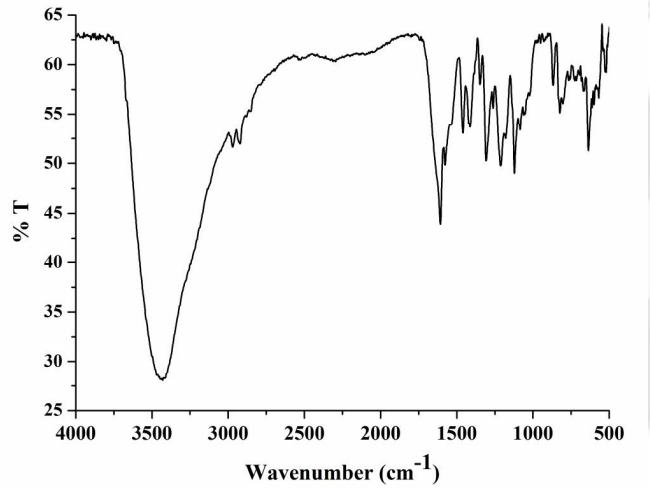

Figure A2.13 FT-IR spectrum of complex **3.3** in KBr pellet.

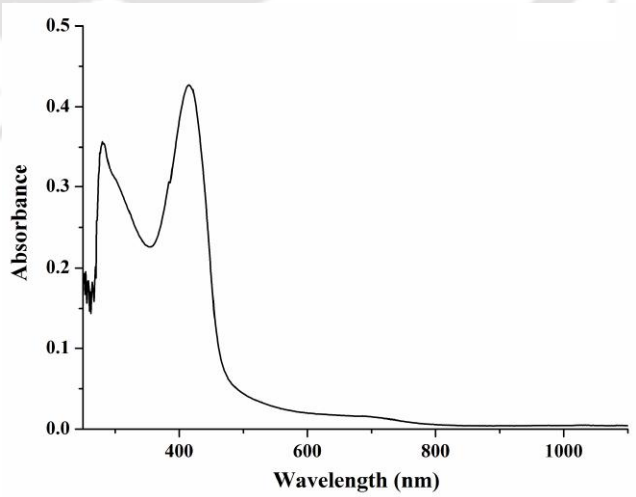

Figure A2.14 UV-visible spectrum of complex **3.3** in methanol.

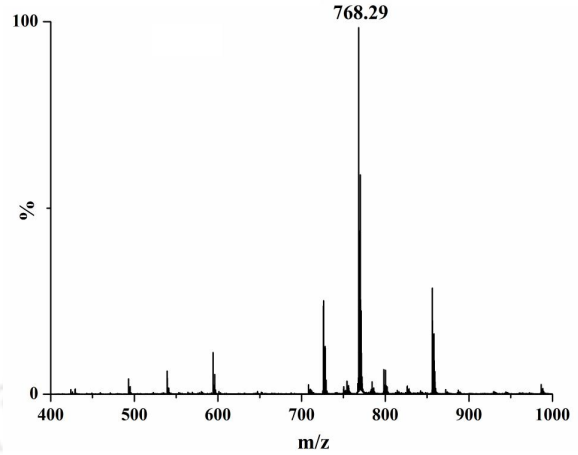

Figure A2.15 ESI-mass spectrum of complex **3.3** in methanol.

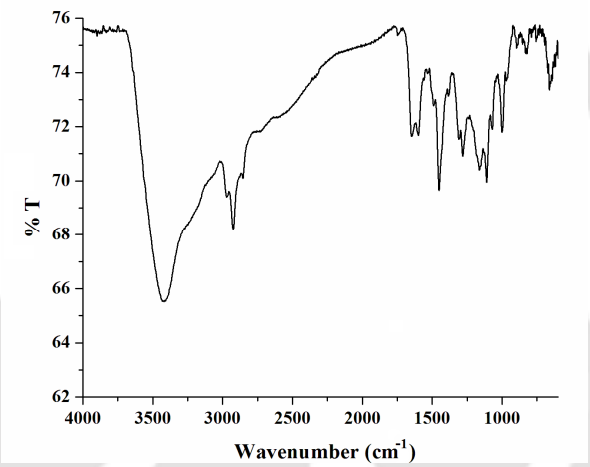

Figure A2.16 FT-IR spectrum of modified ligand **L2′** in KBr pellet.

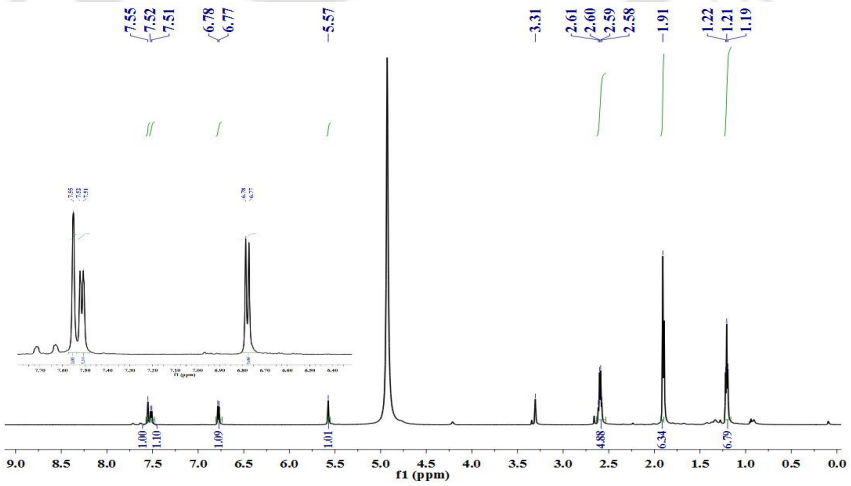

Figure A2.17 ^{1}H NMR spectrum of modified ligand **L2′** in CD_3OD.

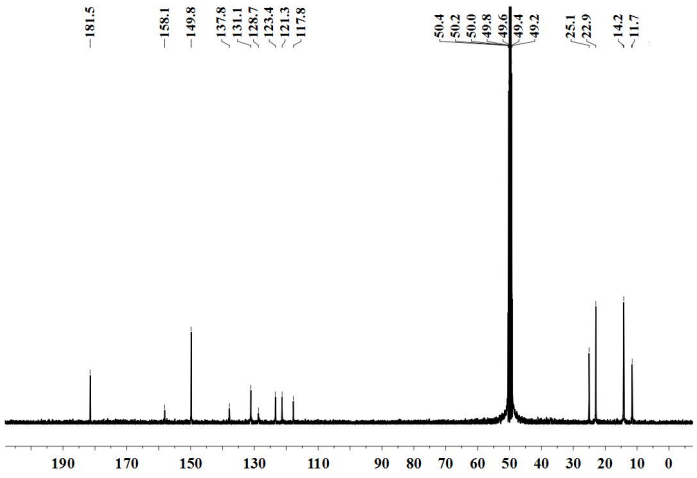

Figure A2.18 ^{13}C NMR spectrum of modified ligand **L2′** in CD_3OD.

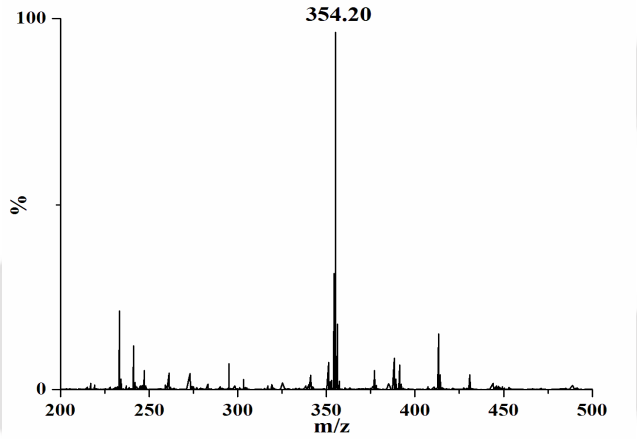

Figure A2.19 ESI-mass spectrum of modified ligand **L2′** in methanol.

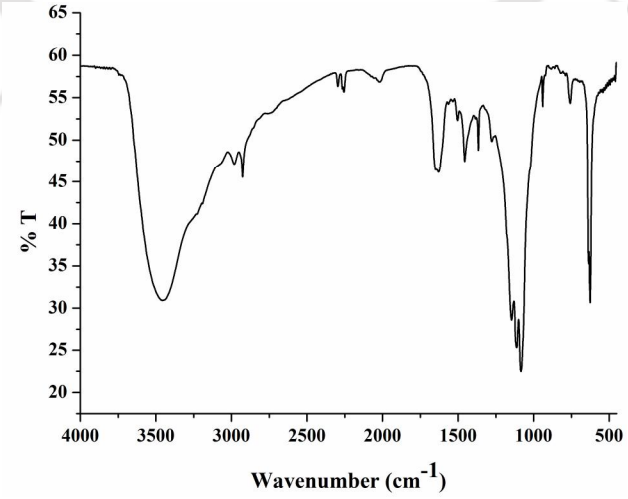

Figure A2.20 FT-IR spectrum of complex **3.1a** in KBr pellet.

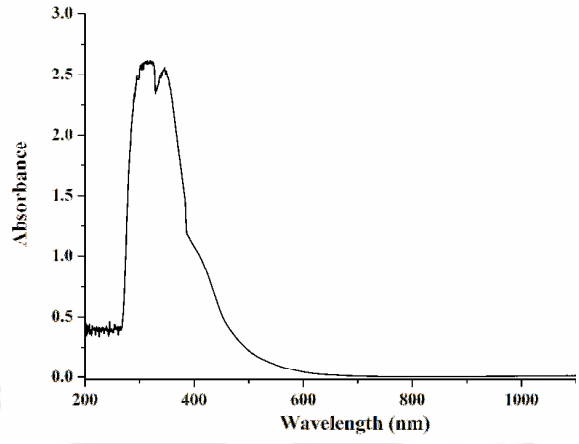

Figure A2.21 UV-visible spectrum of complex **3.1a** in methanol.

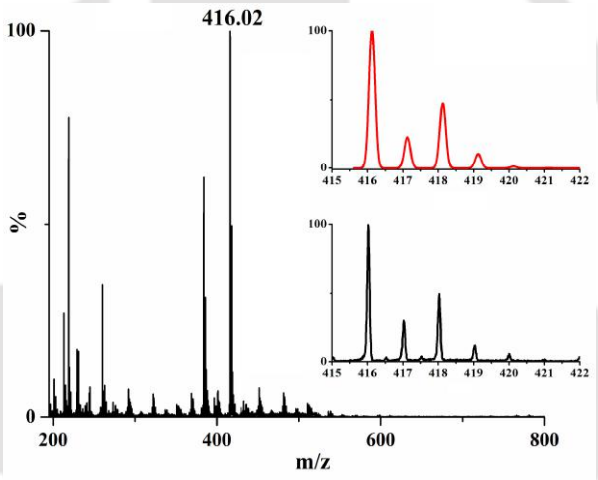

Figure A2.22 ESI-mass spectrum of complex **3.1a** in methanol. Inset shows the simulated (red) and experimental (balck) isotopic distribution pattern.

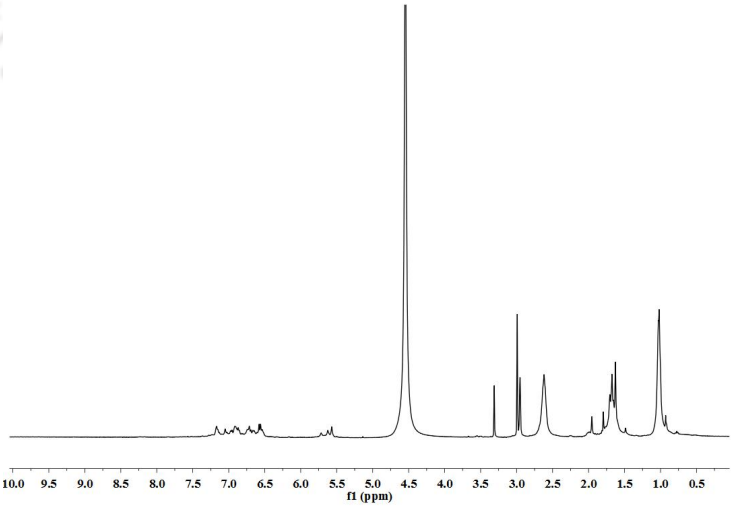

Figure A2.23 ^{1}H NMR spectrum of **3.1a** in CD_3OD and CD_3CN mixture.

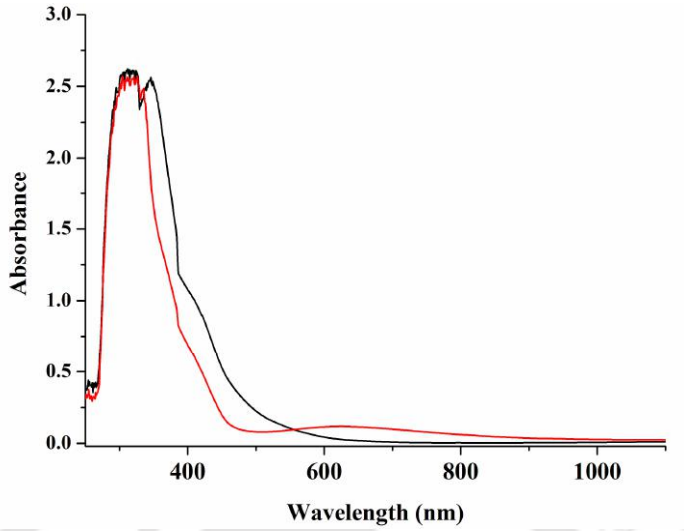

Figure A2.24 UV-visible spectra of complex **3.1a** (black) and after purging NO (red) in acetonitrile.

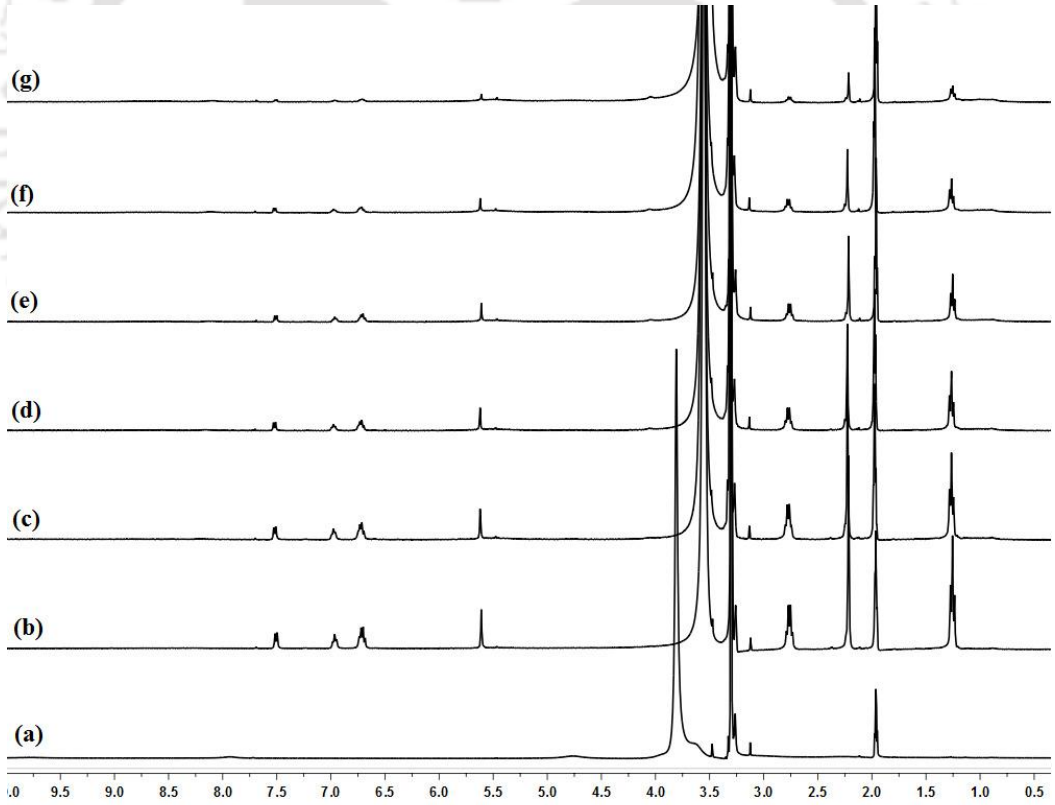

Figure A2.25 ^{1}H-NMR spectra complex **3.1** before and after purging NO in CD_3OD and CD_3CN mixture. (a) Represents complex **3.1**; (b) – (g) represent the spectra of complex **1** after the addition of NO. Spectra are recorded in 2 hours intervals.

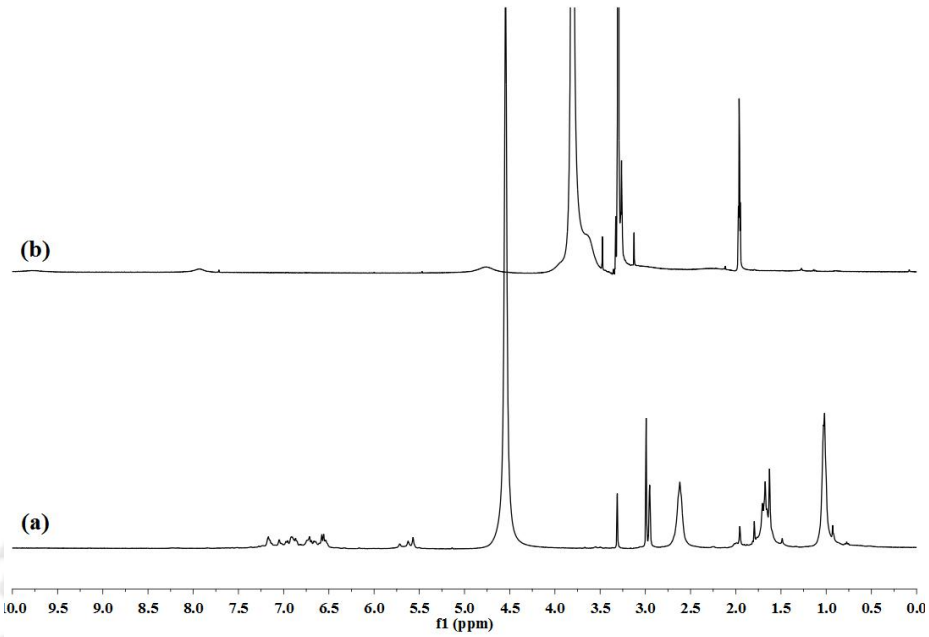

Figure A2.26 ^{1}H NMR spectrum of (a) complex **3.1a** and (b) after addition of NO in CD_3OD and CD_3CN mixture.

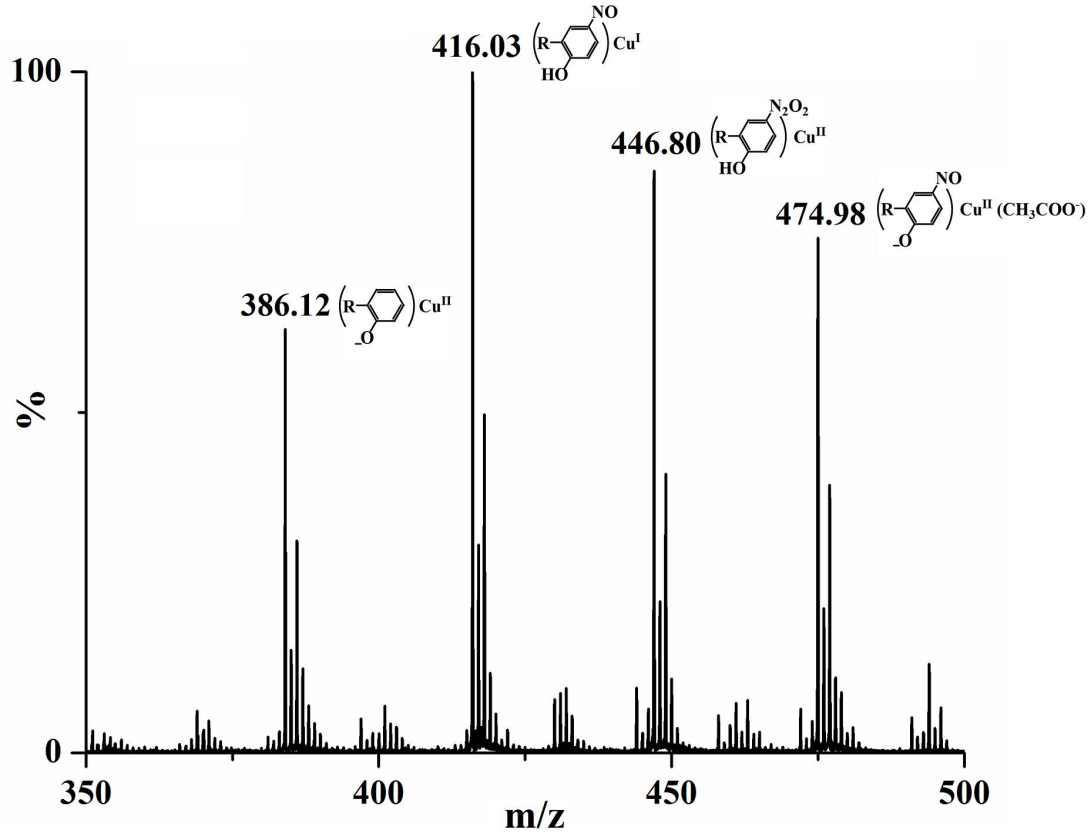

Figure A2.27 ESI-mass spectrum of the reaction mixture of Complex **3.1** and NO in methanol and acetonitrile mixture (1:5).

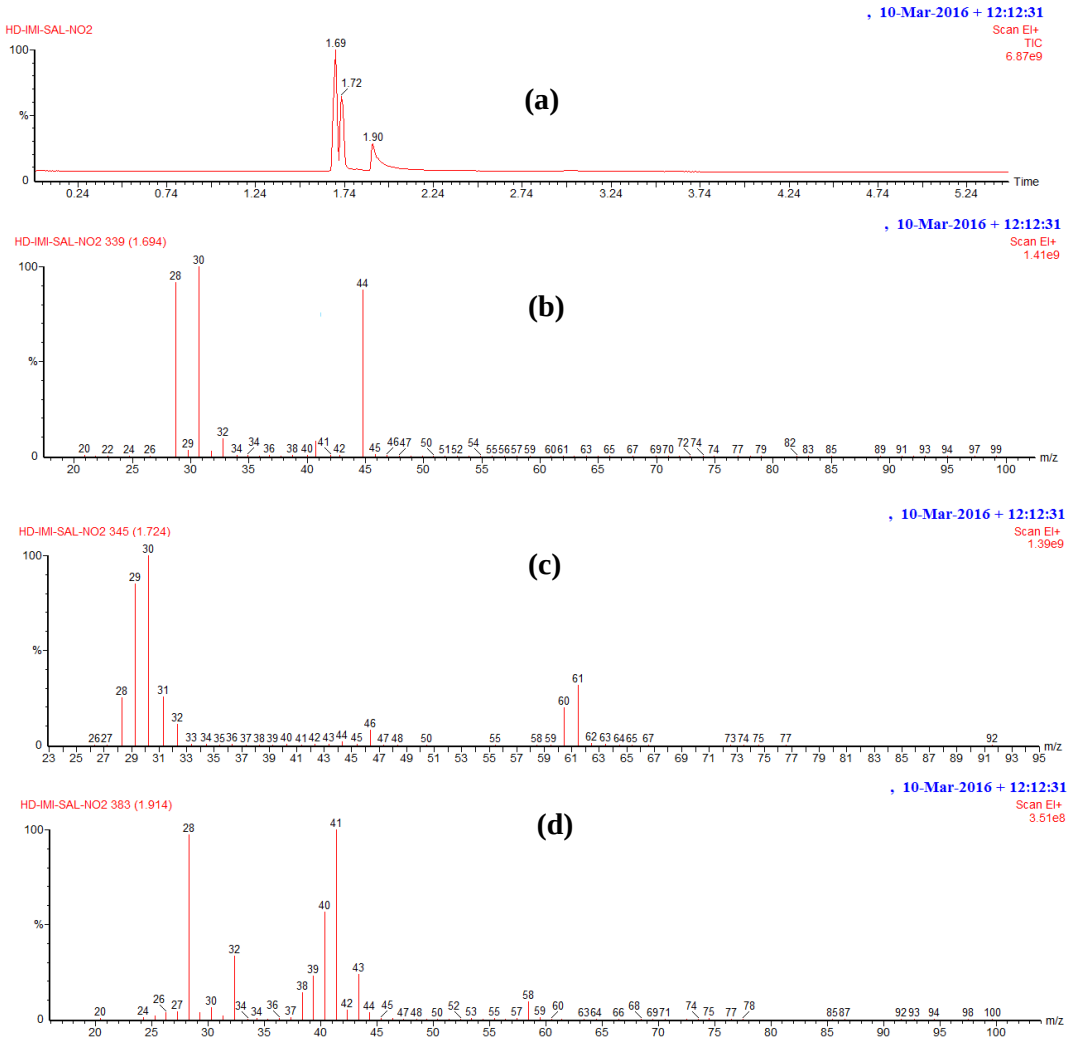

Figure A2.28 GC-mass spectra of headspace gas after 1 day of purging NO in the solution of complex 3.1 (methanol: acetonitrile, 1:5, v/v). (a) Chromatogram, (b) mass spectrum of nitrous oxide at retention time 1.694 minute, (c) mass spectrum of methyl nitrite at retention time 1.724 minute (d) mass spectrum of acetonitrile solvent at retention time 1. 914 minute.

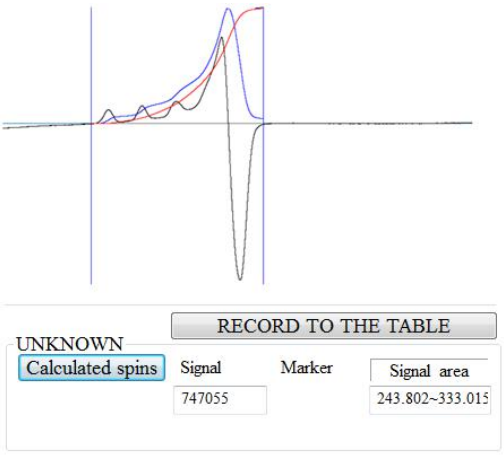

Figure A2.29 Double integration of EPR spectrum of complex **3.1** (concentration 0.5 M) in methanol and acetonitrile mixture (1:5, v/v) at 77 K.

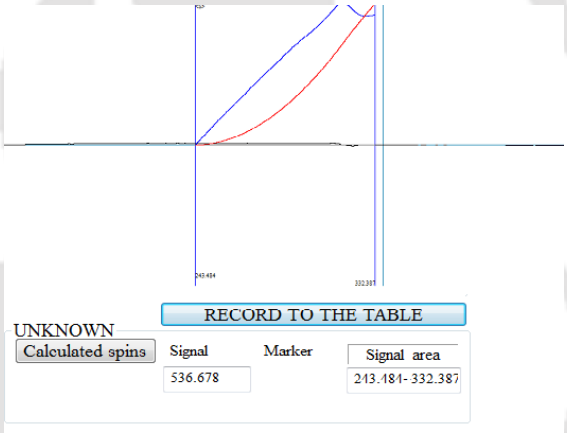

Figure A2.30 Double integration of EPR spectrum of complex **3.1** (concentration 0.5 M) just after adding of NO in methanol and acetonitrile mixture (1:5, v/v) at 77 K.

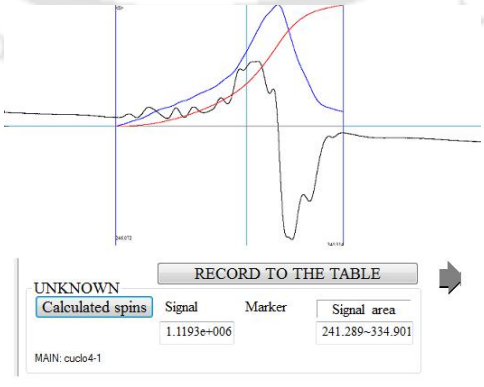

Figure A2.31 Double integration of EPR spectrum of complex **3.1** (concentration 0.5 M) after 24 hours of adding NO in methanol and acetonitrile mixture (1:5, v/v) at 77 K.

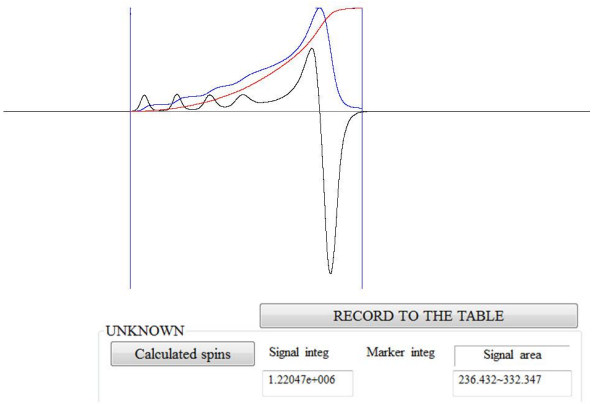

Figure A2.32 Double integration of EPR spectrum of complex **3.1** (concentration 0.5 M) after adding excess of NO in methanol and acetonitrile mixture (1:5, v/v) at 77 K.

Table A2.1. Selected bond lengths (Å) of complexes **3.1, 3.2** and **3.3**.

Atom	**3.1**	**3.2**	**3.3**
Cu(1)- N(1)	1.958 (4)	1.945 (5)	2.010 (3)
Cu(1)- N(3)	2.041 (5)	1.951 (7)	1.994 (3)
Cu(1)- O(1)	2.236 (4)	-	2.342 (3)
Cu(1)- O(2)	1.931 (4)	-	-
Cu(1)- O(4)	1.988 (4)	1.909 (6)	-
Cu(2)- N(5)	1.961 (4)	1.961 (6)	-
Cu(2)- N(7)	2.015 (5)	1.948 (6)	-
Cu(2)- O(1)	1.933 (4)		-
Cu(1)- O(3)	-	1.910 (5)	-
Cu(2)- O(5)	-	1.930 (7)	-
O(4)- N(9)	-	1.315 (6)	-
O(6)- N(11)	-	1.306 (7)	-
O(5)- N(12)	-	1.30(1)	-
N(9)- N(10)	-	1.26 (1)	-
N(11)- N(12)	-	1.26 (1)	-
Cu(2)- O(2)	2.266 (4)	-	-
N(1)- C(6)	1.384 (7)	10415(7)	1.392 (4)
O(1)- C(9)	1.302 (6)	-	-
O(2)- C(41)	1.327 (6)	-	-
O(3)- C(39)	1.26 (1)	-	-
O(4)- C(39)	1.26 (1)	-	-
O(2)- N(5)	-	-	1.297 (5)
C(18)-N(11)	-	1.427(8)	-
C(37)-N(9)	-	1.430(9)	-

Appendix III

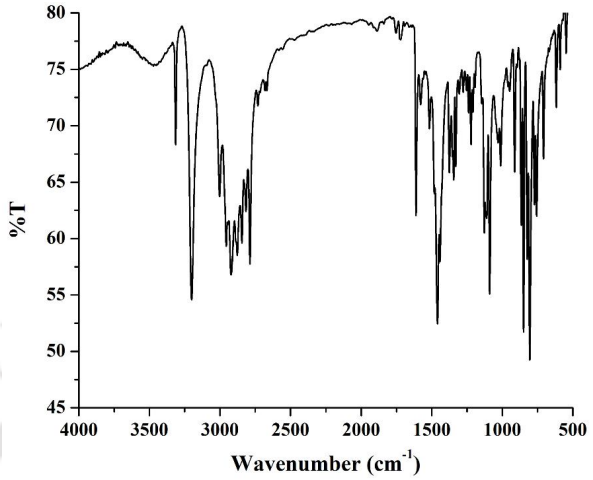

Figure A3.1 FT-IR spectrum of **L3** in KBr pellet.

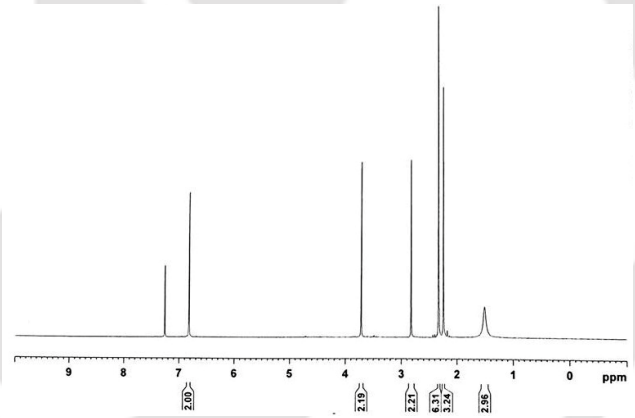

Figure A3.2. ^{1}H-NMR spectrum of **L3** in $CDCl_3$.

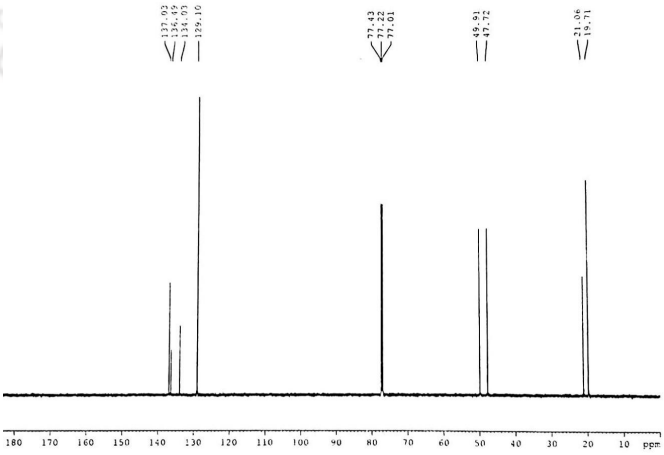

Figure A3.3 ^{13}C-NMR spectrum of **L3** in $CDCl_3$.

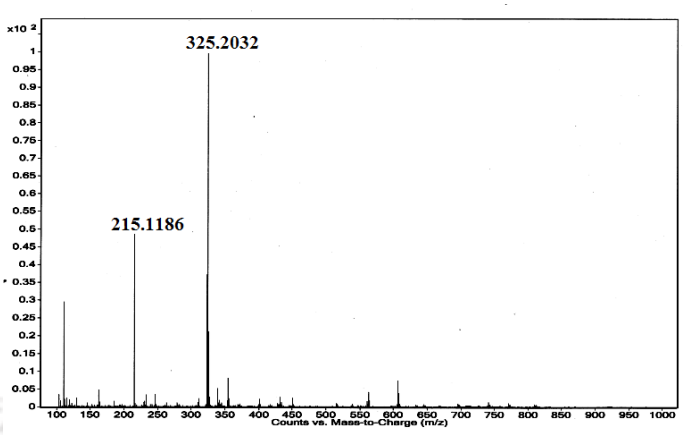

Figure A3.4 ESI-mass spectrum of **L3** in methanol.

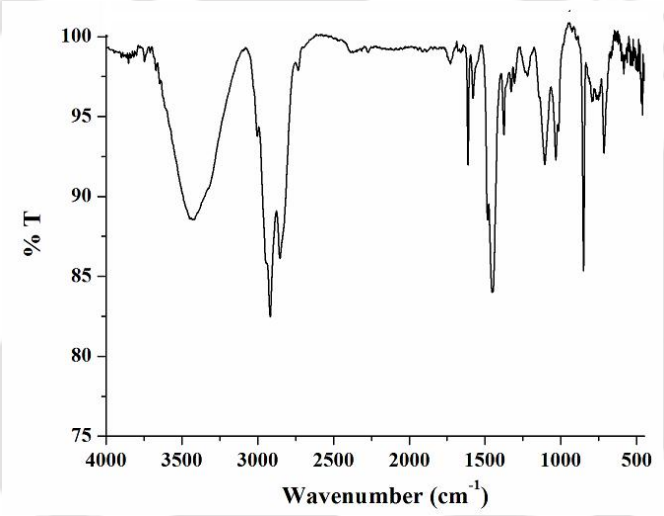

Figure A3.5 FT-IR spectrum of ligand **L4** in KBr pellet.

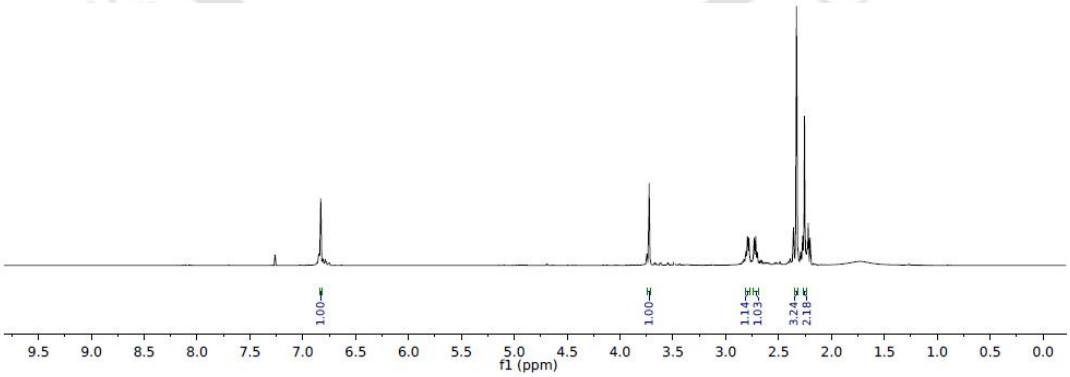

Figure A3.6 ^{1}H-NMR spectrum of **L4** in $CDCl_3$.

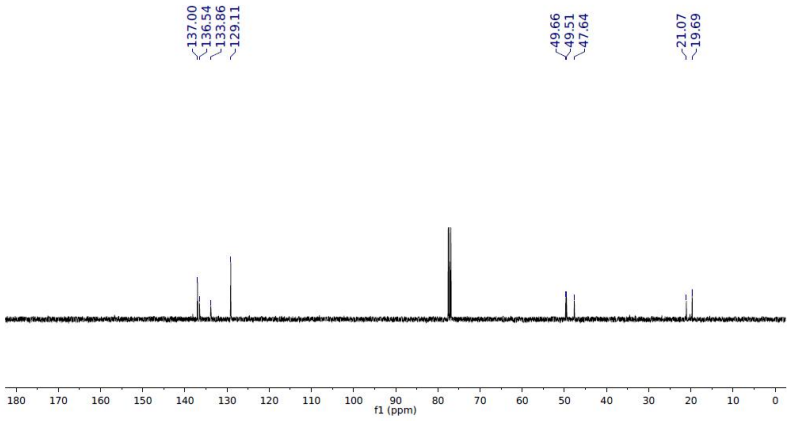

Figure A3.7 ^{13}C-NMR spectrum of **L4** in $CDCl_3$.

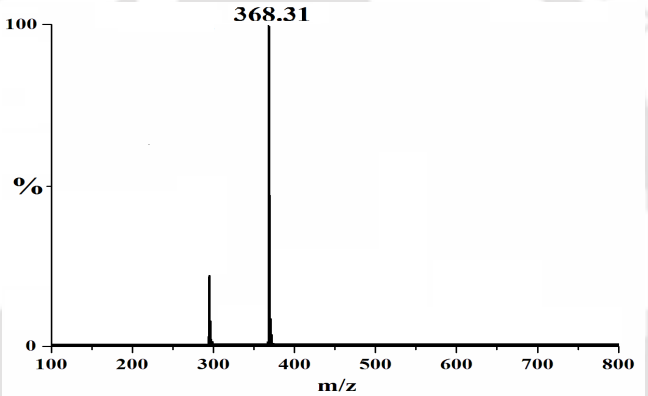

Figure A3.8 ESI-mass spectrum of **L4** in methanol.

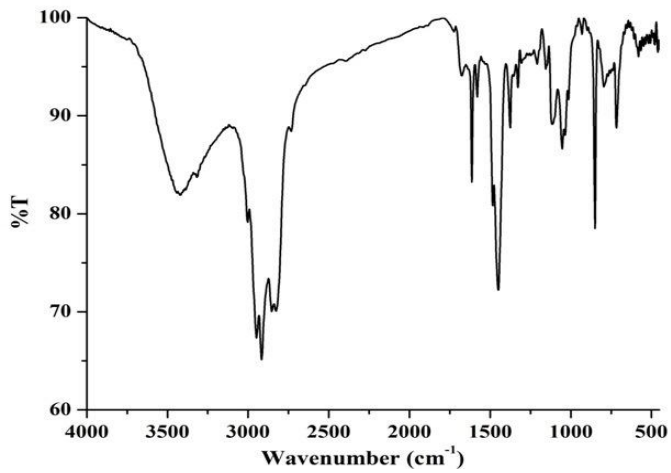

Figure A3.9 FT-IR spectrum of ligand **L5** in KBr pellet.

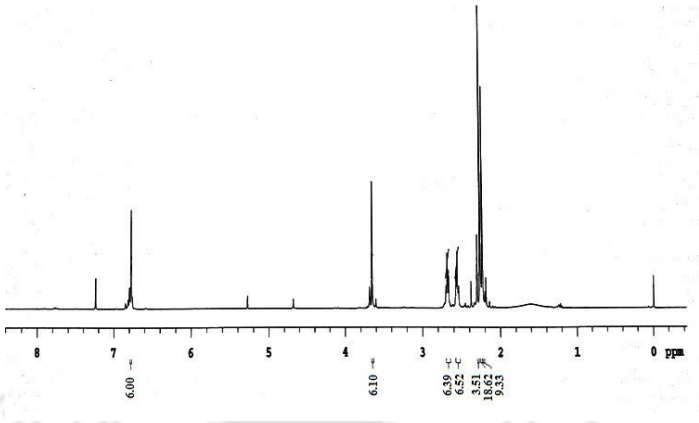

Figure A3.10 ^{1}H-NMR spectrum of **L5** in $CDCl_3$.

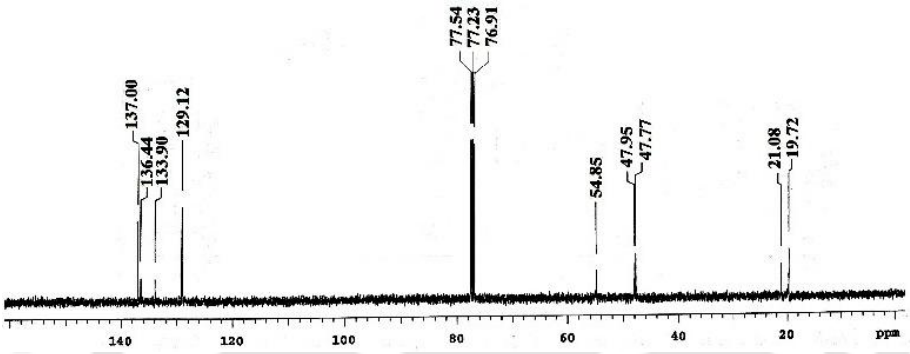

Figure A3.11 ^{13}C-NMR spectrum of **L5** in $CDCl_3$.

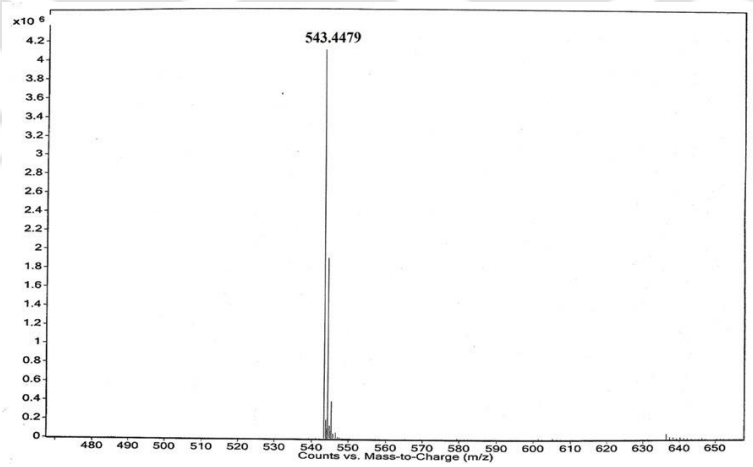

Figure A3.12 ESI-mass spectrum of **L5** in methanol.

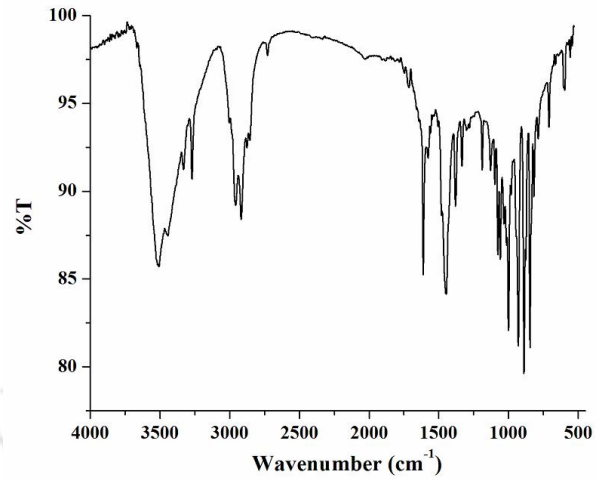

Figure A3.13 FT-IR spectrum of complex **4.1** in KBr pellet.

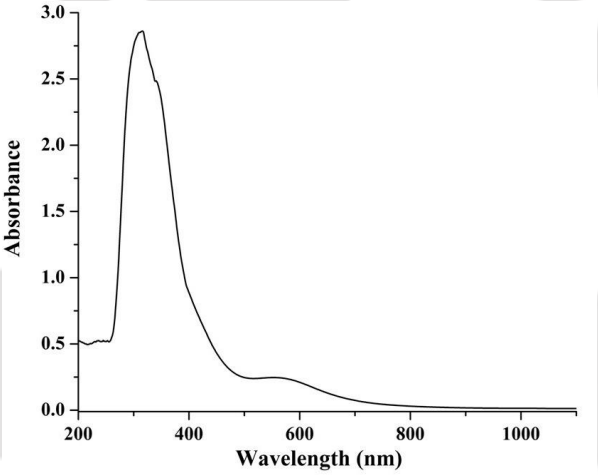

Figure A3.14 UV-visible spectrum of complex **4.1** in methanol.

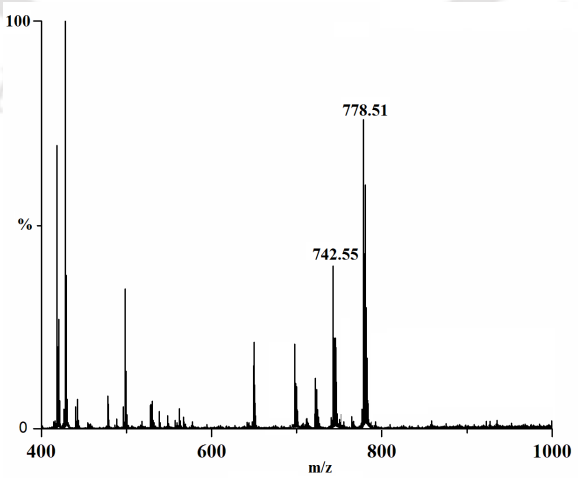

Figure A3.15 ESI-mass spectrum of complex **4.1** in methanol.

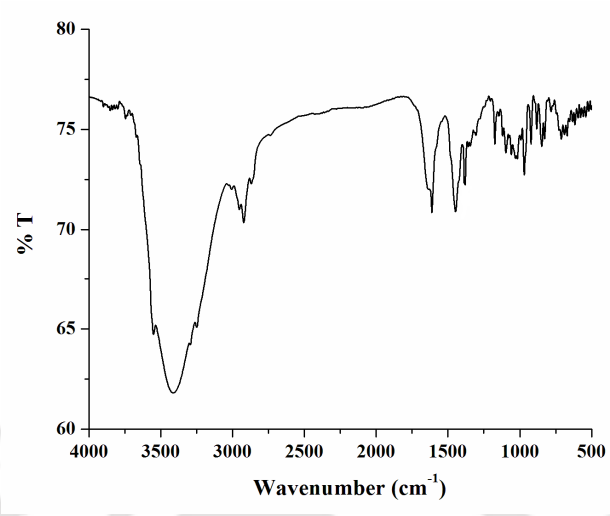

Figure A3.16 FT-IR spectrum of complex **4.2** in KBr pellet.

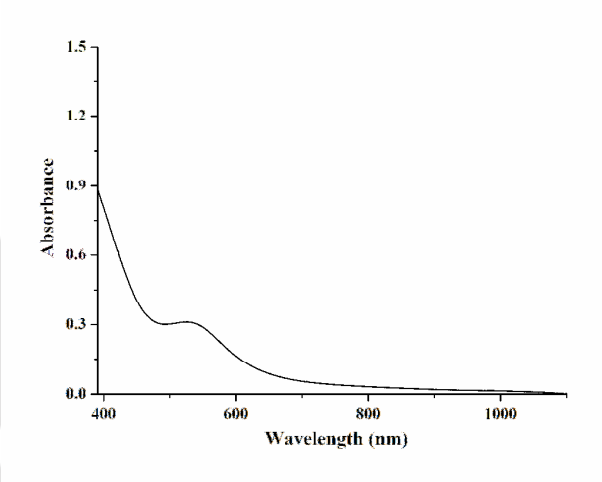

Figure A3.17 UV-visible spectrum of complex **4.2** in methanol.

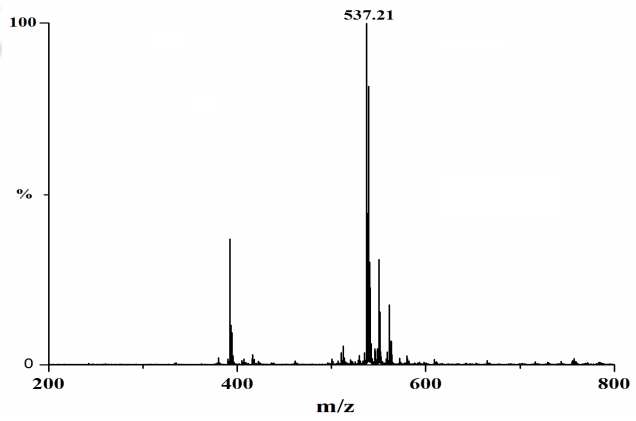

Figure A3.18 ESI-mass spectrum of complex **4.2** in acetonitrile.

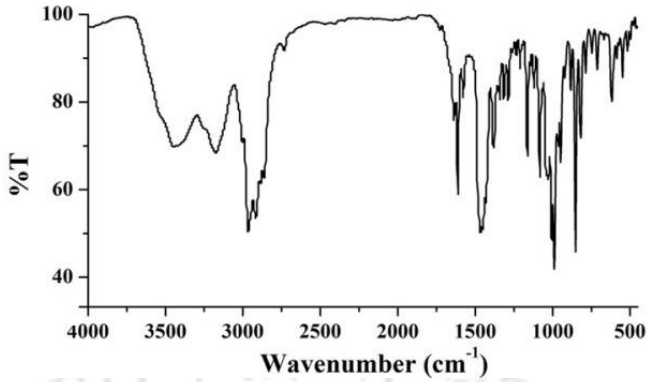

Figure A3.19 FT-IR spectrum of complex **4.3** in KBr pellet.

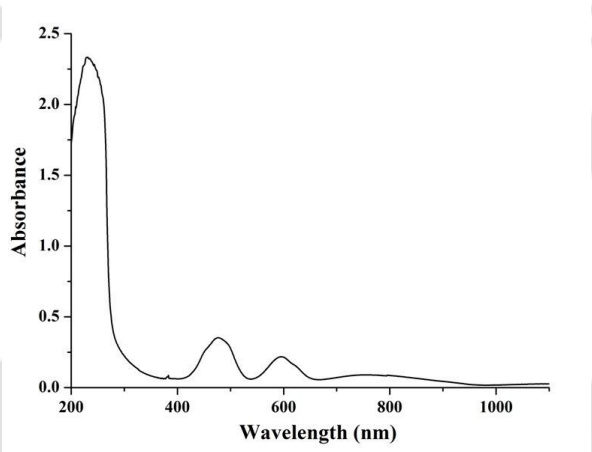

Figure A3.20 UV-visible spectrum of complex **4.3** in methanol.

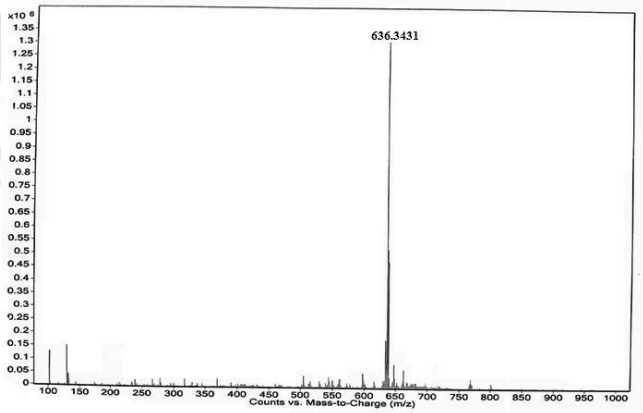

Figure A3.21 ESI-mass spectrum of complex **4.3** in methanol.

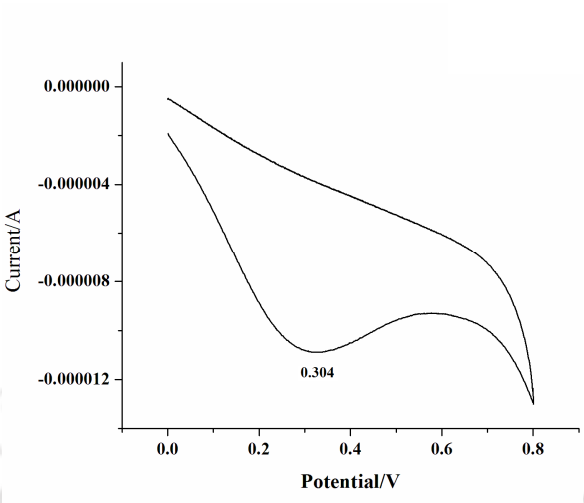

Figure A3.22 Cyclic voltammogram of complex **4.1**.

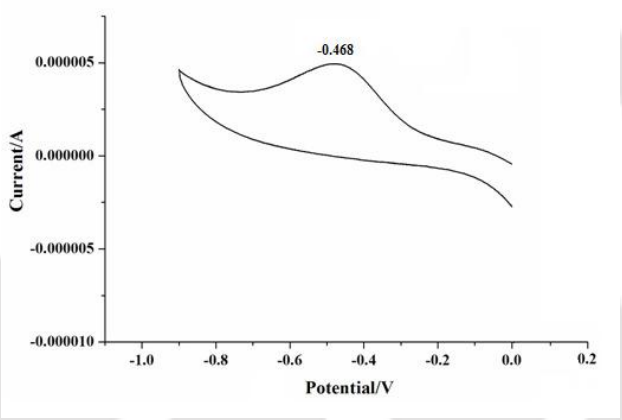

Figure A3.23 Cyclic voltammogram of complex **4.1**.

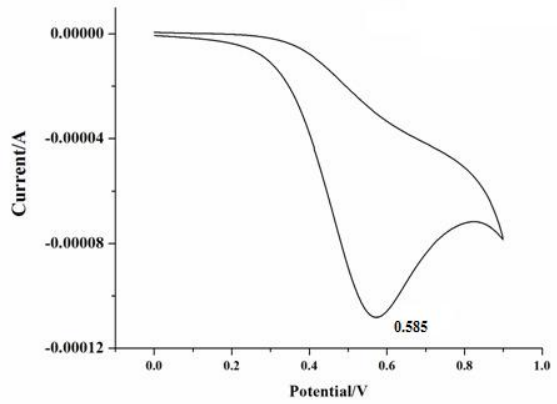

Figure A3.24 Cyclic voltammogram of complex **4.2**.

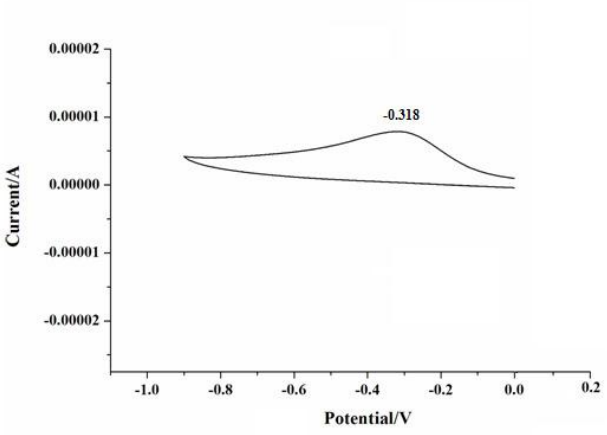

Figure A3.25 Cyclic voltammogram of complex **4.2**.

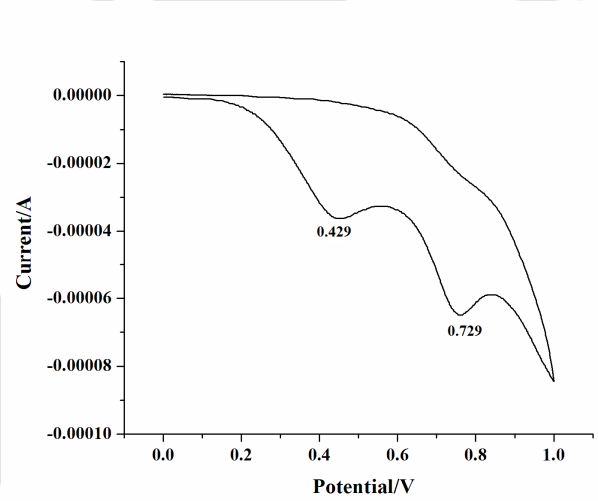

Figure A3.26 Cyclic voltammogram of complex **4.3**.

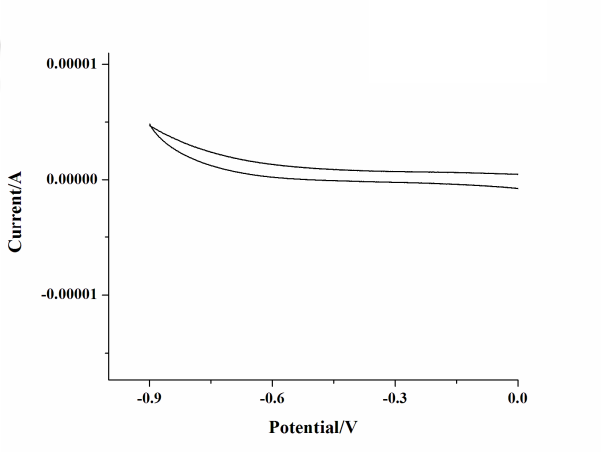

Figure A3.27 Cyclic voltammogram of complex **4.3**.

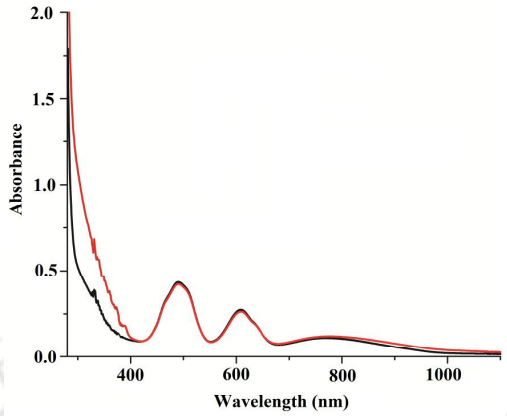

Figure A3.28 UV-visible spectra of complex **4.3** (black) and upon purging excess NO (red) in methanol.

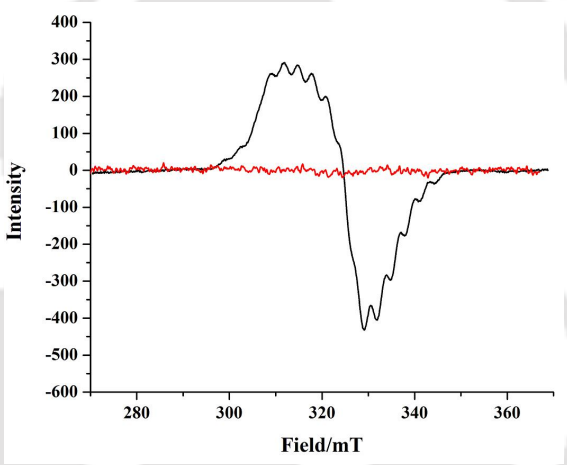

Figure A3.29 X-band EPR spectra of complex **4.1** (black) and upon purging excess NO (red) in methanol.

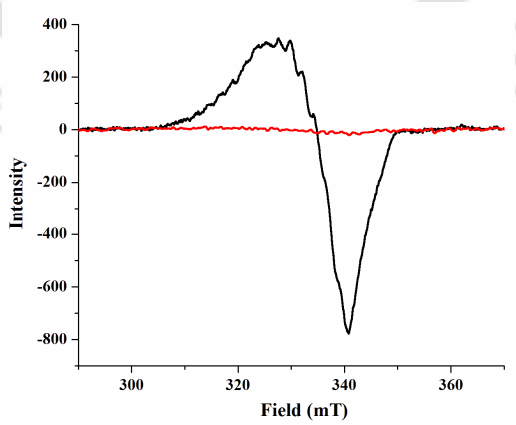

Figure A3.30 X-band EPR spectra of complex **4.2** (black) and upon purging excess NO (red) in methanol.

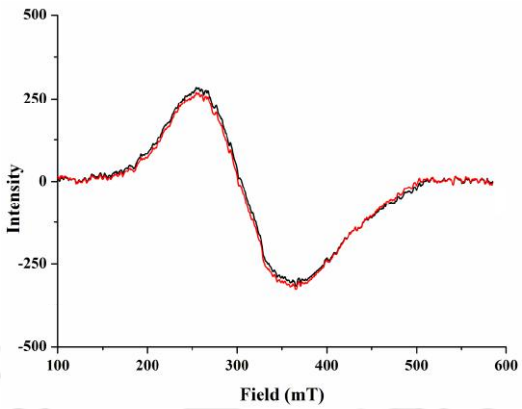

Figure A3.31 X-band EPR spectra of complex **4.3** (black) and upon purging excess NO (red) in methanol.

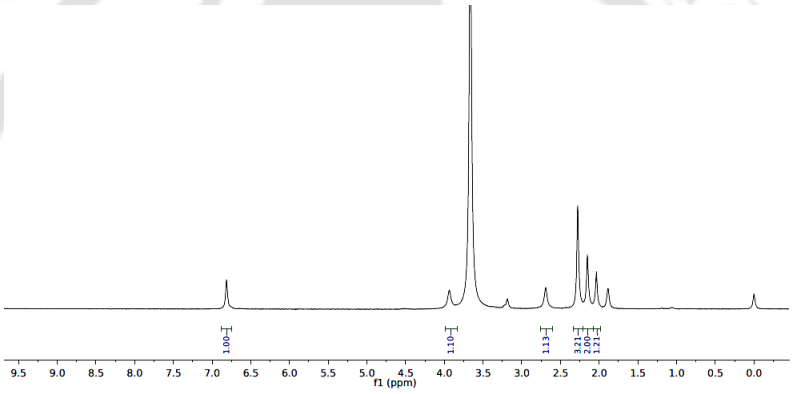

Figure A3.32 ^{1}H-NMR spectrum of complex **4.4a** in CD_3OD.

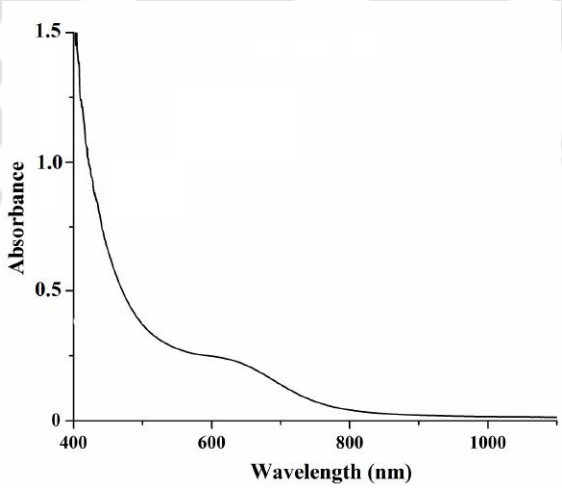

Figure A3.33 UV-visible spectrum of complex **4.4a** in methanol.

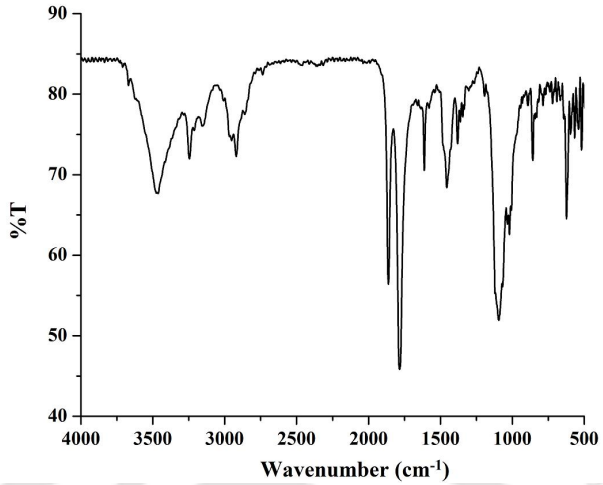

Figure A3.34 FT-IR spectrum of complex **4.4b** in KBr pellet.

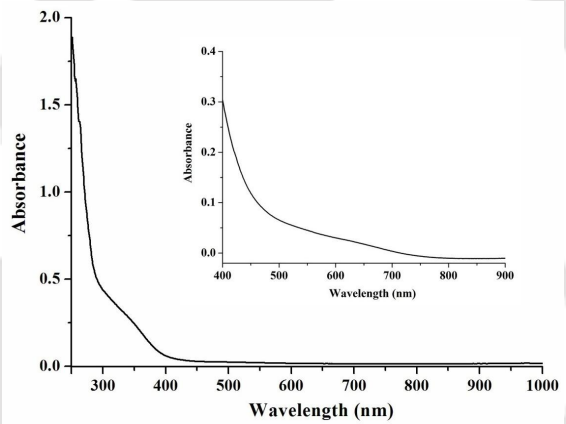

Figure A3.35 UV-visible spectrum of complex **4.4b** in methanol. Inset shows the *d-d* transition region.

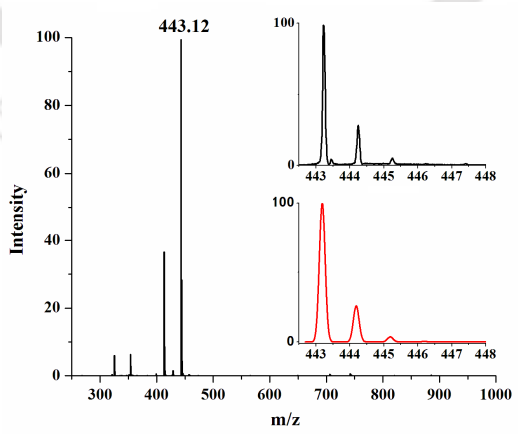

Figure A3.36 ESI-mass spectrum of complex **4.4a** in acetonitrile. Inset shows the simulated (red) and experimental (black) isotopic distribution pattern.

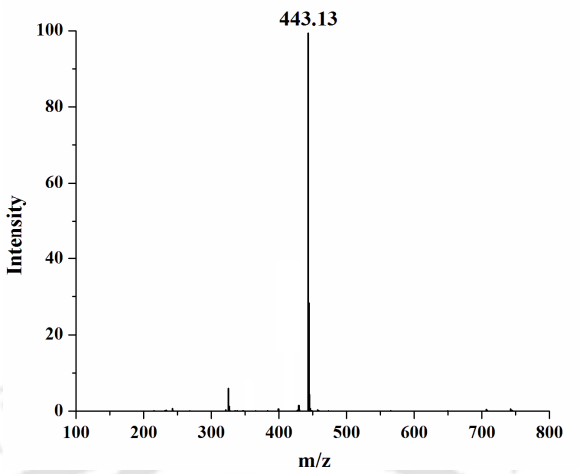

Figure A3.37 ESI-mass spectrum of complex **4.4b** in acetonitrile.

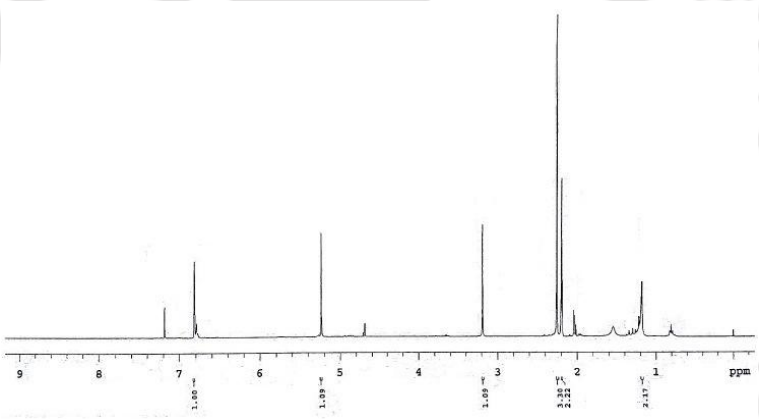

Figure A3.38 ^{1}H-NMR spectrum of modified ligand **L3**$^{/}$ in $CDCl_3$.

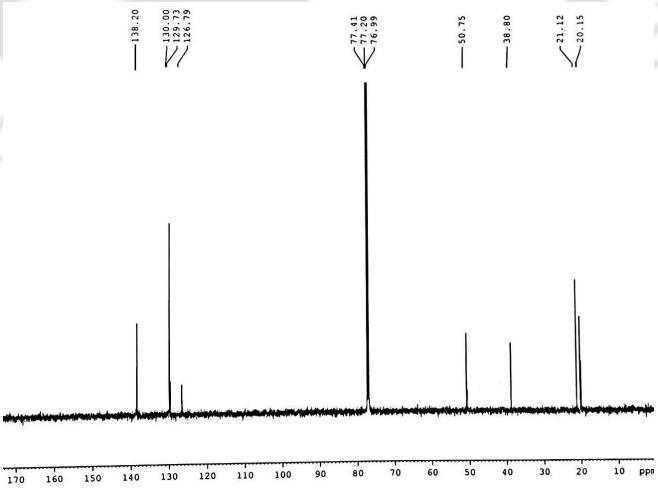

Figure A3.39 ^{13}C-NMR spectrum of modified ligand **L3**$^{/}$ in $CDCl_3$.

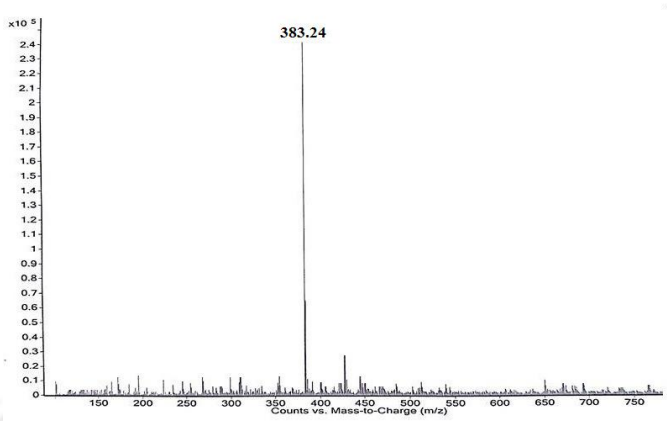

Figure A3.40 ESI-mass spectrum of modified ligand **L3′** in methanol.

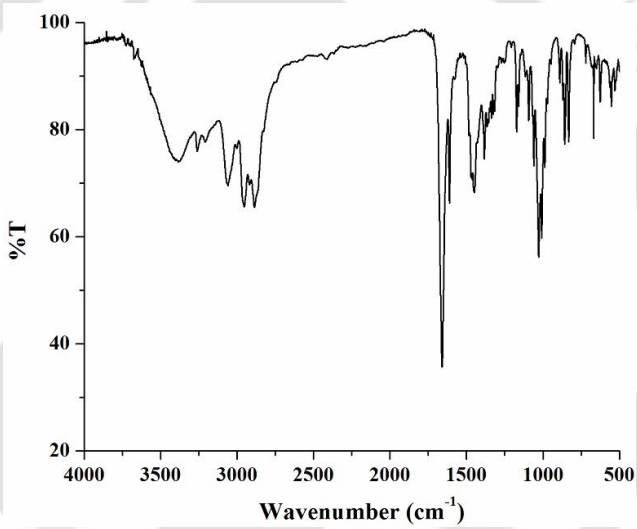

Figure A3.41 FT-IR spectrum of complex **4.5** in KBr pellet.

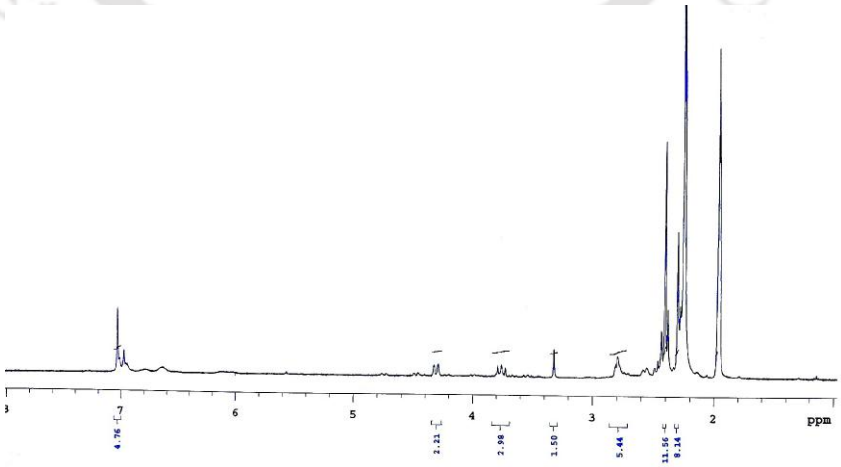

Figure A3.42 ^{1}H-NMR spectrum of complex **4.5** in CD_3CN.

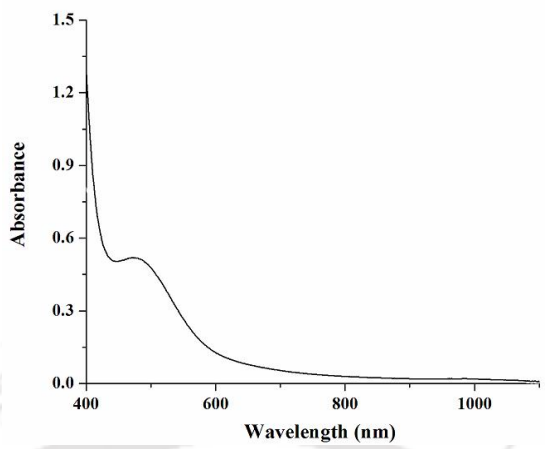

Figure A3.43 UV-visible spectrum of complex **4.5** in methanol.

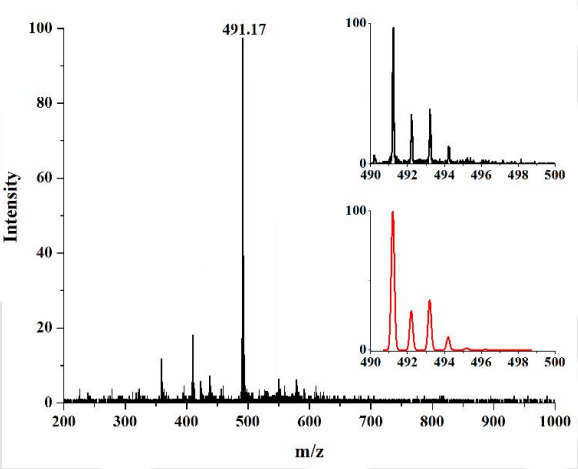

Figure A3.44 ESI-mass spectrum of complex **4.5** in acetonitrile. Inset shows isotopic distribution pattern. Black line corresponds experimental and red line corresponds simulated mass spectra.

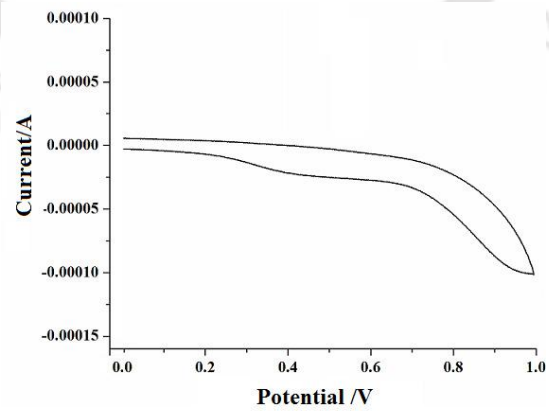

Figure A3.45 Cyclic voltammogram of complex **4.4a**.

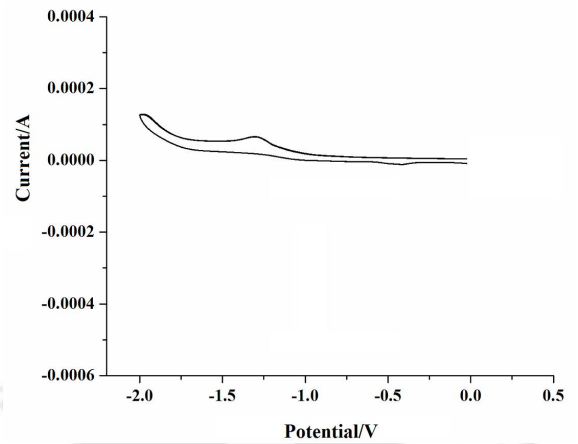

Figure A3.46 Cyclic voltammogram of complex **4.4a**.

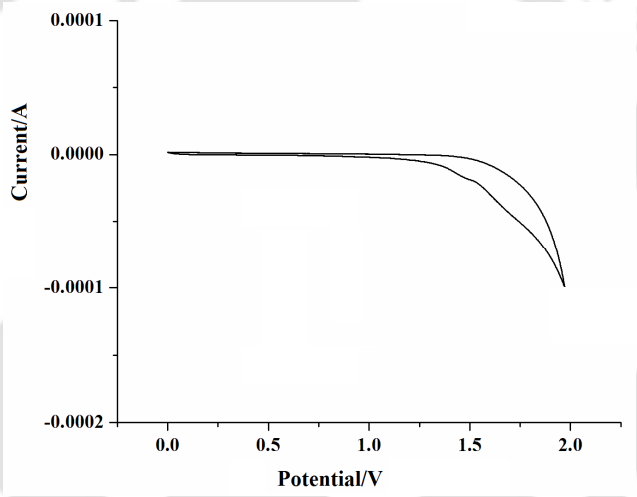

Figure A3.47 Cyclic voltammogram of complex **4.5**.

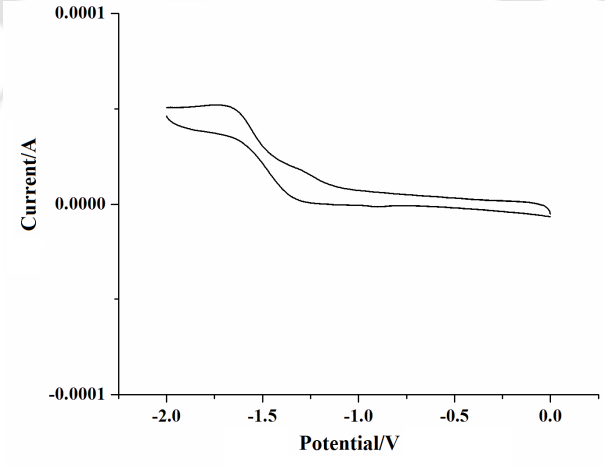

Figure A3.48 Cyclic voltammogram of complex **4.5**.

Appendix IV

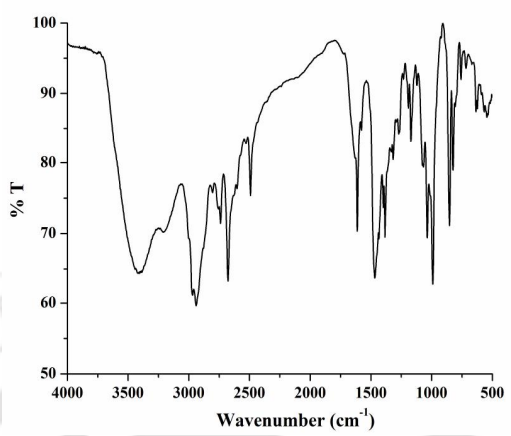

Figure A4.1 FT-IR spectrum of complex **5.1** in KBr pellet.

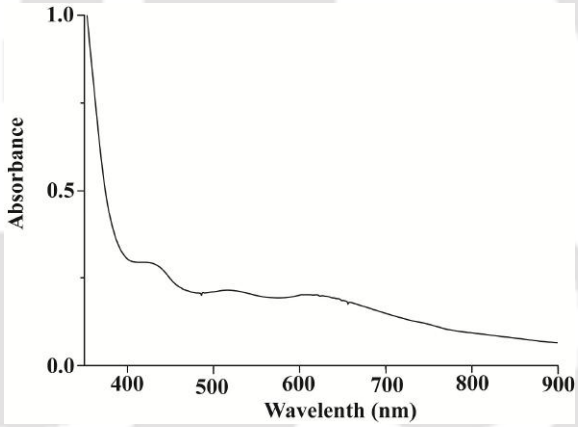

Figure A4.2 UV-visible spectrum of complex **5.1** in methanol.

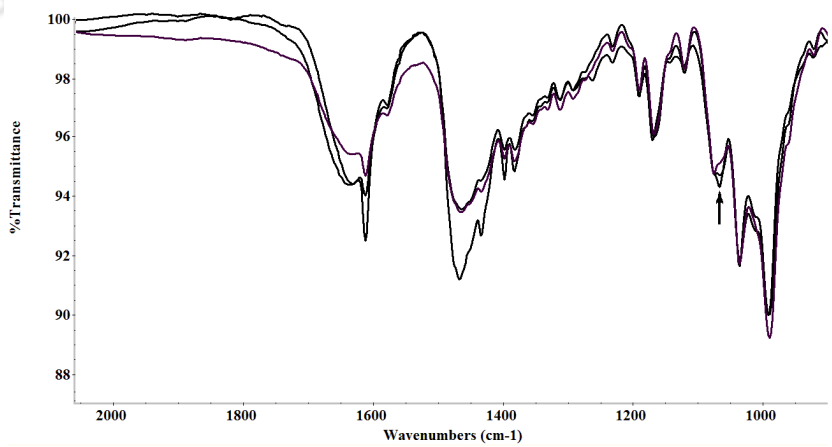

Figure A4.3 FT-IR spectral change during the decomposition of complex **5.1** at room temperature in KBr pellet.

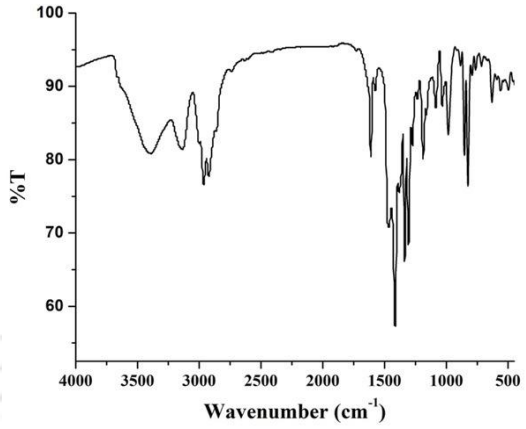

Figure A4.4 FT-IR spectrum of complex **5.2** in KBr pallet.

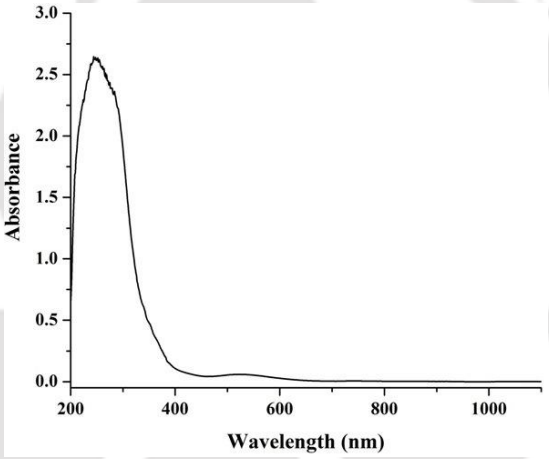

Figure A4.5 UV-visible spectrum of complex **5.2** in methanol.

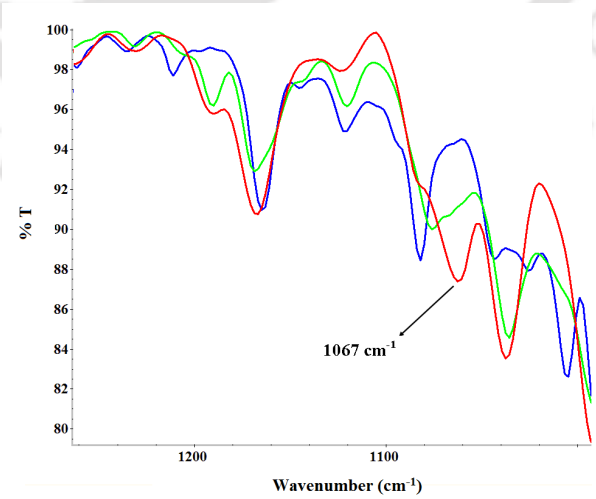

Figure 4.6 Solution FT-IR spectra of complex **4.3** (blue), complex **5.1** (red) and complex **5.2** (green) in acetonitrile at room temperature.

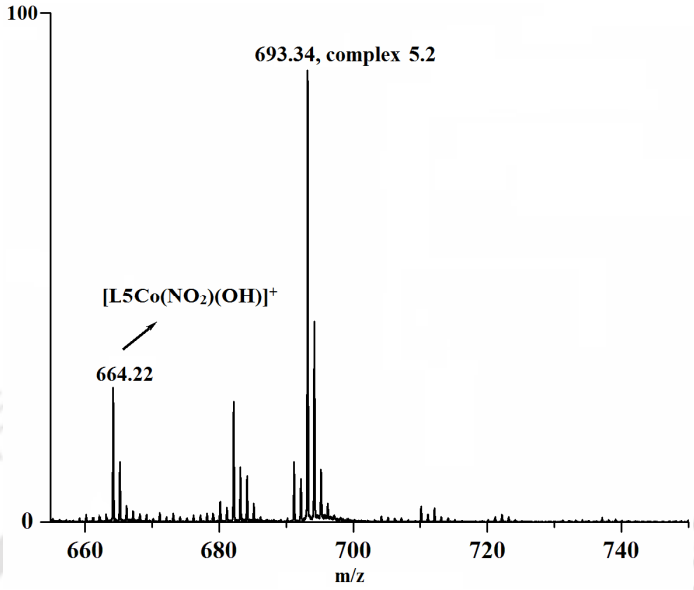

Figure A4.7 ESI-Mass spectrum of complex $[L5Co(OH)(NO_2)]^+$, obtained from reaction of peroxynitrite intermediate and 2,4-di-*tert*-butylphenol.

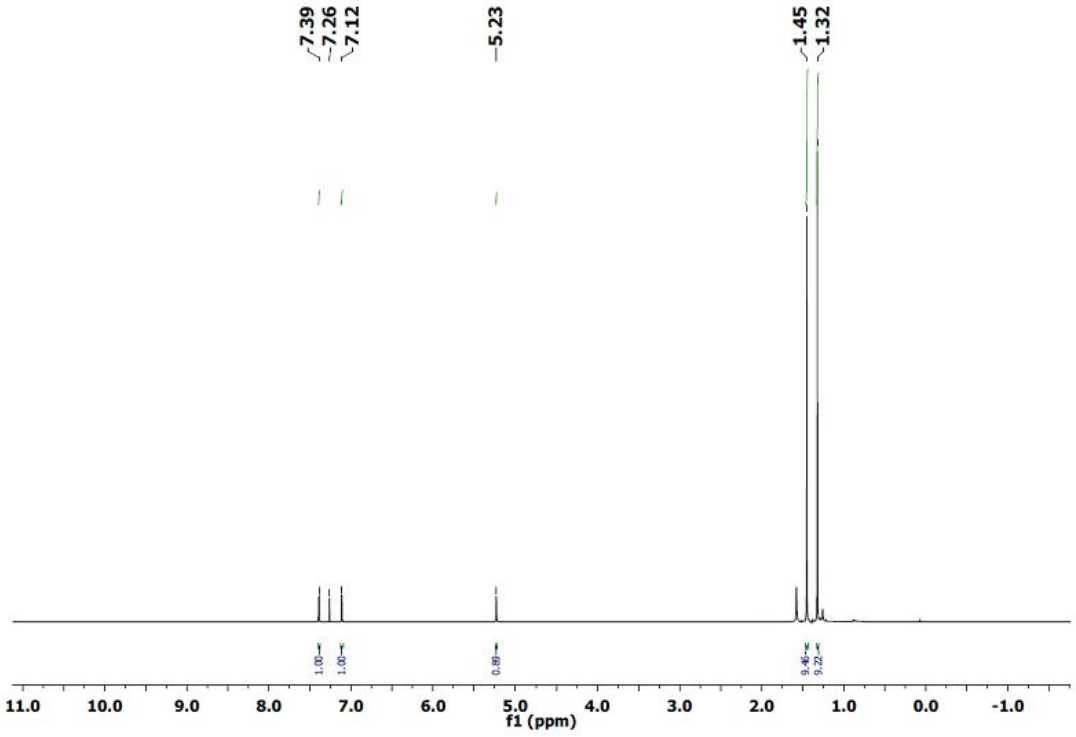

Figure A4.8 ^{1}H-NMR spectrum of 2,2′-dihydroxy-3,3′,5,5′-tetra-*tert*-butylbiphenol in $CDCl_3$.

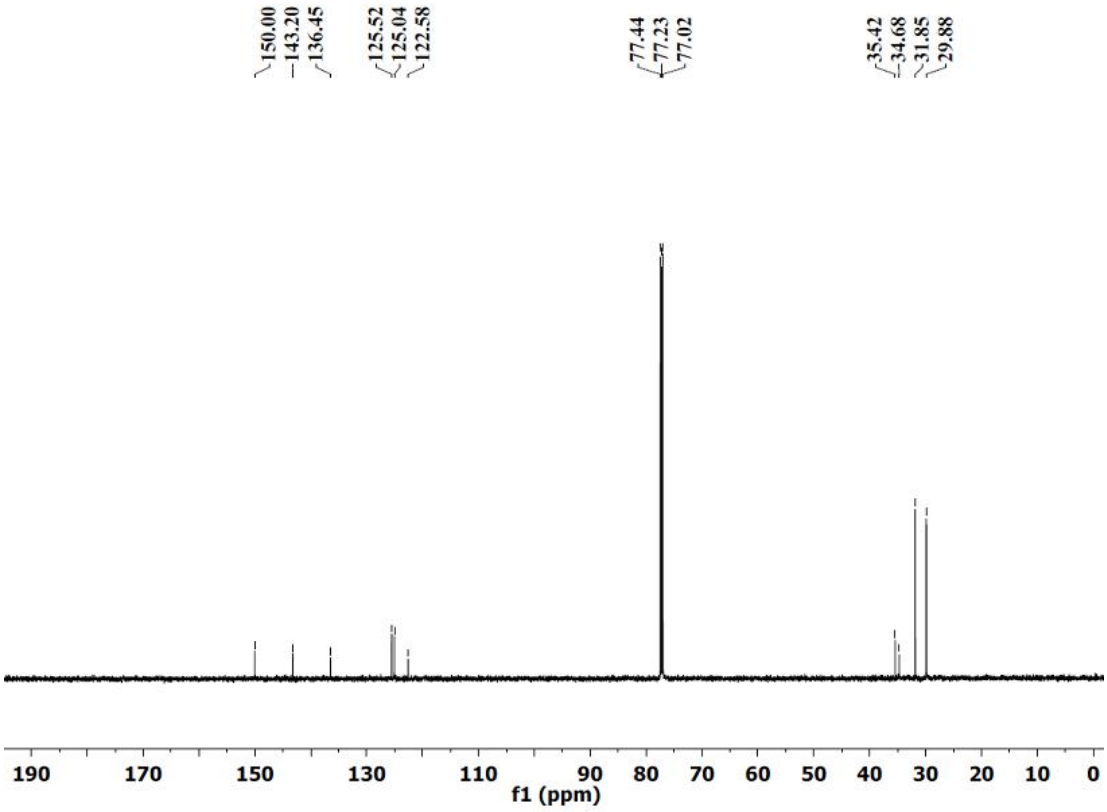

Figure A4.9 ^{13}C-NMR spectrum of 2,2′-dihydroxy-3,3′,5,5′-tetra-*tert*-butylbiphenol in $CDCl_3$.

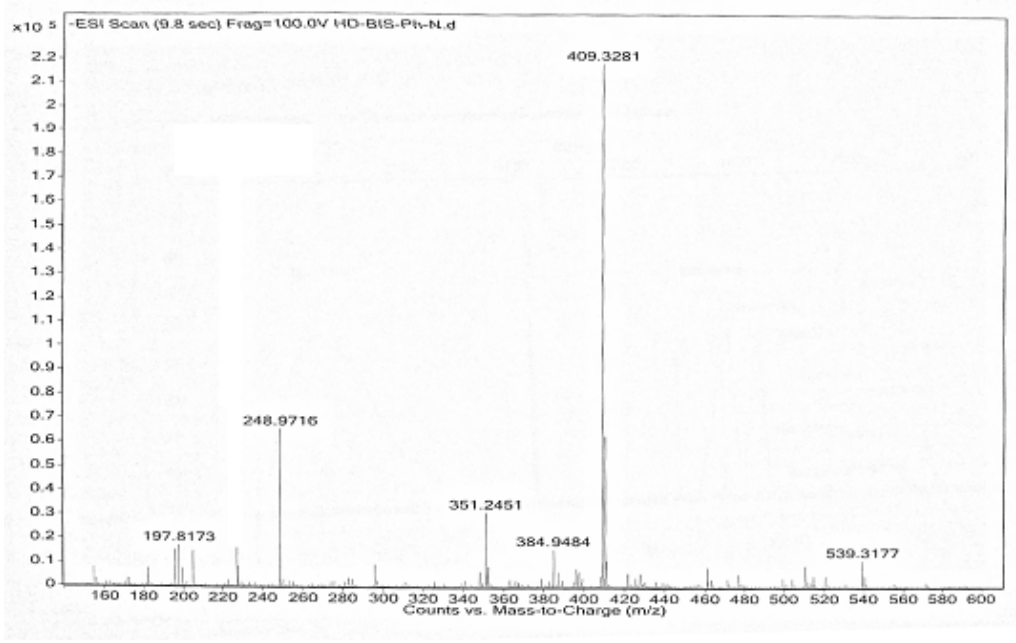

Figure A4.10 ESI-Mass spectrum of 2,2′-dihydroxy-3,3′,5,5′-tetra-*tert*-butylbiphenol in acetonitrile.

List of Publications

(1) "A stable nitrous oxide complex of copper(II)" **Deka, H**.; Ghosh, S.; Banergee, S.; Saha, S.; Gogoi, K.; Vanka, K.; Mondal, B. (*communicated*).

(2) "Nitric oxide reactivity of a Cu(II) complex of an imidazole based ligand: Aromatic C‑nitrosation followed by the formation of N‑nitrosohydroxylaminato complex" **Deka, H**.; Ghosh, S.; Gogoi, K.; Saha, S.; Mondal, B. Inorg. Chem. DOI: 10.1021/acs. inorgchem.7b00069.

(3) "Effect of ligand denticity on the nitric oxide reactivity of cobalt(II) complexes" **Deka, H**.; Ghosh, S.; Saha, S.; Gogoi, K.; Mondal, B. *Dalton Trans.* **2016,** *45*, 10979.

(4) "Reductive nitrosylation of nickel(II) complex by nitric oxide followed by nitrous oxide release" Ghosh, S.; **Deka, H**.; Dangat, Y. B.; Saha, S.; Gogoi, K.; Vanka, K.; Mondal, B. *Dalton Trans.* **2016,** *45*, 10200.

(5) "Oxo transfer from nitrogen dioxide to nitrito group in a copper(II) complex" Gogoi, K.; **Deka, H**.; Kumar, V.; Mondal, B. *Inorg. Chem.*, **2015,** *54*, 4799.